Ovarian Signalling:Insights into the P13K/PKB/Foxo and the Ras/Raf/MEK/ERK Pathways

Nicola Cahill
Technological University Dublin

Recommended Citation

OVARIAN SIGNALLING

INSIGHTS INTO THE PI3K/PKB/FOXO AND THE

Ras/Raf/MEK/ERK PATHWAYS

by

Nicola A. Cahill

M.Phil. Biomedical Science

2008

Department of Biological Sciences,
Dublin Institute of Technology,
Kevin Street,
Dublin 8

ABSTRACT

The ovaries are a pair of female reproductive organs that are involved in the production of gametes 'oogenesis' and the production of hormones 'steroidogenesis' to mediate the oestrous cycle, preparation of the uterus for pregnancy and the preparation of the breast for lactation (www.lab.anhb.uwa.edu.au/mb140/corepages/femaleRepro). The oestrous cycle is controlled by the release of the pituitary gonadotrophins, follicle stimulating hormone (FSH) and lutenising hormone (LH).The physiological responses of ovarian steroidogenesis, oogenesis, folliculargenesis, ovulation and lutenisation to the gonadotrophins are accomplished by the activation of greater than one hundred ovarian target genes (Hunzicker-Dunn *et al* 2006). These processes are dependant on the interplay between the steroid/gonadotrophin hormone signalling pathways and the peptide signalling pathways that cross talk and intercommunicate to induce these ovarian genes (Richards J S *et al* 2002). Two such critical pathways are the PI3K pathway and the Ras/Raf/MEK/ERK cascade. FSH stimulates these pathways in a unique time dependant and synergistic manner (Campbell *et al* 1998) (Wayne *et al* 2007).

Ras is a G protein known as Rat sarcoma homologue and a well known proliferative factor where oncogenic Ras is associated with approximately 20-30% of all human cancers (Bos 1989). Ras plays a key role in both pathways as it stimulates the Ras/Raf/MEK/ERK pathway directly and acts as a supportive activator of the PI3K cascade (Wayne *et al* 2007). Ras works by transducing extracellular ligand mediated stimuli such as growth factors, cytokines and hormones that hit receptor tyrosine kinases (RTK's), non receptor tyrosine kinases (NRTK's) and G protein coupled receptors (GPCR's) to mediate signal transduction that influences growth, differentiation and apoptosis. Ras serves as a binary molecular switch and its bioactivity is controlled by a regulated GDP/GTP cycle (Campbell SL *et al* 1998).

In this study the K-Ras isoform was engineered to be made constitutively active in the ovary. By introducing a glycine to aspartic acid mutation at residue 12 of the *ras* gene, Ras was locked in a constitutively active GTP state and thus the mutation deemed Ras to be insensitive to GTPase activating protein (GAP) stimulation. (Bourne *et al* 1990) A *Lox-Stop–Lox K-ras* conditional mouse strain capable of controlled timing and location of constitutively active Ras expression was utilised (Tuveson *et al* 2004) (Jackson *et al* 2001).

The main objectives of this project were to study the effects of constitutively active Ras on ovarian cell function and morphology, to study the effects of constitutively active Ras on vital ovarian signalling genes *Fshr, Lghcr* and *Mkp-3* and to study the effects of constitutively active Ras on p-ERK and p-PKB; protein intermediates of the Ras/Raf/MEK/ERK cascade and the PI3K cascade respectively. These studies were conducted on $LSL\text{-}K\text{-}ras^{G12D}$;*Amhr2-Cre* knock-in and $LSL\text{-}K\text{-}ras^{G12D}$;*Cyp19-Cre* transgenic mouse models. Results showed that engineering Ras to be constitutively active causes an ovulatory malfunction. Possible reasons include the formation of tumour like follicles, follicles with odd shaped oocytes and abnormal protein and mRNA expression, reduced oocyte number, down regulation of gonadotrophin receptors and or the up regulation of the *Mkp-3* gene a phosphatase and newly suspected negative control component of the Ras/Raf/MEK/ERK pathway.

Control of the PI3K cascade is critical to maintaining the proliferative and cell survival balance. PTEN is a negative regulator involved in the control of the PI3K pathway. Thus the secondary objectives of this study were to study the effect of a *Pten* conditional knock out on ovarian morphology and to study the effect of a *Pten/K-ras* double knock out on ovarian morphology using $Pten^{flox/flox}$;$Amhr2^{Cre/+}$ and $Pten^{flox/flox}$;$K\text{-}ras^{flox/+}Amhr2^{cre/+}$ mouse models respectively. Conditional *Pten* knock out morphology studies demonstrated a luteal cell pre tumour phenotype and the *K-Ras/Pten* double knock out studies presented with thecal cell thickening suggesting that both the *Pten* and *K-ras* gene products work together to augment signalling control and uphold a normal ovarian physiology.

DECLARATION

I certify that this thesis, which I now submit for examination for the award of MPhil, is entirely my own work and has not been taken from the work of others save and to the extent that such work has been cited and acknowledged within the text of my work.

This thesis was prepared according to the regulations for postgraduate study by research of the Dublin Institute of Technology and has not been submitted in whole or in part for an award in any other Institute or University.

The work reported on in this thesis conforms to the principles and requirements of the Institute's guidelines for ethics in research.

The Institute has permission to keep, to lend or to copy this thesis in whole or in part, on condition that any such use of the material of the thesis be duly acknowledged.

Signature _Nicola Gately_ Date

        Candidate

TABLE OF CONTENTS   **Page No.**

7) BIBLIOGRAPHY 82

ACKNOWLEDGEMENTS

ABBREVIATIONS

AC-Adenylate cyclase

ADAMTS-1- a disintegrin-like and metallopeptidase with thrombospondin motifs-1

AREG- amphiregulin

CA- constitutively active

cAMP- cyclic adenosine monophosphate

CBP- CREB binding protein

CDKI- cyclin dependent kinase inhibitor

CKO-conditional knock out

CL- corpus luteum

COC- cumulus oocyte complex

Cox-2- cyclo-oxygenase enzyme 2

CRE- c AMP response element

CREB- c AMP response element binding

CREB-CRB- CREB binding protein

CYP19- aromatase

DAX-1- Dosage sensitive sex reversal-Adrenal hypoplasia congenita gene on X chromosome, gene *1*

eCG-equine chorionic gonadotrophin

E-estradiol

EGF-Epidermal growth factor

EGFR-Epidermal growth factor receptor

EPACS-exchange proteins activated by cAMP

ERK- extracellular signal related kinase

FOXO 1a- forkhead transcription factor 1

FSH- Follicle stimulating hormone

FSHR- follicle stimulating hormone receptor

GAP-GTPase activating protein

GC's – granulosa cells

GDP-guanosine diphosphate

GEF's- guanine nucleotide exchange factors

GF's- growth factors

GLUT-1- glucose transporter-1

GnRH-gonadotrophin releasing hormone

GPCR's- G protein coupled receptors

GSK-3β- Glycogen synthase kinase 3 beta

GTP-guanosine triphosphate

HA- hyaluronic acid

HAS-2-hyaluronic acid synthase 2

hCG- human chorionic gonadotrophin

IGF-1-Insulin like growth factor 1

IGF-1R- insulin like growth factor 1 receptor

LH- lutenising hormone- (hCG analogue)

LHR- lutenising hormone receptor

LIF- lymphocyte inhibiting factor

LRH-1- liver receptor homologue 1

MAPK- Mitogen activated protein kinases

MKP-3/ Mkp-3 (protein/gene- or DUSP 6) - dual specific phosphatase

NRTK's non- receptor tyrosine kinases

PDK 1-phosphinositide dependant protein kinase 1

PH domain- pleckstrin homology domain

PI3K-Phosphoinositide-3 kinase

PKA- protein kinase A

PKB- protein kinase B

PMSG- Pregnant mare serum gonadotrophin- (FSH analogue)

PR- progesterone receptor

PRKO-progesterone receptor knock out

Ptd Ins 3,4,5 P$_3$ or PIP$_3$- phosphatidylinositol 3, 4, 5 triphosphate

Ptd Ins 4,5 P$_2$- phosphatidylinositol 4, 5 diphosphate

Pten- Phosphate and tensin homologue (gene)

PTEN- phosphate and tensin homologue (Protein)

P 450 SCC/ *P450 SCC*- P450 side chain cleavage (protein/mRNA)

ras (gene)- rat sarcoma homologue gene

RAS/Ras- rat sarcoma homologue protein

RTK's- receptor tyrosine kinases

SCC- cholesterol side chain cleavage (p450 enzyme)

SF-1 -steroidogenic factor 1

SFK's- Src family of tyrosine kinases

Sgk- serum glucocorticoid kinase

SRC- Rous sarcoma oncogene

Tcf/Lef -T-Cell factor/ Lymphoid enhancer factor

TGF-β- transforming growth factor beta

Versican/ *Versican*- Versican (Protein/mRNA)

INTRODUCTION

1.1) FEMALE REPRODUCTION AND OVARIAN PHYSIOLOGY

The ovaries are a pair of female reproductive organs known as the gonads. They are located in the pelvis, one on each side of the uterus. The functions of the ovary include production of the gametes "oogenesis" and secondly production of the female hormones, "steroidogenesis" to augment the oestrous cycle and to prepare the uterus for pregnancy and the breast for lactation (www.lab.anhb.uwa.edu.au/mb140/corepages/femaleRepro/femaleRepro.htm). The reproductive processes in female mammals are characterized by cyclic alterations in the female tract and sexual receptivity. The recurrent period of receptivity, or "heat" is called Estrus. The oestrous cycle of the mouse lasts 4-6 days, this is substantially shorter to the human primate equivalent called the menstrual cycle, which lasts on average 28 days (*Fig.1.1a*). Mice are polyestrous animals with many cycles recurring throughout the year. The cycle involves the whole of the reproductive tract, this includes the ovary, uterus and vagina. It is possible to determine the sexual status of the female mouse by examination of vaginal fluid smears (*Fig.1.1b*) (www.embrology.med.unsw.edu.au/ otherEmb/mouse2.htm).

Fig. 1.1a. **THE HUMAN MENSTRUAL CYCLE**
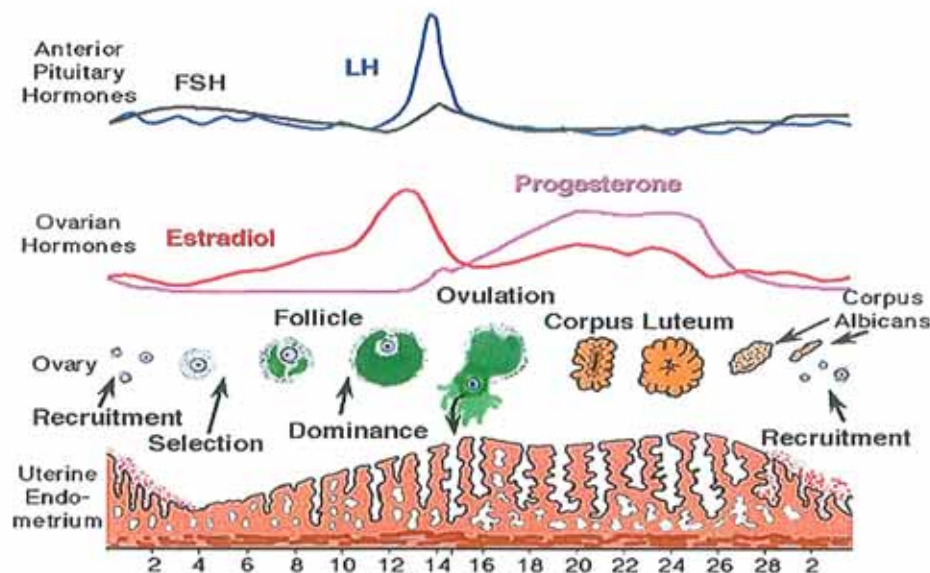
www.wisc.edu/ansci_repro/lec_11/menstrual.jpg

Fig.1.1b. THE MOUSE ESTROUS CYCLE

STAGE	OVARY	UTERUS	VAGINA	SMEAR
Diestrus	Small follicles are present with large corpora lutea from the former ovulation. These secrete for a very short time Unless pregnancy Or pseudopregnancy intervene	Small and anaemic, low motility, lumen small and slit-like. Cells of the uterine mucosa columnar; polymorphonuclear leucocytes in stroma; endometrial glands collapsed and atrophic.	The epithelium is thin and mitotic figures are infrequent. Leucocytes abundant in the stroma migrate through the epithelium into the vaginal lumen.	Stringy mucous in which are entangled many leucocytes and a few nucleated epithelial cells.
Proestrus	Some follicles grow rapidly.	Becomes more vascular, water content increases and the organ distends. Contractility is more pronounced. Epithelial cells become higher (continuing into estrus). Leucocytes disappear from mucosa. Endometrial glands hypertrophy.	Epithelum thickens, numerous mitoses in inner layers. Old layers of epithelium line the lumen. Leucocytes no longer migrate through the epithelium. Superficial epithelial cells slough off into lumen.	Largely small, round, nucleated epithelial cells, singly or in sheets. None to few leucoytes
Estrus	Ovulation in the rat is spontaneous and occurs about 10 hours after the beginning of estrus. "Heat" (receptivity) lasts about 13 hours. Usually 10-20 eggs ovulated each time.	Gains maximum vascularisation. Epithelial cells reach maximum development. No leucocytes.	Outer layer of epithelial cells become cornified and sloughed into the lumen. In early estrus these cells retain their nuclei, but in later stages no nuclei visible and the cells are irregular, flat, cornified plates. The skin around the vaginal orifice becomes swollen.	Contains hundreds of large cornified cells with degenerate nuclei. Towards the end of estrus the smear becomes "cheesy" - masses of adherent cornified cells.
Metestrus	Many corpora lutea, which secrete only for a very short time, and small follicles.	Epithelium continues vacuolar degeneration and replacement. Leucocytes in stroma. Decrease in size and vascularity.	Deeper layers of the estrous epithelium now line the lumen, the older, superficial layers having become cornified and sloughed off. Reduction of mitotic activity ,leucocytes in stroma & migrating into the lumen	Many leucocytes and a few cornified cells.

www.embrology.med.unsw.edu.au/otherEmb/mouse2.htm

2

1.2) HORMONE DYNAMICS

Cyclic changes in ovarian activity are controlled by the pituitary secretion of FSH and LH (*Fig.1.2*). The production of these gonadotrophins is in turn controlled by the hypothalamus as it analyses hormonal signals relayed from the ovary. During the latter half stages of the oestrous cycle a high output of progesterone and oestradiol acting via the hypothalamus suppresses the pituitary secretion of FSH and LH. On formation and eventual degradation of the corpus luteum, production of oestrogen and progesterone decreases releasing the suppression of pituitary FSH and LH secretion. Ovarian follicles possess a threshold requirement for FSH, when the threshold is overcome growth and eventual oestradiol secretion of a select group of follicles occurs. The hypothalamus detects this oestradiol and recognises that the threshold has been reached. An intermediate level of FSH production must be exceeded before the ovulatory response is stimulated. Likewise a maximum level must not be exceeded as this could result in multiple follicle stimulation and multiple ovulations. This maximum level sits marginally above the threshold so precise feedback control of FSH by oestrogen is employed. The dominant follicle moves favourably towards ovulation, produces a rapid increase in oestradiol, producing cervical mucus and suppressing FSH below the threshold thus removing the support required by less dominant follicles which are competing to ovulate. A fall in FSH switches on the ovarian maturing mechanism in the dominant follicle rendering it receptive to LH. The high oestrogen conditions act by a positive feedback to the hypothalamus to cause the pituitary to release the LH surge to augment ovulation. The formation of the corpus luteum then leads to increases in oestrogen and progesterone to augment changes in the uterus and vagina to facilitate a possible pregnancy. If pregnancy does not occur the corpus luteum degrades and hormone production wanes. However, unlike in the human where lack of pregnancy results in an eventual drop in progesterone leading to menstruation, a shedding of the uterine wall matter, menstruation does not occur in the murine oestrous cycle

(www.billings.ovulation.method.org.au/act/physiol.shtml).

3

Fig.1.2 **HORMONE DYNAMICS**
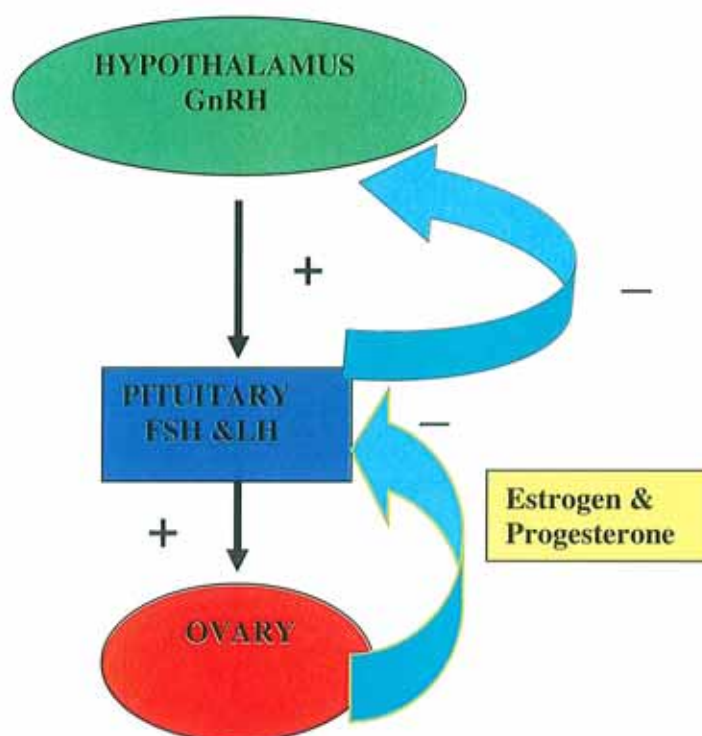
Key: (+) Positive feedback, (-) Negative feedback.

Fig.1.2 Diagram of the positive and negative feedback control mechanisms governing gonadotrophin stimulation and secretion from the hypothalamus, pituitary and ovary. Release of gonadotrophin releasing hormone (GnRH) from the hypothalamus positively stimulates the release of FSH and LH from the pituitary which positively stimulates the ovary into folliculargenesis and ovulation. When GnRH has stimulated sufficient FSH and LH release, the pituitary hormones work back via negative feedback to stop the further release of GnRH. Similarly the release of estrogen and progesterone form the ovary works in a negative feedback manner to control the release of the pituitary hormones.

1.3) OVARIAN PHYSIOLOGY AND HISTOLOGY

The ovarian follicle plays a critical role in female reproduction. The ovarian follicle goes through a series of growth stages during folliculargenesis to ultimately form a mature graffian follicle ready for ovulation. Typically the follicle contains an oocyte surrounded by epithelial-type granulosa cells, a basal lamina and peripheral thecal cells (*Fig.1.3a*). At the first stage of follicular development the primordial follicle is made up of a small oocyte arrested in meiotic prophase and a single layer of follicular squamous cells bound by a basal lamina. The follicle then develops into a primary follicle. The primary follicle is made up of an enlarged oocyte surrounded by a zona pellucida a layer rich in glycosaminoglycans. The membrana granulosa consists of layers of stratified cuboidal epithelial cells

4

whose outmost layer lies on the basal lamina. The inner highly vascularised layer of steroid secreting cells, fibroblasts and collagen fibers form the theca interna of the primary follicle. The theca externa is composed of smooth muscle cells and loose connective tissues. Finally the secondary antral follicles and graafian follicles form. Within these follicles the oocyte enlarges further, it undergoes its first meiotic division and one daughter cell receives the majority of the cytoplasm and becomes the secondary oocyte. It begins the second division and is arrested at metaphase. The other daughter cell receives minimal cytoplasm and becomes the first polar body. Granulosa cells then form in a thickened complex around the oocyte called the cumulus oocyte complex (COC). A hyaluronic acid (HA) rich antrum then surrounds the COC complex to meet the theca cell layers (*Fig.1.3a*) (www.lab.anhb.uwa.edu.au/mb140/corepages /femaleRepro/female

Repro.htm).

Fig.1.3a OVARIAN HISTOLOGY

Primary follicle

Oocyte

Cumulus cells

Granulosa Cells

HA rich Matrix

Thecal cells

Secondary follicle
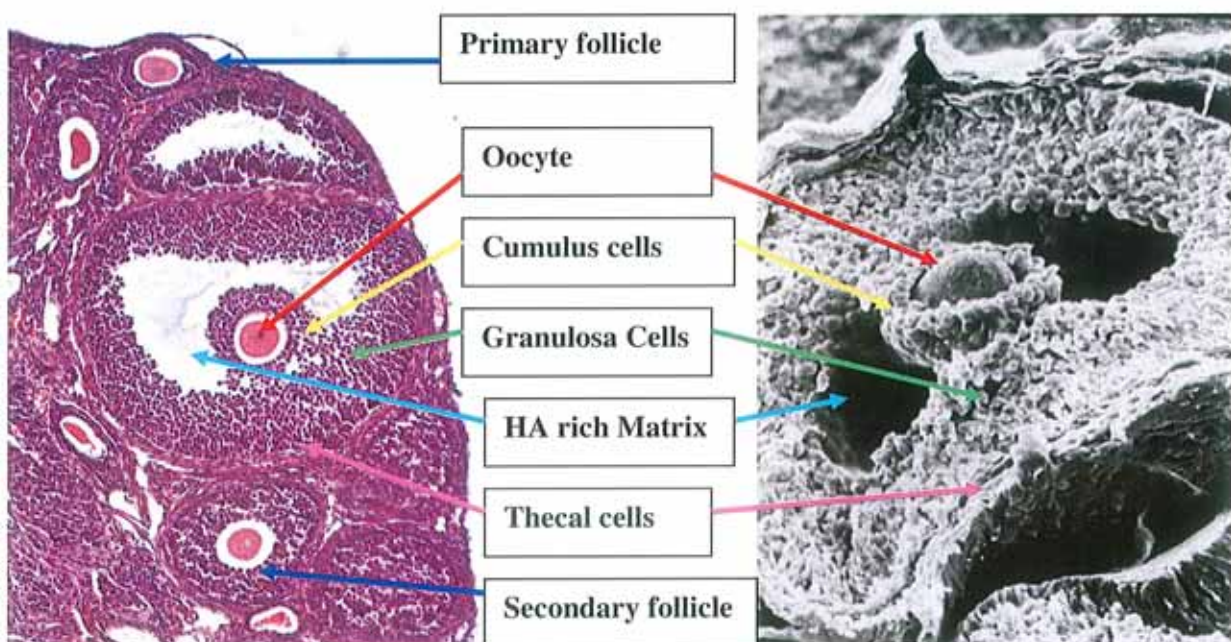
Fig.1.3a The diagram shows the histology of the pre-ovulatory follicle. It shows the stages of folliculargenesis with increased layering of granulosa cells during maturation from the primary follicle, secondary follicle and the mature follicle. In the more mature follicles it demonstrates the outer thecal cells and shows the oocyte surrounded by the Cumulus-Oocyte Complex made up of a hyaluronic acid and granulosa cell matrix which provides a structural support and an optimal communicative/signalling microenvironment for the ovarian cells to communicate.

Follicular maturation is cyclic due to the cyclic recruitment of immature follicles by the gonadotrophin follicle stimulating hormone (FSH) (Hunzicker-Dunn *et al* 2006). Typically only a single follicle sustains its inherent gametogenic potential and goes to maturation whereas the other follicles become atretic. The chosen follicle is derived from a group of growing follicles drawn from a pool of non proliferating early follicles in fetal development. Follicular selection is dependant upon the interplay between gonadotrophin hormone secretion, steroid production and maturation specific alteration in the responsiveness of the ovary to gonadotrophins (Hadley *et al* 2007).

Fig.1.3b **HORMONAL CONTROL OF FOLLICULARGENESIS AND OVULATION**
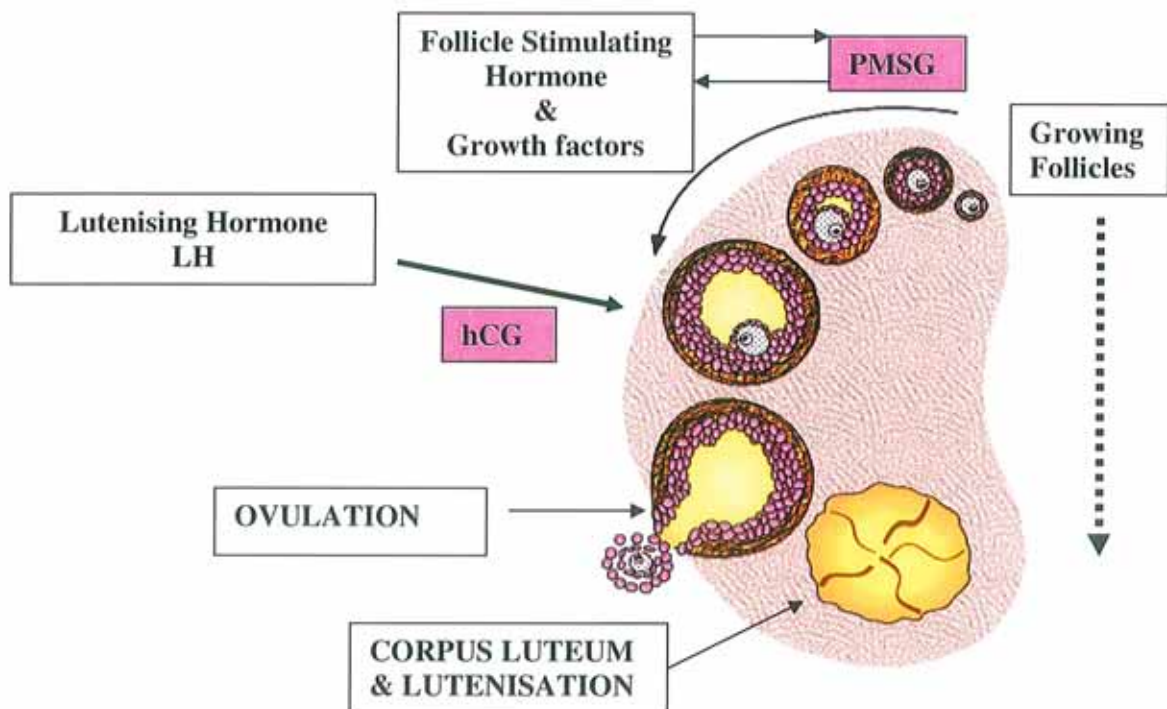
Fig.1.3b The diagram demonstrates pregnant mare serum gonadotrophin (PMSG) a Follicle Stimulating Hormone (FSH) analogue augmenting folliculargenesis. At a critical stage of folliculargenesis when the follicle is mature enough the human chorionic gonadotrophin hormone (hCG) a Lutenising hormone (LH) analogue augments ovulation.

FSH mediates the growth, proliferation and differentiation of ovarian follicles that is folliculargenesis characterized by increased vascularisation of the theca iterna layer, formation of the fluid filled atrum within the maturing follicle and development of the two classes of granulosa cell, the outer mural granulosa cell layer and the inner oocyte surrounding cumulus layer (Hunzicker-Dunn *et al* 2006) and (Richards *et al* 1998).

6

At a critical follicular maturation stage on acquiring the lutenising hormone receptor (LHR), Lutenising hormone (LH) drives ovulation and lutenisation of the follicle that is, matrix expansion of the cumulus oocyte complex, rupture and liberation of the ovum from the follicle and terminal differentiation of the granulosa cells to luteal cells to form the corpus luteum (*Fig.1.3b*) (Gonzalez-Robayna IJ *et al* 1999), (Richards *et al* 1998),(Hadley *et al* 2007), (Russell D L *et al* 2003).

1.4) STEROIDIGENESIS

Steroidogenesis is crucial to folliculargenesis and ovulation. The biosynthesis of steroid hormones requires a battery of oxidative enzymes located in both the mitochondria and endoplasmic reticulum. The rate-limiting step in this process is the transport of free cholesterol from the cytoplasm into the mitochondria (Breckwoldt M *et al* 1996). Within the mitochondria, cholesterol is converted to pregnenolone by an enzyme in the inner membrane called CYP11A1 or P450 side chain cleavage. Pregnenolone itself is not a hormone, but is the immediate precursor for the synthesis of all of the steroid hormones. Thus, within the ovarian granulosa cells p450 SCC enzyme works to convert cholesterol to pregnenolone where pregnenolone serves as a substrate for vital ovarian progesterone and androgen production.

During the follicular phase estrogen is the main steroidal product of the ovary. As follicular maturation progresses, induction and activation of the granulosa cell p450 aromatase enzyme or (CYP19) increases the ability of the granulosa cells to aromatase and convert the thecal cell derived androgen to estrogen. In the ovary estrogen is responsible for control of ovulatory cyclicity and ovum maturation. During the terminally differentiated luteal phase progesterone is the predominant hormone post ovulation. During the pre-ovulatory LH surge, LH acts directly on the granulosa cells and initiates lutenisation and enhancement of progesterone production and secretion. Thus, progesterone represents an early step in the biosynthesis of estrogen and androgen in the thecal cell (*Fig.1.4*) (Hadley M.E *et al* 2007). The corpus luteum is deemed to be the main supplier of progesterone. Luteal cells are the main source of progesterone following lutenisation. Unusually apoptotic cells are still active in steroidogenesis until total collapse.

Progesterone's main role does not impinge on the ovary; its main role is for the growth and development of the oviduct for ovum transport, to prepare the tract for implantation and in rodents induces sexual receptivity (Breckwoldt M *et al* 1996) (Hadley M.E *et al* 2007).

Fig.1.4 THE MAJOR PATHWAYS IN STEROID BIOSYNTHESIS

www.vivo.colostate.edu/hbooks/pathway/endocrine/basics/steroiogensis/htm

1.5) OVARIAN GENES

The physiological responses to FSH are accomplished by the activation of more than 100 target genes in the granulosa cells (Hunzicker-Dunn *et al* 2006). Thus, at the cellular level follicular selection, folliculargenesis and ovulation are dependant on the interactions of steroid/gonadotrophin hormone signalling pathways in addition to peptide signalling pathways where these multiple pathways cross talk and inter communicate to induce genes that promote granulosa cell proliferation, survival, ovulation and apoptosis (*Fig.1.5*) (Richards *et al* 1998)(Richards,2001 a &b).

8

Fig.1.5 **THE COLLABORATIVE IMPACT OF PEPTIDE AND HORMONE SIGNALING ON OVARIAN PHYSIOLOGY.**
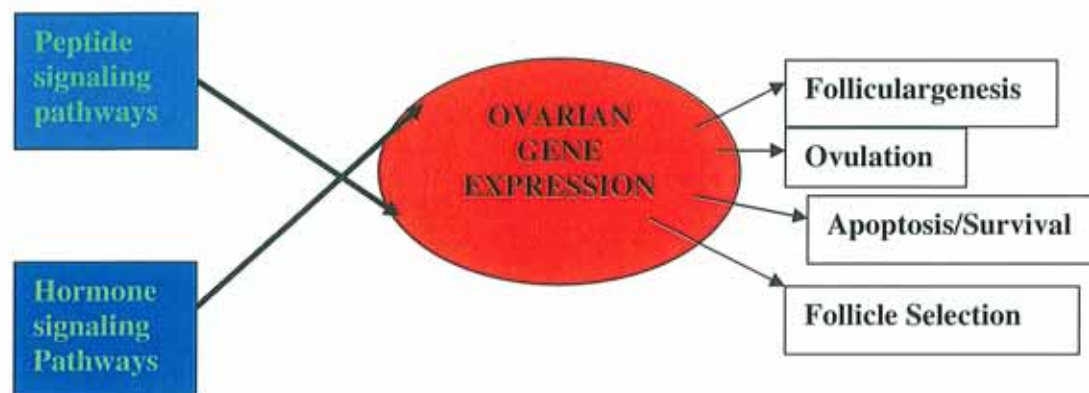
Fig.1.5 The diagram represents the importance of hormonal and peptide signalling pathway synergy whereby peptides and hormones activate pathways that cross talk in order to maintain ovarian gene expression control and ovarian function.

Like FSH, the LH surge initiates the expression of critical genes for ovulation, terminal differentiation and apoptosis. LH down regulates genes associated with follicle function like aromatase and cyclin D2 and transiently induces genes required for ovulation like the progesterone receptor (PR). During lutenisation, granulosa cells become refractory to further cAMP stimulation and genes such as *Side Chain Cleavage p450* enzyme are constitutively expressed at elevated levels (Richards, 2001a) (Robker RL *et al* 1998 a&b) (Gonzalez-Robayana IJ *et al* 1999). Additionally products of some other FSH and LH induced genes selectively impact the formation and expansion of the cumulus oocyte complex (COC) matrix essential for extrusion of the oocyte. Such inducible factors involved in ovulation include, Cox-2, an enzyme vital for the production of prostaglandin E2, an essential factor for complete cumulus expansion and the progesterone receptor to mediate the effects of progesterone. Cox-2 and PR are confirmed as essential ovulatory genes as both progesterone receptor knock out and Cox-2 -/- mice are anovulatory. Other inducible factors include the HAS-2 gene that mediates matrix hyaluronic acid (HA) production and TSG-6, a hyaladherin that binds HA and Versican (Ochsner *et al* 2001) (Russell D.L *et al* 2003) and (Richards *2001a*). Versican a vital ovarian matrix protein and ADAMTS-1 a PR dependent protease is hypothesized to be a Versican substrate to degrade the follicle wall and augment rupture.

9

During ovulation the production of a specialized hyaluronan HA rich matrix cross linked by associated HA binding factors causes expansion of the cumulus oocyte complex (COC). HA production and stabilisation are essential for successful ovulation. Versican is one such HA binding protein playing an important role in morphogenesis. Versican isoforms V0, V1 and V3 are detected in the granulosa cells of primary and growing follicles, the isoforms are LH induced in mural granulosa cells and are most intensely detected in the COC matrix of ovulatory follicles (Russell DL et al 2003). In addition to binding HA and cross-linking of the expanding cumulus matrix Versican has the potential to mediate several of the functional properties of the ovulating follicle. Properties such as maintenance and remodeling of the ovarian matrix and follicle wall, promotion of cell detachment and migration during vascularisation of the corpus luteum. However, the functional activity of Versican may depend on proteolytic cleavage, as studies by Russell DL et al 2003 have shown Versican to be a substrate to the protease ADAMTS-1. Where ADAMTS-1 is deficient as in the progesterone receptor knock out mouse (PRKO) mouse it does not alter the localization of immunoreactive Versican, however ADAMTS-1 may merely generate products with additional or specific functions to the intact molecule (Russell D.L et al 2003).

1.6) PEPTIDE SIGNALING PATHWAYS

Peptide signaling pathways include those stimulated by Insulin like growth factor-1(IGF-1). IGF-1, estradiol and FSH comprise a major regulatory system where IGF-1 has the ability to enhance FSH action in the granulosa cells. By complex mechanisms IGF-1 is known to enhance the FSH induced enhancement of progesterone, estrogen and cAMP production and LH receptor (LHR) induction (Hadley et al 2007). Other peptide signaling initiators include Wnts/Frizzleds, fibroblast growth factor (FGF) and transforming growth factor-beta (TGF-B) family members which include activin and inhibin. Likewise, the orphan nuclear receptors, steroid receptors and their ligands colloborate with these multiple signalling cascades to augment ovarian function. Each of the above factors is expressed and acts in a cell specific manner at defined stages of follicular growth (Richards et al 1998).

These factors act by autocrine, paracrine and intracrine mechanisms supplementing endocrine pituitary gonadotrophin action (Richards J.S *et al* 2002a&b). Their subsequent activated target genes work in synergy with hormone signalling cascades to potentiate folliculargenesis and steroidogenesis.

In comparison the Wnt/Frizzled pathways govern ovarian embryogenesis and possibly function to support ovulation and lutenisation processes which are chiefly governed by gonadotrophin and peptide directed pathways. Wnts are secreted locally and act upon their GPCRs called Frizzleds to activate the canonical pathway which leads to the hyperphosphorylation of the cytoplasmic protein dishvelled (Dvl) and subsequently glycogen synthase kinase 3 beta (GSK-3beta) leading to the release of beta catenin. This then dimerises with the T-Cell factor/Lymphoid enhancer factor (Tcf/Lef) family of transcription factors to regulate genes like c-myc and DAX1 (*Dosage sensitive sex reversal - Adrenal hypoplasia congenital gene on the X chromosome, gene 1*). It is hypothesized that the effectors of the Wnt/Frizzled pathway change as the follicle terminally differentiates to luteal cells and so controls patterns in gene expression. However one such Wnt induced on the LH surge known as Wnt-4 is shown to regulate DAX-1 in the ovary. Beta catenin can enhance the transcription factor SF-1, transactivation of DAX-1 and as DAX-1 is a co-repressor to the ophan nuclear receptor SF-1, DAX-1 may antagonize genes regulated by SF-1 like *Fshr*, *p450 SCC* and *CYP19*. As LRH-1 is hypothesized to work in a similar manner in steroidogenesis as its family member SF-1, thus DAX-1 may impinge on the functions of LHR-1 also (*Fig.1.6*) (Richards *et al* 2002b).

Fig.1.6 THE Wnt ACTIVATED PATHWAYS
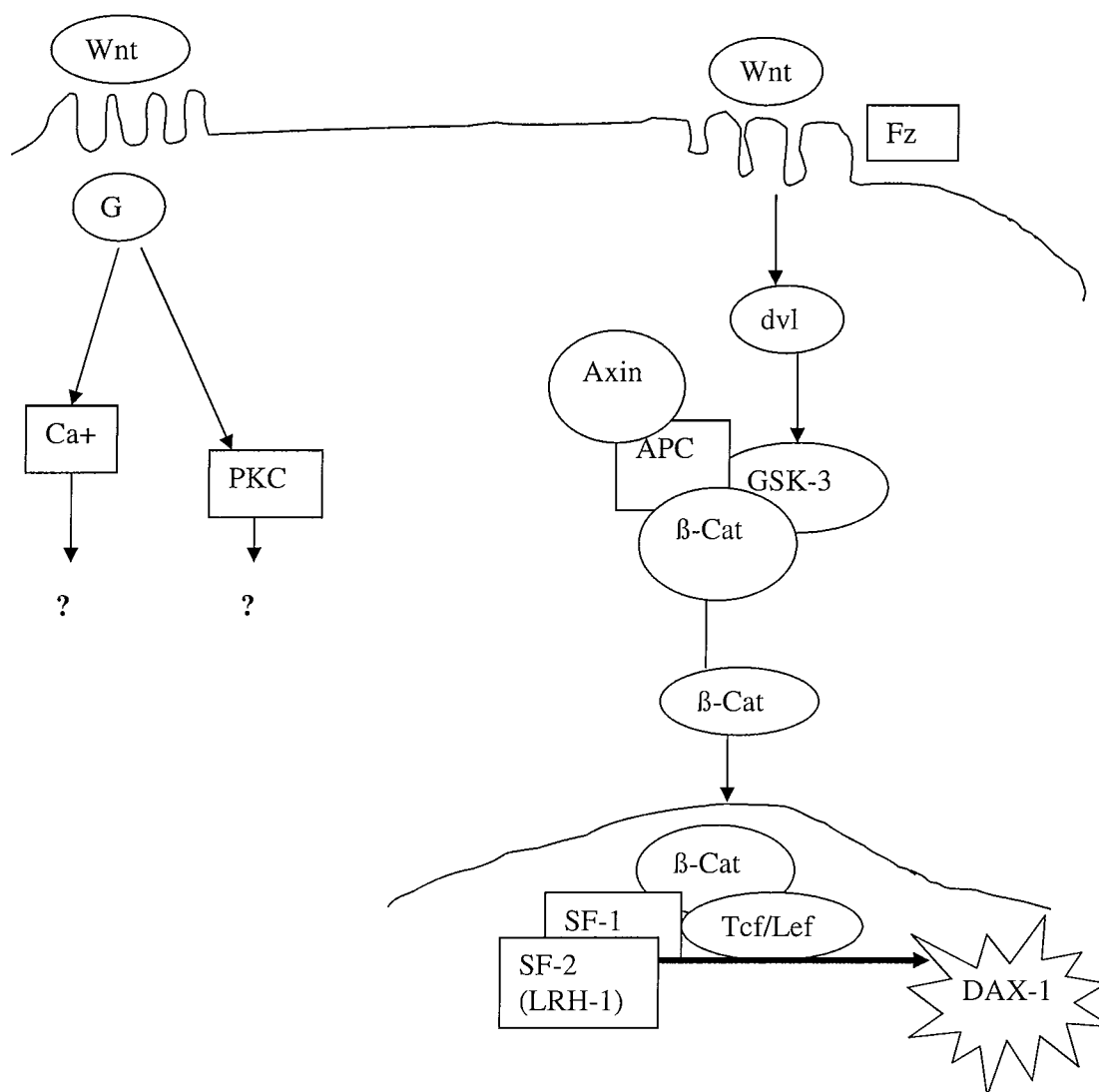
(Richards *et al 2002b*)

Fig.1.6 Diagram showing Wnt signalling activating the canonical pathway. Activation of the canonical pathway is hypothesized to play a role in the ovary whereby activation of DAX-1 via Wnt-4 antagonises vital ovarian genes regulated by the transcription factor SF-1 such as the *Fshr* gene and the rate limiting enzyme *p450 SCC* gene. Wnt signaling is shown to be diverse as it demonstrates activation of the protein kinase C (PKC) pathway, and calcium activated pathways in addition to the canonical pathway.

Liver receptor homologue–1 (LRH-1) a well known family member of Steroidogenic Factor-1 (SF-1) is an orphan nuclear hormone receptor and transcription factor vital for organogenesis (Hinshelwood *et al* 2005). Both are potential regulators of granulosa cell gene expression and are regulated under different hormone conditions. At a biochemical level both LRH-1 and SF-1 are shown to activate consensus motifs in the promoters of aromatase and other steroidogenic enzyme genes similarly. SF-1 is expressed in the granulosa cells and expression is highest in ovarian interstitial and thecal cells.

Conversely, LRH-1 is specifically expressed in the granulosa and luteal cells and not in the theca cells. However, *Lrh-1* mRNA is expressed at higher levels in the ovary then the liver and other tissues and it is specifically expressed in the ovarian granulosa and luteal cells. Additionally it is known to activate liver P450 cytochrome enzymes. Therefore it is hypothesized that LRH-1 may control target gene expression in granulosa cells in association with SF-1. It is now known that the PKA and p38 MAP kinase pathways more than the P13-Kinase pathway impact the transcription of LRH-1 reporter genes in granulosa cells (Falender A.E *et al* 2003).

1.7) OVARIAN BIOCHEMISTRY

FSH stimulates growth and differentiation of the pre-ovulatory follicle. However FSH induces multiple signalling cascades responsible for the induction of gene expression in target granulosa cells, for the coordinated induction of steroidogenic enzymes, the LHR, cell cycle regulatory proteins among other regulatory factors (Hunzicker-Dunn *et al* 2006). The rapid activation via a series of phosphorylation events of multiple signalling molecules impacts upon the diverse effects in granulosa cells. FSH orchestrates the coordinate activation of three diverse membrane associated cascades, Adenylate Cyclase (AC), RAS (rat sarcoma homologue) and the SRC (Rous sarcoma oncogene) family tyrosine kinases (SFKs) that converge downstream to activate specific protein kinases ERK1/2 (Extracellular Signal Related Kinase 1/2) and protein kinase B (PKB) to control granulosa cell function and differentiation (*Fig.1.7*) (Wayne C.M *et al* 2007).

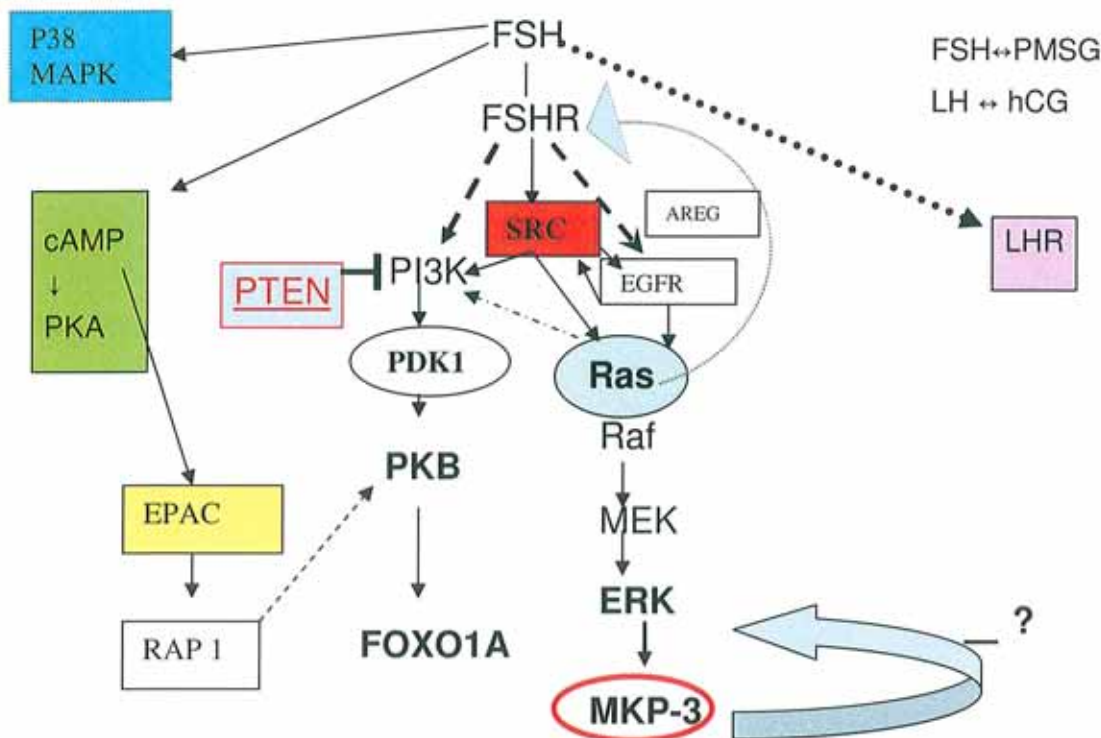*Fig.1.7* DIAGRAM OF PI3K AND RAS SIGNALING PATHWAYS

Fig.1.7. Diagram showing follicle stimulating hormone (FSH) stimulating the PI3K and Ras/Raf/MEK/ERK pathways in a PKA independent manner via signalling through the FSH receptor (FSHR) and the SRC molecule a member of the SFKs. SRC kinase activity then activates the MAPK cascade Ras/Raf/MEK/ERK directly or indirectly by activating the EGFR. Simultaneously FSH can induce the expression of EGFR ligands such as amphiregulin (AREG) to interact with the EGFR to activate Ras.Ras activation, activates MKP-3 a phosphatase that is hypothesized to dephosphorylate ERK to negatively regulate the Ras cascade (blue arrow). Ras is also hypothesised to work upstream to the level of the FSH receptor (blue dotted arrow) in addition to activating Ras down stream effectors. The PI3K cascade is also shown to be activated by the same cAMP/PKA independent pathway (FSH-FSHR-SFK-PI3K) and is shown to be negatively regulated by PTEN. FSH mediated signalling through SRC activates PI3K and results in the phosphorylation of the down stream intermediates PDK1 (3-phosphoinositide-dependent kinase-1), protein kinase B (PKB) and the FOXO1A (forkhead transcription factor).However PKB activation is independent of RAS. Ras can also support the activation of PI3K and PKB (dashed arrow). FSH activation of the EPAC1-RAP1 pathway is shown to support the activation of PKB (dashed arrows).

FSH signals via a seven transmembrane FSH receptor which is found exclusively on the granulosa cells. Approximately 1600-4500 receptors per cell are present (Hunzicker-Dunn *et al* 2006). The FSH receptor is a G-protein coupled receptor that activates adenylate cyclase to increase the production of the second messenger cAMP. cAMP then activates the cAMP dependent kinase, protein kinase A (Richards, 2001b).Traditionally signalling through the cAMP /PKA pathway alone was thought to account for all genes up regulated and down regulated during folliculargenesis and ovulation. However, recent studies have demonstrated that there are new signalling pathways and mechanisms existing for hormones, growth factors and cAMP action in ovarian cells (Richards 2001).

New evidence shows that activation of SRC (a member of the SRC family kinases –SFKs), Ras and epidermal growth factor receptor (EGFR) are crucial for granulosa cell differentiation (*Fig.1.7*) (Wayne *et al* 2007).

The cAMP/PKA pathway was shown to mediate specific signalling events, including the transcription of specific genes, via the cAMP regulatory element binding protein-CREB binding protein complex (CREB-CBP) which involves CREB binding cAMP response elements (CREs) in proximal promoter regions of specific genes such as aromatase and inhibin to facilitate transcription. Recent studies show that PKA is not the sole intracellular target of cAMP (Richards 2001b). Elevated levels of cAMP activates other transcription factors apart from CREB in the ovary such as the Estrogen Receptor (ER) α and β. Molecular events such as phosphorylation of PKB an intermediate of the PI3K cascade and phosphorylation of ERK1/2 an intermediate of a MAPK cascade are known to occur independently of PKA activation (Gonzalez-Robyana I-J *et al* 2000). Other targets for mediating cAMP action are known as the EPACs (exchange protein activated by cAMP) (Richards 2001b).These cAMP bound proteins have been shown to have an affinity for cAMP equivalent to that of the regulatory subunit of type 1 PKA. On binding cAMP, EPACS activate small GTP binding proteins RAP1/2 and possibly activate RAS by exchanging bound GDP for GTP. EPAC1/RAPGEF3 and EPAC2/RAPGEF4 are two such EPACs found in the granulosa cells however EPACs are not the key mediators by which FSH mediates PKA independent signalling. Instead EPACs are proposed to exert a supportive role to enhance the true PKA independent mechanisms (*Fig.1.7*) (Wayne *et al* 2007). It is therefore critical to understand how the endogenous levels and activities of small GTPases such as Ras which are activated by EPACS interact with their presumed target kinase in response to different hormone conditions and elevated levels of cAMP in order to mediate signalling. (Richards 2001b) (de Rooij *et al* 2000) (Kawasaki *et al* 1998).

Additionally, new families called activators of G protein signalling have been proposed to stimulate G proteins independently of receptor activation. It is also hypothesized that the $\alpha\beta\gamma$ subunits of the GPCRs have functions beyond regulating the $G\alpha$ subunit of the GPCRs and thus are also involved in directing alternative signalling pathways. It is known that $\beta\gamma$ proteins can activate the $p100\gamma$ isoform of PI3K therefore linking the GPCR and PI3K pathways (Hunzicker-Dunn *et al* 2006).

In summary, FSH stimulates the Ras/Raf1/MEK/ERK1/2 cascade, the p38MAPK and PI3K/PKB pathways in a unique time dependant and synergistic manner. FSH can rapidly activate the EPAC1-RAP1 pathway and simultaneously activate the SRC/EGFR/RAS mediated pathway. FSH mediated activation of RAP1 requires cAMP mediated activation of EPAC and once activated RAP1 can mediate its supportive role in the PKA independent phosphorylation of PKB/FOXO. It is in the same way through the activation of RAP1 that p38 MAPK and ERK kinases may be activated. In contrast FSH activation of RAS is suspected to involve multiple factors. FSH activation of RAS requires SRC family tyrosine kinase (SFK) and EGFR tyrosine kinase activities. The EGFR can be activated directly by SFKs and or by FSH induction of EGF like factors, including amphiregulin (AREG). SFKs are key components for the activation of both the RAS and PI3K cascades and so demonstrate themselves as key components in PKA independent mediated signalling (Wayne *et al* 2007).

1.8i) THE PI3K CASCADE AND REGULATION

Activation and potentiation of the PI3K/PKB cascade can come from a number of sources, FSH/PKA dependant mechanisms, FSH/IGF-1 stimulation and the FSH/PKA independent mechanisms. Ras can support the activation of PI3K and downstream PKB. However, dominant negative expression of Ras whereby Ras has a dominant loss of function mutation does not eliminate FSH activation of the PI3K pathway (Wayne *et al* 2007). Mutant K-Ras can directly activate PI3K however, it is unknown if normal Ras has this ability (Campbell *et al* 2007). Activation of the PI3K cascade involves recruitment of PI3K to the cell surface receptor where it phosphorylates phosphatidylinositol 4, 5 diphosphate (Ptd Ins 4, 5 P2) to generate phosphatidylinositol 3, 4, 5 triphosphate (Ptd Ins 3,4,5 P3). Ptd Ins 3, 4, 5 P3 acts as a second messenger to bind pleckstrin homology domain (PH) domain

containing proteins such as PDK1 a down stream kinase essential for the mediated activation of the anti-apoptotic factor PKB. Elevated levels of this second messenger elicit cell behaviours that favour oncogenesis (Sulis M.L *et al* 2003) (Yamada *et al* 2001). Under such conditions PDK1 mediates the over activation of downstream kinases such as PKB. PKB is a terminal kinase in a cascade that controls cell survival and proliferation thus sustaining folliculargenesis. Many substrates phosphorylated by PKB are inactivated or degraded such as BAD, Caspase 9 and the forkhead family of transcription factors (Richards *et al* 2002). Phosphorylation of FKHR (FOXO-1) by PKB restricts nuclear localization of these factors, thus, impeding transcriptional activation of FOXO target genes. Three genes hypothesized to be regulated by FKHR include the pro apoptotic Fas L, p27kip an inhibitor of the cell cycle and IGF protein-1, a presumed inhibitor of IGF-1 (Richards JS *et al* 2002a). FKHR is highly and specifically expressed in the granulosa cells of the pre-ovulatory follicle thus suggesting a key role in promoting follicle growth. Efficient expression and phosphorylation is dependant on the precise interplay between Estradiol, IGF-1 and the gonadotrophins where the function of FKHR and other members of the FOXO family are said to be dependant not only on their transcriptional activites but is also dependant on the hormonal milieu, cell context and the levels of pro and anti apoptotic factors and so the different forkhead proteins may have a different function depending on cell type and differentiation stage. Estradiol causes the coordinated induction of FKHR mRNA and up regulates other components of the IGF signaling pathway including IGF-1R B subunit and the GLUT-1 transporter thus indicating that it enhances granulosa cell function in hypophysectomised rats by regulating three targets that control cellular energy flow, glucose metabolism and cell survival (Richards *et al* 2002a).

Additionally, IGF-1 helps maintain expression of the estrogen receptor beta thus suggesting that both Estradiol (E) and IGF-1 comprise of an autocrine regulatory system in granulosa cells promoting cell survival and proliferation. In contrast to basal levels of FSH and Estradiol, LH decreases the expression of FOXO.

So granulosa cells become resistant to apoptosis insult when stimulated to undergo lutenisation. In this case factors impacting on proliferation like E and IGF-1 are lost and pro-apoptotic factors like FKHR and Fas L are lost. Factors hypothesized to augment lutenisation such as Sgk, p21 CIP, Jun D and FKHRL1 are acquired (*Fig.1.8i*) (Richards *et al* 2002a).

Fig.1.8i THE INTERPLAY OF FSH AND IGF-1 SIGNALING ON GRANULOSA CELL PROLIFERATION AND DIFFERENTIATION.

Fig.1.8i. Diagram showing the FSH-FSHR mediated activation of cAMP-GEFs to support the PKA independent phosphorylation of PKB/FOXO1A via PI3K activation. Activation of PKB causes phosphorylation and inactivation of FOXO1A thus impeding activation of the pro apoptotic target genes such as Fas L thus promoting survival and proliferation. Additionally the IGF-1-IGF-R autocrine signaling pathway is shown to support activation of the PI3K cascade.

1.8ii) PTEN -the negative regulator

PTEN (phosphates and tensin homologue) is a negative regulator of the PI3K (phosphatidyl inositol-3 kinase) cascade. PTEN negatively regulates the PI3K pathway by dephosphorylating the second messenger phosphatidylinositol 3, 4, 5 triphosphate (PIP$_3$). By doing so PIP$_3$ levels and overactive signalling are kept low. *Pten* is a tumour suppressor gene frequently mutated in a variety of human cancers and inactivation of *Pten* in mouse models has confirmed PTEN to be a bona fida tumour suppressor. Thus without PTEN the PI3K pathway is constitutively active thus stimulating uncontrolled cell division, cell size and apoptosis inhibition (*Fig.1.8ii*) (Sulis M.L *et al* 2003).

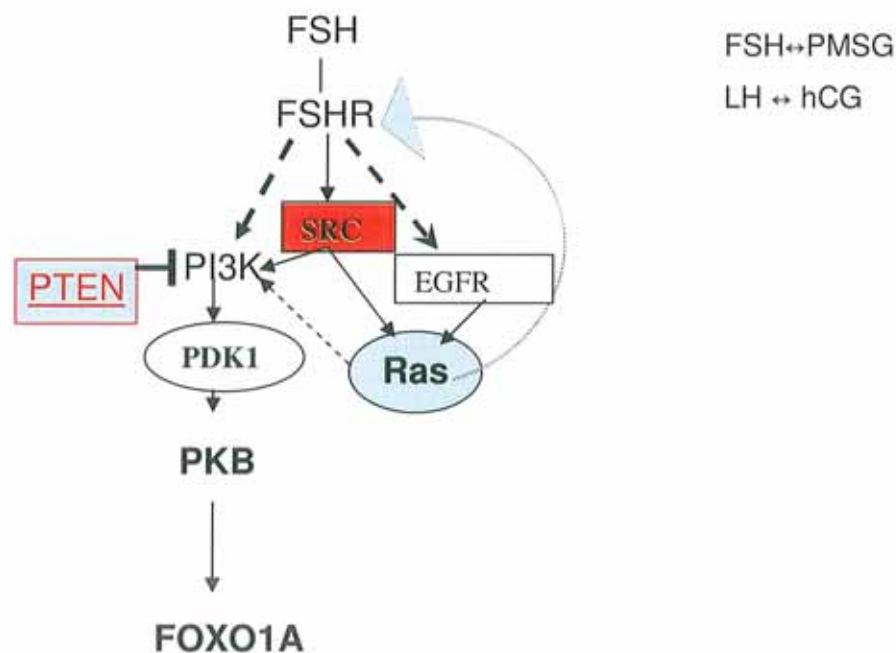*Fig.1.8ii* DIAGRAM OF PI3K AND RAS SIGNALING PATHWAYS

Fig.1.8ii. Diagram showing the PTEN tumour suppressor protein to negatively regulate the survival PI3K pathway. PTEN interacts with the PI3K molecule to prevent phosphorylation and activation of the down stream intermediates PDK1 (phosphinositide dependant protein kinase 1), protein kinase B (PKB) and the forkhead transcription factor FOXO1A.

1.8iii) RAS

Ras is a G protein known as Rat sarcoma homologue and a well known proliferative factor where oncogenic Ras is associated with approximately 20-30% of all human cancers (Bos 1989). Ras G proteins are positioned on the inner surface of the plasma membrane and serve as binary molecular switches to transduce extracellular ligand mediated stimuli such as growth factors, cytokines and hormones. These stimuli hit receptor tyrosine kinases (RTK's), non receptor tyrosine kinases (NRTK's) and GPCRs to mediate signal transduction that influences growth differentiation and apoptosis. Ras bioactivity is controlled by a regulated GDP/GTP cycle (*Fig.1.8iii*). This cycle is modulated by guanine exchange factors (GEFs), which promote the active GTP state, and GAPs that promote formation of the GDP inactive state (Campbell SL *et al* 1998). In this study the K-Ras isoform was engineered to be made constitutively active. By introducing a glycine to aspartic acid mutation at residue 12 of the *ras* gene, Ras was locked in a constitutively active GTP state and the mutation deemed Ras to be insensitive to GAP stimulation (Bourne *et al* 1990). The determination that mutated *ras* genes were present in a variety of cancers linked the growth promoting effects of mutated Ras to the aberrant regulation of signalling pathways seen in cancer (Tuveson, DA *et al* 2004). Interestingly, gene targeting studies have determined the K-Ras isoform to be essential for normal development in mice as opposed to other H-Ras and N-Ras isoforms (Koera K *et al* 1997). It has been reported that different mutant amino acids in the Ras proteins activate different down-stream signalling pathways and lead to distinct transforming capabilities in human and mouse tumours. (Cespedes *et al* 2006). Some reports show that binding between Ras and down stream Raf is strengthened in the fibroblast cells of the same *K-ras* ^{G12D} knock-in mouse strain (Tuveson *et al* 2004). Other reports suggest that *K-ras* ^{G12D} models induce tumourigenesis by activating PI3K/PKB and p38 MAPK cascades (Cespedes *et al* 2006).

Fig.1.8iii. CELLULAR LOCATION AND ACTIVATION OF THE RAS/RAF/MEK/ERK PATHWAY IN-VIVO
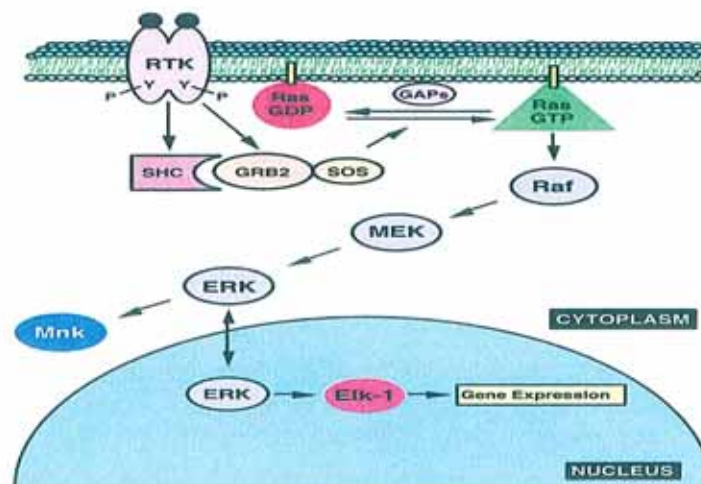
Fig.1.8iii Demonstrates the activation of a receptor tyrosine kinase (RTK) at the plasma membrane. This activates the signalling complex and adapter proteins SHC-GRB2-SOS. This complex in turn switches Ras from an inactive GDP state to an active ATP state however the switch is reversible. Ras activation activates the cytoplasmic MAPK cascade Ras/Raf/MEK/ERK. Activated ERK translocates to the nucleus and impinges on gene expression.

Ras plays a pivotal role in governing FSH mediated signalling as it is a point of convergence for many signaling pathways. It marks the start of the Ras/Raf/MEK/ERK cascade which can be initiated and potentiated through the unique and combined efforts of gonadotrophin and peptide signalling in the ovary. Remarkable evolutionary conservation of the Ras cascade reflects the central role of Ras in diverse organisms. Ras signalling has emerged to involve a complex array of signalling pathways where crosstalk feedback loops, branch points and multi-component signalling cascades impinge on the Ras protein (Campbell *et al* 1998). Ras functions as a relay switch down stream of cell surface receptor tyrosine kinases and upstream of cytoplasmic cascades of kinases the MAPKs (mitogen activated protein kinases). The mechanism by which FSH activates Ras is likely to involve more than one pathway. It is also hypothesized that FSHR like other GPCRs can activate Ras directly as seen in other cells namely male mouse Leydig cells. In Leydig cells the LHR activates Ras and induces phosphorylation of a Ras downstream target, ERK1/2 via a RTK mechanism. This links together the possibility that gonadotrophin receptors are linked to Ras and tyrosine kinase activity.

As mentioned FSH activation of Ras and downstream signalling require a multitude of factors, including the SRC family tyrosine kinases (SFKs) the EGFR and the FSH induced and activated EGF like factors (Wayne *et al* 2007).

The SFKs are hypothesised to be activated via gonadotrophins via recruitment of the SRC to the GPCRs via scaffold effects driven possibly by beta arrestins and G protein receptor kinases. Undoubtedly FSH induces folliculargenesis and LHR production and it is suggested that LH through its receptor induces the formation of EGF (epidermal growth factor) like factors such as (amphiregulin) AREG. AREG then works on the EGFR to activate Ras/Raf/MEK/ERK cascade to impinge on the transcriptional regulation and expression of steroidogenic enzyme genes like aromatase and P450 cholesterol side chain cleavage, Nr5A1/2 i.e. (LRH-1 and SF-1) and genes favouring a luteal cell phenotype thus governing differentiation (Wayne *et al* 2007). In the case of AREG mediated phosphorylation of PKB/FOXO "c-abl" a SRC kinase phosphorylates the EGFR to prevent its degradation and so prolong possible activation and signalling.

Undoubtedly the balance of ovarian genes expressed to bring about folliculargenesis and differentiation are dependant on multiple pathways and synergistic timing. Collectively the pathways work together to hit their individual and shared gene targets where ultimately activation of ERK, PKA and PKB dictate terminal differentiation of granulosa cells to non dividing steroid producing cells (Wayne *et al* 2007).

1.8iv) THE Ras/Raf/MEK/ERK CASCADE AND ITS REGULATION

Ras directly activates the downstream pathway Raf/MEK/ERK1/2 via series of phosphorylation events and mediates its actions through an interaction with multiple effectors. Activation of this MAP kinase cascade is reversible even in the presence of activating stimuli indicating that protein phosphatases may provide an important mechanism of control. MAP kinases are activated by phosphorylation of specific tyrosine and threonine residues localised within the activation loop motif of the kinase domain. ERK/MAP kinase catalytic activation requires phosphorylation by the upstream dual specificity MAP kinase kinase/ERK kinase called MEK, which in turn is phosphorylated and

activated by a MAP kinase kinase kinase called Raf (*Fig.1.7*). Raf is not the sole downstream target of Ras, and Raf may associate with a plethora of effectors in order to transduce Ras mediated signals through multiple pathways. ERK/MAP kinases are involved in cell cycle progression, mitogenesis and oncogenic transformation. Additionally, Ras activation of Raf independent pathways are also crucial to sustain Ras effects by induction of EGFR dependent autocrine growth pathways (*Fig.1.7*). In summary different cell stimuli activate preferentially distinct MAP kinases hence many growth factors and G-Protein linked receptors, cell adhesion molecules and some oncogenes are linked to the activation of ERKs (Campbell *et al* 1998).

Once ERK 1 and 2 are activated the MAPKs translocate to the nucleus to phosphorylate and activate transcription factors and other kinases and phosphatases such as the dual specific phosphatase MKP-3 to maintain folliculargenesis and ovulation. MKP-3 is a cytoplasmic member of the dual specific phosphatases that is selective for the dephosphorylation and subsequent inactivation of ERK1/2 map kinases, therefore working in direct opposition to MAP kinases (Karlsson *et al* 2004) (Camps *et al* 2000) (Camps *et al* 1998)(Keyse, 2000). In addition MKP-3 determines the subcellular localisation of its substrate ERK1/2 as MKP-3 has the ability to shuttle between the nucleus and the cytoplasm; however it is largely expressed in the cytoplasm. MKP-3 is suggested to bind ERK independently of it's phosphorylation state and once it has dephosphorylated ERK it can retain inactive ERK in the cytoplasm (Karlsson M *et al* 2004), thus possibly dampening down the proliferative effects of Ras. Studies in Saccharomyces cerevisiae, Drosophila and mammalian cell lines (Karlsson *et al* 2004) and in chicken ovarian granulosa cells (Woods and Johnson, 2006) have demonstrated that the expression of certain MKPs is induced in response to MAP kinase activation. This suggests that MKP-3 may be a component of a negative feedback loop and MKP-3 therefore presents itself as a possible tumour suppressor. MKP-3 therefore determines the timing and duration of MAPK activation in terms of switch like or proportional response to agonists thus impinging on the spatio-temporal control of MAP kinase signaling. Precise spatio-temporal regulation of MAP kinase signaling may involve constant movement of ERK2 between the nucleus and the cytoplasm and the competition between activator

MEK and inactivating MKP-3 to maintain a fine balance for growth differentiation and survival in the ovary. It is believed that the different temporal patterns of ERK activation elicited by different growth factors underlie their differential effects to drive proliferation and differentiation where dephosphorylation of ERK regulates the duration and magnitude of activation and the biological outcome of signaling (Karlsson *et al* 2004).

Conversely, it is known that sustained activation of the Ras/Raf/MEK/ERK pathway can also lead to cell cycle arrest in many cell types. Cell cycle arrest is induced by producing and secreting the autocrine-paracrine factor lymphocyte inhibiting factor (LIF). LIF mediates this effect through the gp130/JAK/STAT3 pathway. LIF/JAK/STAT3 independent pathways also exist. Additionally the hypothesised mechanism by which Ras and or Raf activation induces arrest involves induction of cyclin dependant kinases (CDKIs) such as p27, p21 and tumour suppressors. Importantly activation of the Ras/Raf/MEK/ERK pathway has been shown to up regulate other autocrine and paracrine factors in addition to LIF that mediate proliferation and arrest. LIF in certain cells has been proven to activate MAPKs and the PI3K pathway. Activation of the MEK/ERK pathway is necessary for the Raf mediated production of LIF however activation of MEK/ERK is not essential to mediate the effects of LIF. This Ras/Raf mediated growth arrest is proposed as a defense mechanism against inappropriate activation of Ras signal transduction (Park J-I *et al* 2003). Thus for carcinogenesis to occur this growth arrest response must be inactivated, although cell transformation may also require inactivation of tumor suppressor genes or inhibition of negative feedback loops like the MKP-3 –ERK1/2 loop.

1.9) EXPERIMENTAL MOUSE MODELS

1.9i) THE *LSL-K-ras^{G12D}-Amhr2-Cre* AND THE *LSL-K-ras^{G12D}-Cyp-19-Cre* MODELS.

To determine the role of Ras on ovarian physiology/pathophysiology, the effect of constitutively active Ras on vital ovarian gene expression, signalling protein expression and ovarian morphology and function was studied using ovaries from mouse models constructed to express constitutively active Ras. In both the (*LSL*) *Lox-Stop-Lox-K-ras^{G12D}-Amhr2-Cre* and *LSL-K-ras^{G12D}-Cyp19–Cre* models *ras* was engineered to be constitutively active. A glycine to aspartic acid mutation was introduced at residue twelve of the *K-ras* gene to render the Ras G protein insensitive to GAP inactivation thus rendering the Ras constitutively active (Bourne *et al* 1990). A *Lox-Stop–Lox K-ras* conditional mouse strain capable of controlled timing and location of constitutively active Ras expression was utilised. A *Cre* recombinase enzyme controlled the expression of constitutively active Ras. The endogenous K-Ras locus was targeted in the *LSL-K-ras^{G12D}* strain so endogenous levels of K-Ras^{G12D} protein were expressed on stop element removal via *Cre* recombinase (Tuveson *et al* 2004) (Jackson *et al* 2001). The previously reported *Amhr2-Cre* knock-in mouse model (Jamin *et al* 2002) and the newly tested *Cyp-19-Cre* transgenic mouse model were mated to the *R26R* mouse strain. The *R26R* models contain a lac Z gene that produces β Galactosidase and only expresses β galactosidase activity in cells that express *Cre* recombinase. This lac Z allele is separated from a constitutively active ROSA 26 promoter by a lox P-flanked by a neomycin cassette (floxed- Lac Z). *Cre* removes this floxed transcription stop element in the *R26R* background to reveal the Lac Z gene. Therefore *Cre* activity and thus constitutively active Ras location within the ovary can be demonstrated via a β galactosidase assay (Soriano P, 1999). *Cre* expression was achieved by targeting *Cre* to the appropriate locus and lac Z expression driven by the constitutively active promoter. In the *LSL-K-ras^{G12D}-Amhr2-Cre* and *LSL-K-ras^{G12D}-Cyp19–Cre* mouse models the *Cre* recombinase was driven by two different promoters. In the transgenic model the *Cyp-19* or aromatase promoter was used and in the knock-in model the Anti- Mullerian hormone receptor-2 (*Amhr-2*) promoter was used.

1.9ii) *THE Pten* CONDITIONAL KNOCK OUT MODEL

In the conditional *Pten* knock out strains Lox P sequences were inserted into the endogenous *Pten* locus flanking exon 5. Exon 5 encodes a phosphatase domain of PTEN in which many tumour associated mutations are detected. *Pten* $^{loxp/+}$ embryonic stem cells (ES) were injected into C57/B6 mice. Chimeric mice were back crossed to C57/B6. Induction of Lox P sites in to the *Pten* locus does not perturb the normal function of *Pten* and *Cre* recombinase mediates exon 5 excision. By using tissue specific promoters to express *Cre*, it elicited a recombination leading the mutational inactivation of PTEN. Loss of *Pten* in tissue studies to date, have initially not resulted in a tumour like phenotype. Instead the *Pten* conditional knock out has displayed that it requires a period of time to gather a subpopulation of *Pten*$^{-/-}$ cells to transform to malignancy (Lesche R *et al* 2002). To generate a granulosa cell specific conditional knockout *Pten* $^{flox/flox}$ mice were mated to *Cre* recombinase expressing mice either the *Amhr-2-Cre* or the *Cyp-19-Cre* mouse.

1.9iii) *Pten/ K-Ras* DOUBLE KNOCK OUT MODELS

Immature wild type C57BL/6 mice were obtained. *LSL-K-Ras*^{G12D}*;Amhr-2-Cre* and *LSL-K-Ras* ^{G12D}*;Cyp-19-Cre* mice were interbred to *Pten* $^{LoxP/loxP}$ mice to generate *K-ras/Pten* double mutations in ovarian granulosa cells (Fan *et al* 2007 unpublished).

2) AIMS

The Ras/Raf/MEK/ERK and the PI3K/PKB/FOXO cascades are known vital pathways for sustaining the balance between proliferation, differentiation, cell survival and apoptosis thus augmenting folliculargenesis, ovulation and lutenisation. Ras is known to play a pivotal role both as a primary activating component in the Ras/Raf/MEK/ERK pathway and as a supportive auxiliary activator of the PI3K cascade. Thus the primary aims of this project were:

A) To study the effects of constitutively active Ras on ovarian cell function and morphology in mice genetically engineered so as their *ras* gene is permanently switched on. This will determine the extent to which Ras influences the ovarian phenotype and how important control of Ras activation is to function.

B) To study the effects of constitutively active Ras on vital ovarian signalling genes namely the *Fshr* and *Lghcr* genes so as to determine the extent to which Ras activation impinges on vital upstream receptor genes that relay the FSH and LH message allowing successful folliculargenesis and ovulation.

C) To study the effect of constitutively active Ras on the downstream Ras/Raf/MEK/ERK cascade component the *Mkp-3* gene, so as to determine the effect and extent to which Ras activation influences the proposed negative regulatory effects of the *Mkp-3* gene product MKP-3.

D) To study the effects of constitutively active Ras on p-ERK and p-PKB; signalling intermediates of the Ras/Raf/MEK/ERK cascade and the PI3K cascade so as to better understand the controlled mechanics of Ras signalling.

As PTEN is a known important negative regulator of the PI3K cascade thus controlling and balancing the cell survival and proliferative effects of an active PI3K cascade and as Ras was known to influence the PI3K cascade in a supportive role the secondary aims of this study were:

E) To study the effect of a *Pten* conditional knock out on ovarian morphology in mice genetically engineered to knock out their *Pten* gene, so as to determine the importance of PTEN in maintaining normal phenotype.

F) To study the effect of a *Pten/K-ras* double knock out on ovarian morphology so as to determine the effect of PTEN and K-Ras together in ovarian phenotype.

All of the above aims were carried out on mice of the required genotype that had been treated with gonadotrophin representing the normal physiological state to induce ovarian folliculargenesis, ovulation and lutenisation as required. Pregnant mare serum gonadotrophin (PMSG) an FSH analogue was used in place of FSH and human chorionic gonadotrophin (hCG) an LH analogue was used in place of LH.

3) MATERIALS AND METHODS

MATERIALS

3.1 MOUSE MODELS/GENOTYPES USED

1-R26R

2-Cyp- 19-Cre

3-Amhr2-Cre

4-LSL-K-ras $^{G12\,D}$; Cyp19-Cre

5-LSL-K-ras ^{G12D}; Amhr2-Cre

6-Pten $^{flox/flox}$; Amhr2$^{Cre/+}$ (Pten KO)

7-Pten $^{flox\,/flox}$;K-ras$^{flox/+}$Amhr2 $^{cre/+}$ (Pten/K-ras KO)

8-Wild type

3.2 IN- SITU HYBRIDIZATION MATERIALS AND PREPARATIONS

RIBOPROBE PREPARATION MATERIALS.

- RNAse-free conditions.

- DEPC water -Sigma Diethyl Pyrocarbonate *Cat No*. D 5758 & dH$_2$0

- Promega® Riboprobe in-vitro transcription system. *Cat No.* P 1450

- Promega ® TSC Buffer *Code No*. P118B, *Lot No.*13494317

- Promega ® Optimised 5X Buffer

- Dithiothreitol (DTT) 100mM

- Invitrogen® RNaisin *Cat No.* 15518-012, *Lot no.* 1363621

- Invitrogen® RNase inhibitor cloned (1000 U) (10U/µl)

- Amersham Biosciences® α^{35}S UTP 1mCi, *Code No.* SJ 40383, *Lot No.*AC0707

- Promega RQ1 DNAse Buffer *Code No*. M198A, *Lot No. 13573506*

- 10X reaction buffer

- Boehringer Mannheim yeast tRNA 20µg/µl *Lot No.*109495

- Omni Pur® chloroform: isoamyl alcohol 24:1 *Lot No.* 1746B067

- Amresco® phenol-saturated H$_2$O II *Lot No.* 2874B05

- Aaper alcohol, the clear leader®-100% ethanol-Ethyl alcohol USP, absolute-200 proof *No*.06K2823 (RNA free 100% ethanol)

- RNAase free 70% Ethanol

- Fisher Scientific 7.5M Ammonium Acetate (NH$_4$OAC)- *Code No*.A637-500, *Lot No*.054580

- Boehringer Mannheim G-50 quick spin columns *Cat No*. 1273973

- N-Tris (hydroxymethyl) methyl-2 aminoethane-sulphonic acid-(TES) (10:1:0.1%)

- Fisher Scientific ScintiSafe™ Econol, *Code No*. SX-20-5

REHYBRIDIZATION MATERIALS

- Fisher Scientific® Xylene- *Code No*. X5-4 UN1307, *Lot No*. 040649

- Fisher Scientific (PBS) - Na$_2$HPO$_4$ Sodium phosphate dibasic *Code No*. S 373-500, *Lot No*. 040414 and NaH$_2$PO$_4$H$_2$O Sodium phosphate monobasic Code No. S 369-500, *Lot No*.055228A

- Para-formaldehyde EMD™ UN2213, *Code No*.PX0055, *Lot No*. 45105621

- Fisher Scientific Proteinase K 20μg/ml in EDTA solution Lot No. 033866

- Sigma TEA – Trietanolamine *Code No*. T-1502

- Sigma Acetic anhydride

- Fisher Scientific EDTA, *Lot No*. 033866

- Boehringer Mannheim Proteinase K *Cat No*. 3115852

- Fisher Scientific TRIS-HCL *Code No* .BP 152-500 *Lot No*. 020575

- RNAse free water (DEPC), RNAse free 70%, 80%, 95% and 100% Ethanol

HYBRIDISATION MATERIALS

- Riboprobe

- Pre made hybridisation solution- Fisher Scientific- Formamide, Tris-HCL, EDTA, NaPO$_4$, Dextran sulphate *Cat No*. BP 1585-100, 1X Denhardt's and yeast tRNA.

- Heating block/ 55°C incubator

- Humidifying chamber solution- Fisher Scientific 20X SCC, H$_2$O and formamide

30

WASHES MATERIALS

- Water bath and slide jars

- Washing solutions- see In-Situ preparations section

- 20X SCC

- Sigma B-mercaptoethanol *Batch No.*105K0104

- Boehringer Mannheim RNaseA 20μg/ml *Cat No.* 109169

- Light tight box

- X-OMAT film

AUTORADIOGRAPHY AND STAINING MATERIALS

- Water bath, Tin foil, slide mailer and light tight box.

- Fisher Scientific® Glycerol Code No. BP229-1 Lot No. 060127

- KODAK D-19 Developer Cat No. 1464593

- Kodak Fixer *Cat No.*1971746

- Kodak NB2 Liquid emulsion *Cat No.* IB 1654433

IN-SITU HYBRIDISATION SOLUTION PREPARATIONS

DEPC H₂O 0.1mM-   Diethyl pyrocarbonate was added to deionised water at a concentration of 100μl/L, stirred overnight and autoclaved for 45 minutes and allowed to cool.

Plasmid template preparation- The required plasmid was linearised using an appropriate enzyme that cuts only once so that transcription will proceed from the vector transcription site into cDNA to yield a 300-100bp RNA strand probe. To generate antisense and sense templates two different enzyme digests were needed. 10μg of the required plasmid was digested overnight in an enzyme digest solution, and then left at 65°C for 5 minutes to stop the enzyme. The linearised cDNA was then Phenol: Chloroform extracted, ethanol precipitated, washed and dissolved in water to a final concentration of 1mg/μl.

31

e.g. To construct the pHF4 (Mkp-3 probe) plasmid
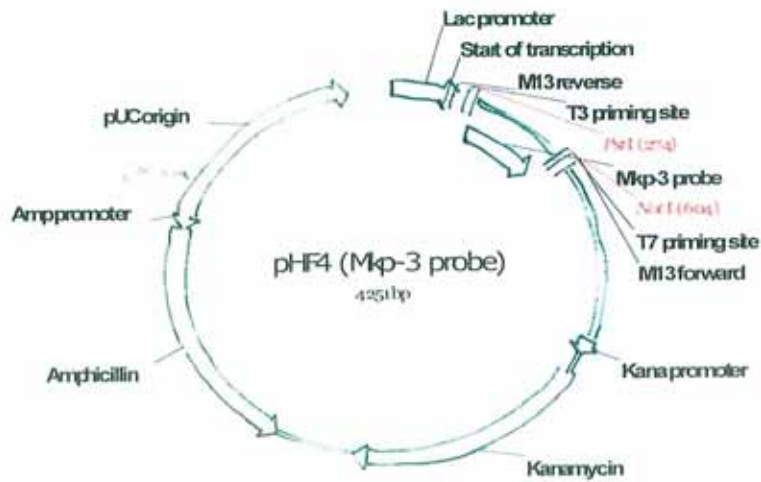
To make an anti-sense probe:

Cut plasmid with Pst1 (NEB buffer 3 + BSA) and transcribe with T7

To make sense probe:

Cut plasmid with Not 1(NEB buffer 3+ BSA) and transcribe with T3.

Para-formaldehyde (PFA) 4%- (30mls)-1.2g of para-formaldehyde in 30mls of 1 X PBS solution heated at 65°C overnight or at 90°C for 1 hour

0.1 M TEA (Trietanolamine) pH 8- 9.29g TEA in 500mls DEPC water and checked with a pH meter.

Proteinase K solution- 20µg/ml proteinase K in 50mM Tris for 60mls: 3mls of 1 M Tris pH 8 was added to 60µl of 0.5 M EDTA pH 8 and 60 µl of proteinase K 20mg/ml and brought up to a final volume of 60mls with DEPC water (one coplin jar)

32

Hybridisation solution 50ml stock- 50% formamide ,0.3M NaCl, 20mM Tris-HCL pH 8, 2.5 mM EDTA pH 8 , 10mM $NaPO_4$ pH, 10% Dextran sulphate, 1 X Denhardt's, 0.5mg/ml yeast tRNA and water and store in aliquots at -80°C.

70% Ethanol (EtOH)/(C_2H_5OH), 0.3 M NH_4OAC (400ml)- 280ml 100% Ethanol, 15mls 8M NH_4OAC, 105mls H_2O.

80% Ethanol (EtOH)/(C_2H_5OH), 0.3 M NH_4OAC (200ml) 160 mls 100% Ethanol, 7.5 mls 8M NH_4OAC, 32 mls H2O.

95% Ethanol (EtOH)/(C_2H_5OH), 0.3 M NH4OAC (200ml)- 190 ml 100% Ethanol, 7.5 mls 8M NH_4OAC, 2 mls H2O.

5X SCC/ 10mM β-Mercaptoethanol- (400ml)-100ml 20x SCC, 280µl ß- Mercaptoethanol up to 400 mls with H_2O (ß-mercaptoethanol was added just before use).

50% formamide/ 2X SCC; 100mM ß-mercaptoethanol- (400mls) - 40ml 20X SCC, 20mls formamide, 160mls H_2O and (1400µl/200ml) ß- mercaptoethanol.

50% formamide/ 2X SCC; 50 mM ß-mercaptoethanol- (400mls)- 40ml 20X SCC, 200mls formamide, 160mls H_2O and (700µl/200ml) ß- mercaptoethanol.

TEN- (0.5 mM NaCl, 10mM Tris pH 8, 5mM EDTA) - (100mls) 5 M NaCl, 10mls 1M Tris, 10 mls 0.5 M EDTA to 1L H_2O

RNase A/TEN- 200µl of 20µg/ml RNase A to 200ml of TEN

0.1X SCC (200mls) - 1ml 20X SCC and 199mls H_2O

2XSCC (200mls) - 20mls 20X SCC and 180mls H_2O

8M NH₄OAC 100mls- 61.664g/100ml.

PBS pH 7.5- 5.68g Na_2HPO_4 80mM, 1.38g NaH_2PO_4 20mM, 2.92g NaCl 100mM, and H_2O to 500mls

TES(10:1:.0.1%)- 500μl of 1M Tris-HCL, 100μl of 0.5M EDTA, 500μl of 10% SDS and 48.9mls DEPC H_2O. Fisher Scientific Tris-HCl and EDTA and Fisher Scientific® SDS *Code No.*BP166-500 *Lot No.*033491

3.3 WESTERN BLOT MATERIALS

- Protein samples and molecular weight marker

- BioRad rack, Plates and electrophoresis apparatus (Western blot apparatus)

- BioRad 1.5 mm 10 well comb

- Fisher Chemalert® Fisher Scientific® Acrylamide *Code No.* BP-170-500

- BioRad TEMED-N,N,N'-N'-tetra-methylethylenediamine *Cat No.* 161-0801

- BioRad Ammonium Persulphate (APS)- *Cat No.* 161-0700

- Sigma Triton-X-100 *Lot.No.* 126H1030

- Fisher Scientific Isobutanol *Code No.* A399-4, *Lot No.* 031612

- Fisher Scientific- Methanol *Code No.* A412-4, *Lot No.* 053816

- Bio-Rad Trans-Blot® SD. Semi-Dry transfer cell *Serial No.153B*R 0146032

- Fisher Scientific® Tween 20 *Code No.* BP337-500 *Lot No.*051388

- Bio-Rad extra thick blot paper 7x 8.4cm, *Cat No.* 1703966

- Bio-Rad nitrocellulose or PVDF membrane.

- Western Super Signal® West Pico chemi-iluminescent substrate/ enhanced chemi-iluminescent substrate for detection of HRP

- Solution A-Western Super Signal® West Pico Stable peroxide solution

- Solution B-Western Super Signal® West Pico luminol/enhancer solution

- Cell signalling technology™ PTEN rabbit monoclonal antibody *Code No.9559*

- Cell signalling technology™ phospho-Akt rabbit monoclonal antibody (p-PKB) *Code No.4058*

- Cell signalling technology™ Phospho-ERK monoclonal antibody.

- GE Healthcare UK -Rabbit secondary donkey anti-Rabbit antibody IgG HRP linked whole Antibody *Cat No.*NA934V *Lot No.*345026

- GE Health Care Extra sensitive substrate- Lumigen ™ PS-3 detection solution A *Lot no.* 71 *Code No.* RPN2132 V1 and Solution B *Code No.* RPN2132V1

WESTERN BLOT SOLUTIONS

- Semi-Dry transfer buffer- 5.82g TRIS, 2.93g Glycine, 20% methanol, 3.75g SDS/1000ml (48mM Tris, 39mM glycine, 0.0375% SDS, 20% methanol)

- 10X TBS (1L)-200ml 1M Tris-HCl pH 7.5, 300ml 5M NaCl, 500ml

- TBST—100ml of 10X TBS- (200ml IM Tris pH 7.5, 300ml 5M NaCl, 500ml H_2O) + 900ml H_2O + 2mls 50% Tween 20

- Blocking buffer- 1X TBST with 5% w/v non fat dry milk- 10g non-fat dry milk and 200ml TBST and mix

WESTERN BLOT 10% ACRYLAMIDE GEL PREPARATION

Running gel, lower (10%)(~15mls/ gel	
Acrylamide (40%)	7.5ml
dH_2O	11.0ml
1M Tris (pH 8.7)	11.2ml
10% SDS	300µL
10% APS (Ammonium persulphate)	120µL
TEMED	20µL

STACKING GEL PREPARATION

<u>Stacking gel, upper</u> (for 2 gels): Acrylamide (40%)	1.3ml
dH$_2$O	7.25ml
1M Tris-HCl (pH 6.8)	1.3ml
10% SDS	104µl
10% APS	52µl
TEMED	11µl

3.4 IMMUNOFLUORESCENCE MATERIALS

- Frozen sections embedded OCT compound (Sakura Finetek USA, INC), fixed in 4% PFA and sectioned at 7-µm

- Amersham Life Science BSA- Bovine serum albumin albumin fraction V RIA grade *Cat No.* 70244

- Fisher Scientific Potassium chloride (KCl) *Code No.* BP 217-500 *Lot No.*897311

- Fisher Scientific Sodium Chloride (NaCl)

- Fisher Scientific (PBS) - Na$_2$HPO$_4$ Sodium phosphate dibasic *Code No.* S 373-500, *Lot No.* 040414 and NaH$_2$PO$_4$H$_2$O Sodium phosphate monobasic Code No. S 369-500, *Lot No.* 055228A

- Para-formaldehyde EMD™ UN2213, *Code No.*PX0055, *Lot No.* 45105621

- Vector Laboratories® Vectashield® mounting medium with Dapi (1.5µg/ml) *Cat no.* H-1200

- MENZEL-GLASER® Super frost® Plus Microscope Slides. *Art no.* J1800AMNZ.

- Coverslips and nail polish

IMMUNOFLUORESCENCE SOLUTIONS

- 10X PBS Phosphate buffered saline – see in-situ materials

- 4% PFA- see in situ materials

- PBS/0.3% triton X-100 10ml-1.5 of 20% triton X-100 to 100ml of 1X PBS

3.5 IMMUNOHISTOCHEMISTRY MATERIALS

- PFA fixed, paraffin embedded sections

- Vector Laboratories VECTASTAIN® Elite® ABC KIT: Rabbit IgG *Cat No.*PK6101

- Vector laboratories DAB peroxidase substrate kit. *Cat No.* SK 4100

- MENZEL-GLASER® Super frost® Plus Microscope Slides. *Art no.* J1800AMNZ.

IMMUNOHISTOCHEMISTRY CHEMICALS

- Fisher Scientific Sodium Citrate *Code No.* BP 327-1 *Lot No.*046500

- Fisher Scientific (PBS)- see immunofluorescence materials

- 4% Para-formaldehyde –see in situ materials

DEHYDRATING; REHYDRATING, MOUNTING, EMBEDDING AND STAINING REAGENTS/INSTRUMENTS

- Histolab® Xylene. *Art Nr.* 02080

- Histolab® 99.5% ethanol

- Histolab® 95% ethanol

- Histolab® 80% ethanol

- dH_2O

- Pertex CE. *Art Nr.* 008111

- Histolab® Mayers Haematoxylin. *Art Nr.* 01820

- Paraffin wax

- VENTANA VIP tissue processor.

IMMUNOHISTOCHEMISRY SOLUTIONS AND REAGENTS

- 10X PBS –see in-situ

- 10mM Sodium citrate buffer. (1L)- 2.94g sodium citrate to 1L dH_2O and adjusted to pH6

- 1% H_2O_2-10mls 30% H_2O_2 to 290ml dH_2O

- Blocking solution 5% normal horse/goat serum in 1X PBS

- ABC reagent- prepared according to manufacturers instructions

- DAB reagent- prepared according to manufacturers instructions

IMMUNOHISTOCHEMISTRY ANTIBODIES

- Santa Cruz™ p21 antibody

- Cell signalling technology™ P450 Side chain cleavage enzyme

3.6 GENOTYPING MATERIALS

DNA EXTRACTION	PCR/GENOTYPING RECIPE
- DNA digestion buffer with proteinase K	-PCR machine, extracted DNA
- Phenol: chloroform: Isoamyl alcohol (25:24:1)	-Forward and reverse primers
- 100% ,70%Ethanol	-Taq polymerase, dNTPs,
- TE Buffer(10mM Tris & 1mM EDTA)	-dH_2O, $MgCl_2$, 10X buffer
- Heating block and eppendorf tubes	-1.5% agarose gel made in TBE buffer

3.7 BETA GALACTOSIDASE/X-GAL ASSAY MATERIALS

- Fresh dissected ovaries

- Tissue Processing, embedding and sectioning materials

- 1XPBS

- Sigma X-Gal stock solution

- 4% PFA

- 70% Ethanol

3.8 H&E MATERIALS

- PFA fixed, processed and paraffin embedded and sectioned ovaries

- Hydrating/dehydrating/mounting materials as mentioned in Immunohistochemistry materials

- Hematoxylin and Eosin stains

3.9 RT-PCR MATERIALS

- 100ηg samples RNA

- ^{32}P-dCTP isotope

- PCR machine

- Invitrogen Superscript One-step RT-PCR system with platinum Taq Kit

- Molecular weight marker

- Oligonucleotides

- Gel apparatus (Rack, plates and electrophoresis tank)

- 1 large 10% acrylamide gel as prepared in the western blot materials section.

- TBE buffer

- Gel dryer

- Light tight cassette

- Kodak Biomax XAR film

- Auto radiography developer.

3) METHODS

3.10-TISSUE SECTION PREPARATION

Mouse ovaries were dissected and immediately fixed in 4% Para-formaldehyde overnight. The ovaries were then washed three times in PBS at 4° C for ten minutes each. Subsequently the ovaries were placed in 70% ethanol and processed. During processing a VENTANA VIP closed system tissue processor:

1) Dehydrated the ovaries in 70% ethanol for one hour at 40°C, two changes of 95% ethanol for one hour each at 40°C and two changes of absolute ethanol at 40°C for one hour each.

2) Cleared the ovaries in three changes of xylene at 40°C for one hour in each well.

3) Infiltrated the ovaries in paraffin wax for one hour at 60°C.

The ovaries were then embedded in paraffin wax and sectioned at 7 μm on a HM 400 microtome and allowed to dry on star frost positively charged glass slides at 42°C overnight.

3.11-H&E STAINING

The required mouse ovary paraffin tissue sections were depariffinised in three changes of xylene for ten minutes each. The sections were hydrated through a graded alcohol series, which included two changes in 100% ethanol for two minutes each and further rehydration through 95%, 70%, 50% ethanol and water for two minutes each. The sections were stained in new and unfiltered haematoxylin for 20-30 seconds and then transferred to running water to blue up. The eosin was applied to the sections for 20 seconds and rinsed. The sections were dehydrated through 95% ethanol for two minutes and then through two changes of 100% ethanol for a minute each. The dehydrated sections were then cleared in two changes of xylene for a minute and mounted in DPX.

3.12-X-GAL/ BETA GALACTOSIDASE ASSAY

The ovaries and or uterus specimens were removed as required from $Rosa^{flox/+;}Amhr-2^{Cre/+}$ and $Rosa^{flox/+;}Cyp-19^{Cre/+}$ genotyped female mice and fixed for 3 hours in 4% PFA at 4° C. The tissues were rinsed in PBS three times for ten minutes each. The tissues were rinsed with tissue rinse solution A for 30 minutes at room temperature. The tissues were rinsed in tissue rinse solution B for 5 minutes. Then the tissues were incubated at 37° C in the dark in an X-Gal working solution diluted I: 40 from the X-Gal stock solution. The tissues were left to incubate for a minimum of 3 hours or until a desired blue colour was achieved in the tissues. The tissues were washed for 5 minutes in two changes of PBS and re-fixed with 4% PFA at 4°C for 1 hour. Finally the tissues were washed for 5 minutes in three changes of PBS and stored in 70% ethanol in preparation for tissue processing and embedding.

3.13-ABC- Elite IMMUNOHISTOCHEMISTRY PROTOCOL

DAY 1

The required ovary paraffin sections (test and negative control sections) were deparaffinised and re-hydrated through xylene x 2 and a graded alcohol series (95% x 2, 80% x 2, ethanol) down to distilled water for three minutes in each bath. A plastic coplin jar (60mls) containing the diluted antigen retrieval solution (1:20 of 200mM Sodium citrate) was placed in a water bath at 90° C and allowed to come to temperature. The required ovarian tissue sections were added to the coplin jar and left for ten minutes at 90° C, and subsequently allowed to rest for a further 30 minutes to ensure maximum antigen retrieval. Sections were rinsed firstly in distilled water and then placed in the appropriate buffer assigned to the antibody. 50μl of normal blocking serum was then applied to the sections for 60 minutes. Nearing the end of the 60-minute incubation, primary antibody was diluted in its appropriate buffer as follows (FKHR antibody was diluted 1:50), (P21 antibody was diluted 1:100) and (P450 Side chain cleavage antibody diluted 1:100). Excess serum was drained from the sections and the primary antibody applied immediately without allowing the sections to dry out. Water only was applied to the negative control section (of the same genotype to test). Sections were placed in a humid

incubating chamber in the refrigerator at 4°C overnight or for one hour at room temperature depending on the antibody conditions favoured by the manufacturer.

DAY2/ An hour later

Sections were rinsed in appropriate buffer, 3 x 5 minutes, keeping the negative controls and different antibodies in separate jars. The ABC- ELITE reagent (20μl reagent A + 20μl Reagent B) in 1ml of buffer) was mixed and kept at room temperature for 30 minutes prior to use. The sections were incubated with 50μl of biotinylated secondary antibody diluted 1:200 in buffer and incubated at room temperature for 30 minutes. Sections were rinsed thoroughly in buffer 3 x 5 minutes and incubated with 50μl of the ABC-Elite reagent for 45 minutes at room temperature. Sections were rinsed with buffer 3 x 5 minutes and 50μl of freshly prepared Vector® DAB substrate applied. Development time for each antibody was determined on the control slides under light microscopy and used for the test ovary sections. Colour development was stopped by rinsing in appropriate buffer and then in distilled water for 5 minutes. The sections were counterstained in Meyers Haematoxylin for three minutes and allowed to blue up in tap water for five minutes. Sections were rapidly dehydrated in two changes of fresh 95% and 100% ethanol and mounted in DPX. Each staining procedure was repeated in triplicate to confirm results.

3.14- IMMUNOFLUORESCENCE METHOD

Ovarian frozen sections of the required genotype and negative control ovary sections (ovary sections of the same genotype as the test sections) were selected and fixed in 4% PFA in PBS for 30 minutes at room temperature. The sections were rinsed three times in PBS for three minutes each and blocked in 5% BSA in PBS/ Triton for 30 minutes. While blocking the primary antibody was diluted as directed (1:100) in PBS/Triton. The blocking solution was aspirated from the sections and the primary antibody diluted as follows (PTEN antibody was diluted at 1:100), (p-PKB antibody was diluted 1:200), and (p-ERK antibody was diluted 1:100).

The primary antibody was applied to the test sections and water only was applied to the negative control section. The sections were incubated overnight at 4°C or at one hour at room temperature. The sections were rinsed three times in PBS for five minutes each. In the dark the sections were incubated in fluorochrome-conjugated secondary antibody diluted (1:250) in PBS/Triton for one hour in the dark. In dimmed light the sections were rinsed twice in PBS for 5 minutes each and contra-stained and mounted with 12μl of vectashield mounting medium containing DAPI. The sides of the cover slip were sealed with nail polish to avoid drying out and the slides examined at the appropriate wavelength. Slides were stored flat in the dark at 4°C.

3.15-GENOTYPING

Mouse-tail tips were digested in 750 μl of DNA digestion buffer/ proteinase K solution at 55°C overnight. 375 μl of phenol: chloroform: isoamyl alcohol (25:24:1) was added and mixed well. The mixture was spun at full speed for 10 minutes. 400μl of the upper layer was taken into a new tube and 1ml of 100% ethanol added and spun at 1400rpm for 10 minutes. The ethanol was removed and the pellet washed with 200μl of 70% ethanol. The 70% ethanol was removed and the pellet left to air dry for ten minutes. To the dry pellet 100ml of TE buffer was added and vortexed. The DNA was then incubated 55°C for one hour and allowed to dissolve. PCR was performed on the dissolved DNA using standardised reagents and optimised PCR programmes.

K-ras /Amhr2 –Cre **Genotyping Reagents (1X reaction)**

1.	10X Buffer-2μl	**2.** DNA- 1μg/μl-1 μl	**3.** MgCl$_2$ 25mM-2μl
4.	d NTP (10mM)- 1μl	**5.** Primer forward -100ηg/μl-1μl	
6.	Primer reverse-100ηg/μl-1μl	**7.** (1U)Taq -0.2μl	**8.** H$_2$O- 11.8μl

Cyp-19-Cre **Genotyping Reagents (1X reaction)**

1.	10X Buffer-2μl	**2.** DNA- 1μg/μl-1 μl	**3.** MgCl$_2$ 25mM-2μl
4.	dNTP (10mM)- 1μl	**5.** Primer forward -80ηg/μl-1μl	
6.	Primer reverse-80ηg/μl-1μl	**7.** (1U)Taq -0.2μl	**8.** H$_2$O- 11.8μl

PCR PROGRAMMES

K-Ras/Amhr2 programme	*Cyp- 19-Cre* Programme
1. 94°C-3 minutes	1. 94°C- 2 minutes
2. 94°C-30 seconds	2. 94°C-30 seconds
3. 60°C-30seconds	3. 55°C-30 seconds
4. 72°C-1 minute	4. 72°C-30 seconds
5. Go to step 2 -35X (cycles)	5. Go to step 2-30X (cycles)
6. 72°C-5minutes	6. 72°C- 5 minutes
7. 15°C forever	7. 15°C forever

Note: The genotype of *Pten* and *R26R* mice were previously confirmed.

3.16-WESTERN BLOT ANALYSIS METHOD

Western Blot apparatus (rack and plates) was assembled and a 10% acrylamide gel mixture minus the TEMED content was made as outlined in the materials section. To create a seal on the base of the western blot plates 200µl of gel mixture minus TEMED was transferred to an eppendorf tube. 2.5µl of TEMED was added to the eppendorf tube, mixed and immediately applied to western blot plate base to provide a seal. TEMED was then added to the pre made gel mixture and the mix immediately added between the plates to a height approximately 4 cm short from the top of the plates. 200µl of water saturated isobutanol was added to remove bubbles and the gel left to set for 10mins. Once set the isobutanol was removed and 2 mls of stacking gel was added and allowed to set with a well comb in place for 15 minutes. The gels were placed in an electrophoresis tank and 1XTBE buffer added. The comb was removed and the appropriate whole ovary lysate protein samples and molecular weight marker were loaded to the wells and the gel run at 150 V for 1 hour. The western blot nitrocellulose or PVDF membrane was wetted in methanol to make it permeable. Excess methanol was removed and the membrane washed in Semi- Dry transfer buffer. The transfer chamber surface and two blotting towels per gel were wetted with semi-dry transfer buffer. The gel was placed on to the transfer

membrane and sandwiched between two wet blotting towels and placed on the transfer chamber surface, excess air was removed with a rolling pin. The gel was transferred to the membrane on the transfer chamber at 15 V for 45mins. Once fully transferred the membrane was blocked in blocking solution (blocking buffer with 0.1% sodium azide) for 30 minutes.

The membrane was incubated in the appropriate primary antibody diluted in blocking solution as follows (PTEN, p-PKB and p-ERK antibodies were diluted 1:1000) and to a final volume of 10mls. The membrane was agitated overnight at 4°C. The membrane was subsequently washed three times in TBST for 10 minutes each. The membrane was then incubated in HRP- conjugated secondary antibody diluted (1:5000) in 10ml of milk with gentle agitation for 30 minutes at room temperature. The membrane was washed in TBST three times for 10 minutes each. The membrane was patted dry on a paper towel and transferred to Western hydrogen peroxide based substrate for two minutes. The excess substrate was removed and the membrane transferred to a plastic sleeve and taped to a labelled cassette that had been exposed to light for 10 minutes. In the dark room Kodak film was placed on top of the membrane and an initial 10 second exposure indicated the proper exposure time. Subsequently the membrane was exposed with new film for the appropriate time and developed.

3.17-IN-SITU HYBRIDISATION METHOD

Using the Promega riboprobe transcription system the pre-made sense and antisense linearized plasmids were firstly transcribed. The following transcription reagents were mixed in a 1.5 ml eppendorf tube: 1 µl Linearised plasmid (1µg/µl), 5µl 5x TSC Buffer, 2.5µl of 100mM DTT, 2.5 µl of 2.5mM GAC ribonucleic acids, 1µl of Rnasin, 2.5 µl of ^{35}S UTP 40 uCi/µl, 9µl H$_2$O and 1.5µl polymerase enzyme.

The transcription mixture was incubated at 37°C for 2 hours. Subsequently the mixture was spun for 10 seconds and 3 µl of (3U) RQ1 DNAse was added and incubated at 37°C for 15 minutes. After a quick spin, 2 µl of 20µg yeast tRNA and 50µl DEPC H$_2$O was added to give a final volume of 80µl. 40µl of Chloroform: Isoamyl alcohol (24:1) and 40µl of Phenol were added for extraction, vortexed and spun for one minute. The aqueous layer was removed to a new tube and the remains of the

original sample tube was back extracted with 20 µl of DEPC H_2O and spun for 1 minute and the aqueous layers pooled. G-50 spin columns were equilibrated with 100µl TES (10:1; 0.1%) by spinning for 1 minute. The flow through was discarded and the sample added to the column. The column was spun for 2 minutes and the flow through collected. The RNA was precipitated by adding 50µl of 7.5M NH_4OAC, 375µl of 100% Ethanol and inverting three times and storing at

- 80° C for 30 minutes, spinning at 4°C for 20 minutes and removing the supernatant from the tube. The tube was filled with 600 µl of 70% Ethanol and spun at 4°C for 10 minutes and the supernatant removed. 100% Ethanol was added to the pellet, immediately removed and the pellet left to air dry. The pellet was then re-suspended in 100µl of 100mM DTT. 4mls of scintillation fluid was added to each scintillation tube needed. 1 µl of appropriate RNA sample (Riboprobe) was added to the fluid and vortexed. The riboprobe was counted in the scintillation counter and the excess sample stored at - 20°C. Counts only between 1/2-1million were accepted.

REHYBRIDIZATION

The required fixed, processed, embedded and sectioned slides (test and immature ovary negative controls) were placed in a coplin jar and filled with 60 mls of the following solutions for the indicated times:

Xylene (10mins 3X), 100% Ethanol (2 mins-3X), 95% Ethanol (2mins), 80% Ethanol (2minutes), 70% Ethanol (2 minutes), PBS (5minutes), 4% Para formaldehyde (20minutes), PBS (5 minutes), Proteinase K solution (7.5 minutes), PBS (quick rinse and then 5 minutes), 4% Para formaldehyde (5 minutes), RNAse free H_2O (1 minute 2X), 0.1M TEA (1 minute) then the 0.1M TEA was poured back into flask and 150µl of Acetic Anhydride added, mixed and left on the slides for 10 minutes, PBS (5 minutes-2X), 70% Ethanol (5minutes-2X) 80% Ethanol (5 minutes), 95% Ethanol (5 minutes), 100% Ethanol (2 minutes-2X).The slides were removed from the coplin jar and allowed to air dry for 15 minutes.

HYBRIDIZATION

For each appropriate slide sample i.e. (ovary tissue sections from mice of the appropriate genotypes) both sense and Anti-sense probes used 5 million counts of Riboprobe in 60 µl of hybridisation solution on each slide via the following calculation.

- No. Slides x 5 million / scintillation reading= amount probe needed (µl)

- (No. Slides x 60µl)- probe amount (µl)= Amount Probe Reagent (µl)

The probes and probe hybridisation solution were mixed together as calculated and the probe mixture denatured at 80°C for 2 mins and the allowed to cool. 60µl of probe was applied to the tissue section and coversliped. The slides were placed in a humidified chamber containing Whatman 3M paper saturated in 150mls of formamide, 75mls of 20X SCC and 75mls H_2O. The edges of a perspex box were covered with parafilm to form a seal and the slides placed on slide grate within the box and incubated overnight at 55° C.

WASHES

Slides were removed from the hybridisation chamber and placed in a slide rack. The slide rack was placed in staining dishes containing 200mls of each wash solution and left for the indicated time and conditions stated. 5x SCC, 10 mM β-mercapto ethanol (140µl/200mls) for 30 minutes at room temperature, after 15 minutes any remaining attached cover-slips were removed. The slides were then incubated in 5 X SCC, 10 mM β-Mercapto-ethanol (140µl/200mls) for 30 minutes at 55°C, then in 50% formamide, 2X SCC, 100 mM β-Mercapto-ethanol (1400µl/200mls) for 30 minutes at 65°C, TEN for 10 minutes at room temperature, followed by incubations in three changes of TEN for 10 minutes each at 37°C, 200µl of 20µg/ml RNAse in TEN for 30 minutes at 37°C, TEN for 15 minutes at 37°C and 50% formamide, 2 X SCC, 50 mM B- Mercapto- ethanol (700µl/200mls) for 30 minutes at 65°C. Subsequently the slides were incubated in 2X SCC for 15 minutes at 65°C, 0.1 X SCC for 12 minutes at 65°C, 70% Ethanol, 0.3 M NH4OAC for 5 minutes twice at room temperature, 80% Ethanol, 0.3 M NH4OAC for 1 minute at room temperature, 95% Ethanol, 0.3 M NH4OAC for 1 minute at room temperature and finally in 100% Ethanol- twice for 1 minute each at room

temperature. The slides were allowed to air dry and were placed flat in a light tight box. In the dark room, a sheet of X-OMAT film was placed flat over the slides and left to develop overnight. The film was developed the next day and the specificity of the probe and the intensity of the signal evaluated so as to determine how long the emulsion is left on before developing.

AUTORADIOGRAPHY AND STAINING

A 10 ml aliquot of Kodak NB2 emulsion was thawed at 42°C for 15 minutes. In the dark room the emulsion and 10mls of 2% glycerol were mixed and inverted once. The mixture was poured in to a slide mailer and each slide was dipped into the emulsion for three seconds. After dipping the slide was allowed to drain for three seconds. The bottom slide edge was then blotted and laid flat in a light tight box for 6 hours. After 6 hours drying the slides were transferred to a smaller box-containing desiccant in the dark room. The slides were stored in an air locked moisture free jar in the dark at 4°C for the appropriate time estimated from the developed film. When the emulsion had been on for an appropriate time the slides were washed in chilled developer for 4 minutes, washed in H_2O for 10 seconds, fixed for 5 minutes in fixer, washed in two changes of H_2O for 5 minutes each, counter stained in haematoxylin for 30 seconds, cleared in H_2O for 5 minutes in running H_2O, dehydrated through 95% ethanol, three 100% ethanol changes and three xylene changes for 1 minute each and finally the sections were mounted in DPX, cover slipped and examined under dark field microscopy.

3.18-TWO STEP RT-PCR METHOD

Reverse transcription PCR was performed using the superscript one step RT-PCR system with Platinum Taq kit (Invitrogen,Carlsbad, CA) and 100ng samples of total ovarian RNA isolated using the RNeasy mini kit (Qiagen Sciences). Reactions were performed as suggested by the manufacturer and additionally 0.625 Ci of $[a-^{32}P]dCTP$ with a specific activity of 3,000 Ci/mmol (MP Biomedicals) were added to each reaction to generate a quantifiable radioactive signal. Cycling conditions for the Mkp-3 reaction, *Fshr* and *Lchgr* was as follows:

Step 1- reverse transcription reagents and PCR programme

Total RNA (300 ng), Oligo dT (500 ng/µl), dNTPs (10mM), 5X buffer, DTT (100mM), RT enzyme 1U, H_2O.

1. 37°C- 45 minutes

2. 65°C-15 minutes

3. 15°C-forever

Step 2 cDNA amplification PCR programme

1. 94°C-3 minutes

2. 94°C- 30 seconds

3. 55°C- 30seconds

4. 72°C-30 seconds

5. Go to step 2 -27X

6. 72°C- 5 minutes

7. 15°C- forever

Preliminary studies determined that the cycle numbers fell within a linear range of PCR amplification. Once reverse transcribed the samples were separated by electrophoresis on 10% PAGE gels for 2 hours at 130V. Once separated the gels were dried and exposed to Biomax XAR film (Eastman Kodak Co.) to generate semi-quantitative images.

3.19-ANIMAL AND HORMONE TREATMENT METHODS

All mouse genotypes under study were housed under a 16 hour light /8 hour dark schedule in the centre of comparative medicine at Baylor College of Medicine and provided food and water freely. Animals were treated under the National Institutes of Health Guide for the Care and Use of Laboratory Animals as approved by the Animal Care and Use Committee at Baylor College of Medicine. Exogenous gonadotrophins were administered to 23-24 day old female mice wild type or mutant and involved injection with PMSG or 4 IU of equine Chorioic Gonadotrophin to stimulate folliculargenesis and 48 hours later injected with 5 IU hCG to stimulate ovulation.

4) RESULTS

Ras is a primary activating component of the MAPK pathway Ras/Raf/MEK/ERK. It also acts as a supportive activator of the PI3K cascade. To determine the function and impact of Ras on vital ovarian genes and proteins of these signal transduction pathways Ras was engineered to be constitutively active. The effects of constitutively active Ras on ovarian function and morphology i.e. (the extent to which Ras influences the ovarian phenotype and how important control of Ras is to function) was assessed via the following histological techniques: H&E, immunohistochemistry, in-situ hybridisation and in situ X-Gal/β galactosidase staining. The effect of constitutively active Ras on vital signalling genes- *Fshr*, *Lghcr* and *Mkp-3* was assessed via RT-PCR. Additionally the effect of constitutively active Ras on vital signalling protein intermediates was assessed via western blot and immunofluorescence staining.

To study the effects of constitutively active Ras on ovarian cell function, morphology, vital signalling genes and signalling protein intermediate expression under controlled conditions, female mice of the LSL-K-ras^{G12D};$Amhr$-2-Cre, LSL-K-ras^{G12D};Cyp-19-Cre and wild type genotypes were successfully breed and obtained from the Baylor College of Medicine Transgenic Mouse Facility (TMF). To confirm the genotypes of the mice used, DNA was extracted from the mouse tail and PCR amplified using conditions as described in the methods. Expected results for the K-ras^{G12D};$Amhr2$-Cre and $Cyp19$-Cre genotypes were PCR products of approximately 600, 300 and 300 base pairs respectively (*Fig.4.1*). Over a hundred mouse models were genotypically analysed.

Assessment of mouse genotypes via mouse tail DNA extraction and PCR amplification

(Fig.4.1). Genotyping for the *K-ras*, *Amhr2-Cre* and *Cyp19-Cre* genotypes
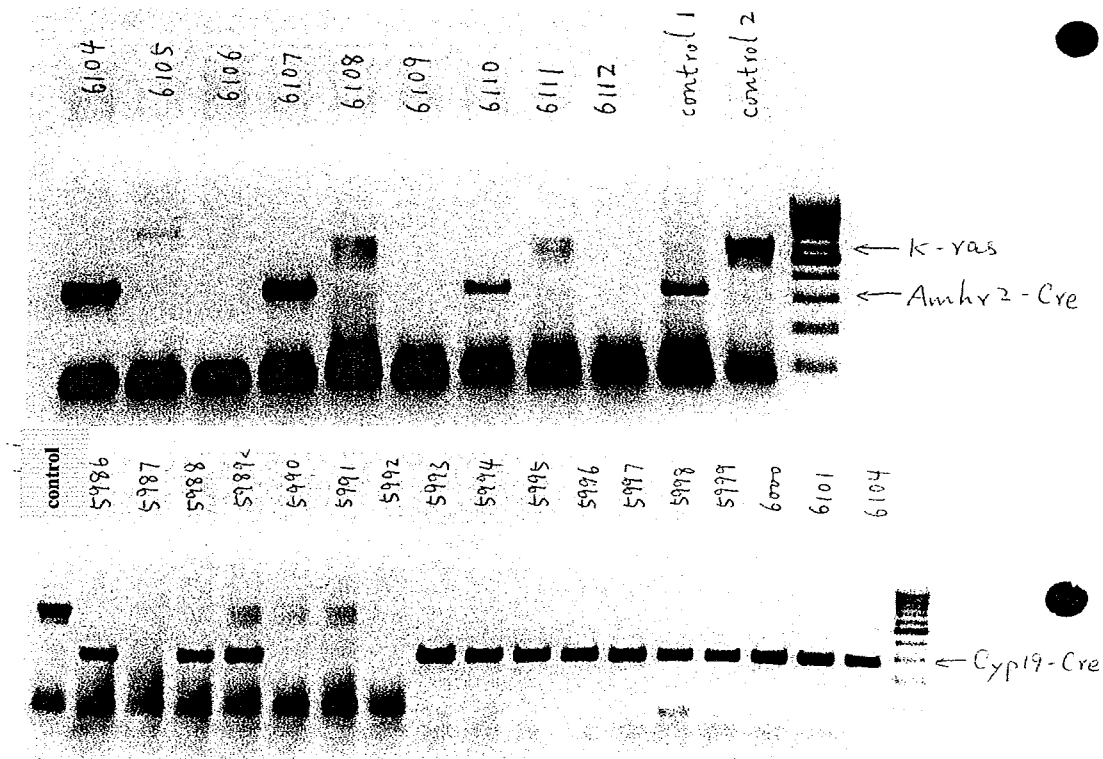

Fig.4.1 showing the genotyping results of a representative number of mice tested for the *K-ras*, *Amhr 2-Cre* and *Cyp-19-Cre* genotypes. The bands represent PCR amplified mouse tail DNA run out and visualized on a 1.5% agarose gel. The *K-ras*, *Amhr 2-Cre* and *Cyp-19-Cre* genotypes are represented by bands of approximately 600, 300 and 300 base pairs respectively. Left of the gel a molecular weight marker is shown.

A histological evaluation of constitutively active Ras expression and function in the mouse ovary via assessment of β- galactosidase expression, macroscopic appearance, H&E staining and in-situ hybridization analysis and immunohistochemistry.

Using mice of the confirmed genotypes as shown above the aim of the first experiment was to determine the ovarian location of constitutively active Ras. The location of constitutively active Ras (CA-Ras) was determined via an in-situ X-gal/β galactosidase assay. Ovaries were removed from the *Amhr2-Cre* and *Cyp-19-Cre*, PMSG treated and untreated mice and stained for β- galactosidase activity. In the *Amhr-2-Cre* and *Cyp-19-Cre* mice, *Cre* recombinase enzyme allows the expression of constitutively active Ras by the removal of stop elements in the genome and so allowing transcription of the *K-ras* gene in both the *LSL-K-ras^{G12D};Amhr2-Cre* and *LSL-K-ras^{G12D};Cyp-19-Cre* models.

51

Thus, wherever *Cre* is expressed constitutively active Ras is expressed. *Cre* allows for the expression of β galactosidase and this was used as a marker for *Cre* activity, and thus CA-Ras expression. Additionally this experiment determined if the *Amhr-2* and *Cyp-19* promoters used in these mouse models were successful drivers of *Cre* in order to study the effects of constitutively active Ras on ovarian morphology and function. The final aim of this experiment was to determine the possibility of *Cre* activity in other reproductive organs outside the ovary namely the uterus.

Fig.4.2 presents the results of this study and demonstrates *Cre* activity in the granulosa cells of all secondary and small antral follicles and at lower levels in earlier follicles in both the *Amhr2-Cre* and *Cyp-19-Cre* models (with and without PMSG treatment). Low *Cre* activity was found in some theca cells and oocytes in the *Amhr2-Cre* model but not in the *Cyp19-Cre* model *(Fig.4.2)*. In the wild type ovary there was no *Cre* activity. *Cre* activity was shown to be negative in the uterus of day 9, 10 and day 11 pregnant mice of genotype Rosa $^{Flox/+;}$ *Amhr-2* $^{Cre/+}$ (data not shown). From this we can infer that Ras expression occurs majoritively in the granulosa cells when driven by the *Amhr2* and *Cyp-19* promoters.

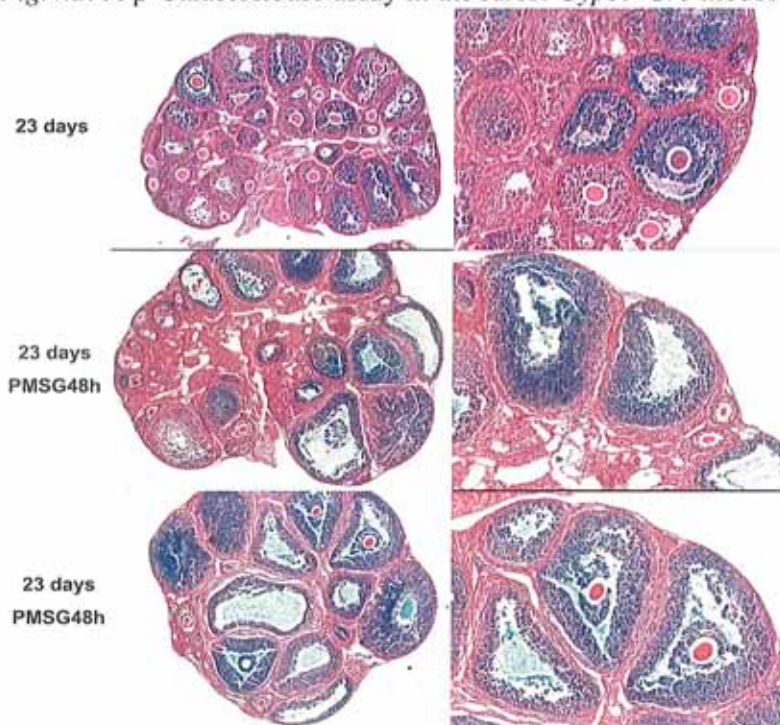*Fig.4.2*: A β Galactosidase assay in the *R26R-Cyp19-Cre* mouse model

Fig.4.2 shows an X gal/β galactosidase in-situ assay on *Cyp19-Cre* ovaries with and without pregnant mare serum gonadotrophin (PMSG) treatment at X5 and X10 magnifications. *Cre* activity is denoted by a blue staining where β-galactosidase on contact with its substrate X gal forms a blue precipitate. The majority of the staining is the ovarian granulosa cells.

Constitutively active Ras was shown to be located mainly in the ovarian granulosa cells via the β-galactosidase assay. The following experiment examined the effect of the *K-ras* constitutively active mutant on the macroscopic ovarian morphology, the morphology of the granulosa cells and any resultant ovarian malfunctions. To examine the effect of constitutively active Ras on ovarian morphology and function a controlled ovarian macroscopic examination and H&E experiment was conducted on the K-Ras mutant models. On macroscopic analysis the dissected Ras mutant ovaries (*LSL-K-ras^{G12D}Amhr2-Cre*) were shown to be up to 4X larger and heavier to wild type mice of the same age (*Fig.4.3*).

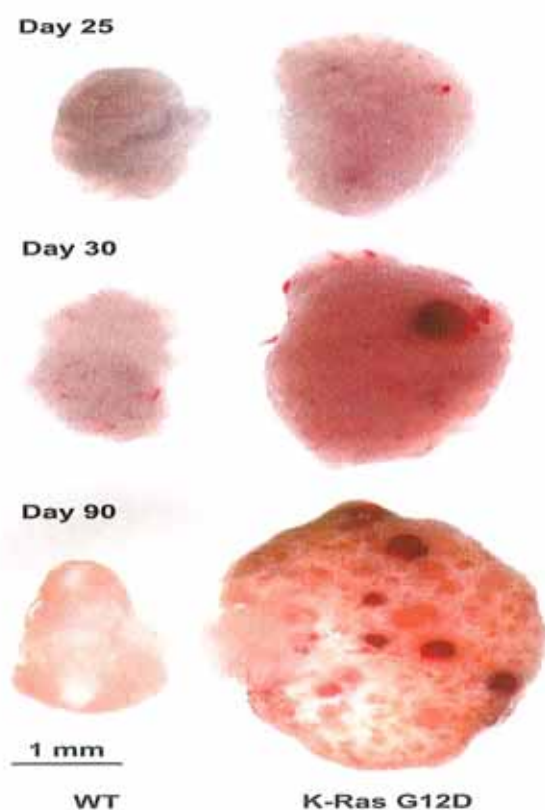Fig. 4.3: *K-ras* Mutant ovaries are 4X larger to wild type

Fig 4.3. Shows a macroscopic image of wild type (left) and *K-ras* mutant ovaries (*LSL-K-ras^{G12D}Amhr2-Cre*) (right) at days 25, 30 and 90. At all time points studied the *K-ras* mutant ovaries are larger and after 90 days are shown to be approximately four times larger. The *K-ras* mutant ovaries also show signs of possible angiogenesis inferring to tumourigenesis.

H&E staining of wild type ovaries demonstrated that most antral follicles had ovulated and lutenised 16 hours post hCG treatment. However in the *K-ras* mutant ovaries many grown antral follicles are still seen with well extended cumulus-oocyte complexes trapped inside i.e. unovulated and unlutenised (*fig.4.4*) In addition many *K-ras* mutant ovaries developed tumour like structures. These large *K-ras* mutant ovaries showing multiple tumour like structures displayed follicle like structures with compressed granulosa cells often without a cavity. An odd shaped oocyte was sometimes enclosed in these structures sometimes being pushed to the outside of the follicle (*fig.4.4*)

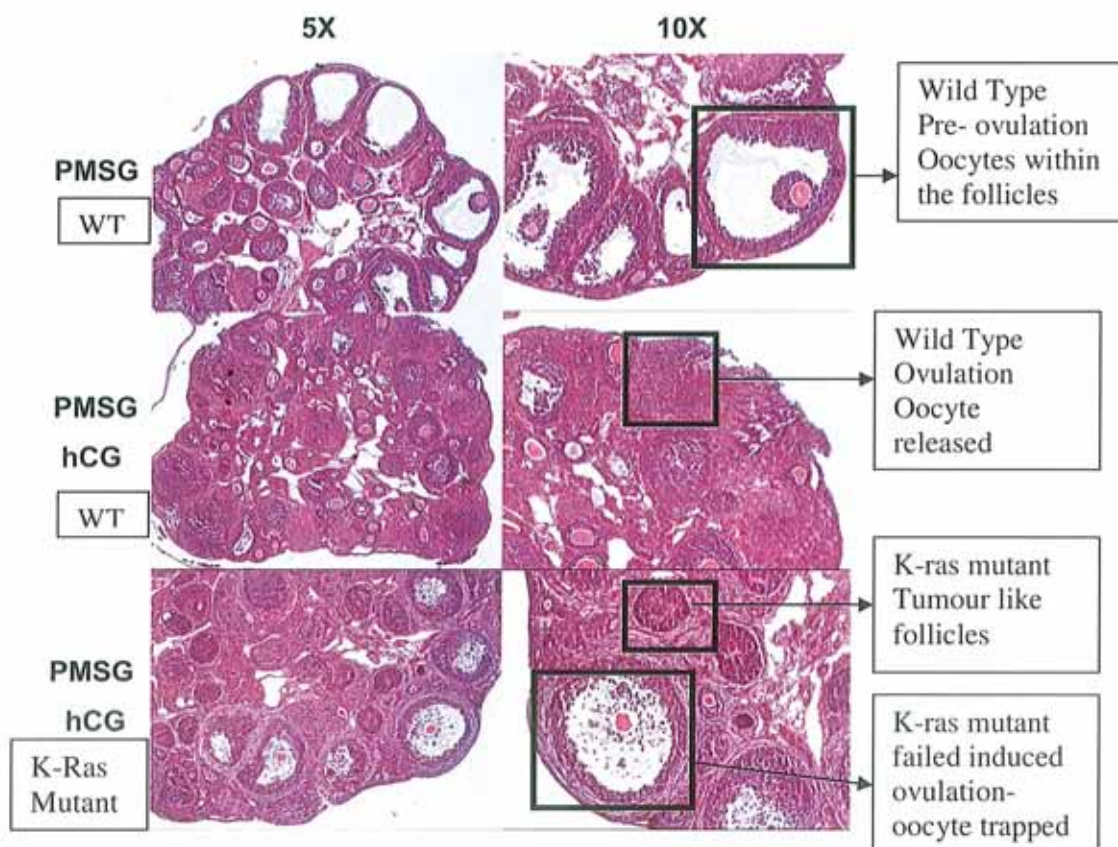*Fig.4.4*: H&E of a Wild Type versus *K-ras* mutant ovary

Fig.4.4 Shows H&E stained sections of wild type (WT) ovaries (top/middle left and right) and *K-ras* mutant ovaries (bottom left and right) PMSG treated and untreated at 5X and 10X magnifications. (top- left and right) shows the WT preovulatory follicle with the oocytes still within the follicle. (middle left and right) shows a WT PMSG and hCG induced ovulated ovary. (Bottom left and right) shows a *K-ras* mutant PMSG and hCG treated ovary presenting with tumour like follicles and a failed induced ovulation.

As the *K-ras* mutant ovary demonstrated an abnormal tumourous phenotype and malfunctioning properties it was necessary to determine possible reasons for the abnormal ovarian structure and function. Thus, controlled In situ hybridisation and immunohistochemistry experiments were conducted on these constitutively expressing *K-ras* ovaries to examine the expression of genes and proteins known to influence folliculargenesis, ovulation and lutenisation.

In situ hybridization experiments on the *K-ras* mutant ovaries demonstrated that liver receptor homologue-1 (*Lrh-1*) mRNA an important granulosa cell marker gene was not expressed in these tumour like structures (*Fig.4.5*). In the wild type ovary LRH-1 was shown to be highly expressed in the granulosa cells. Similarly, little to no expression of *p450 SCC* mRNA was seen in these tumour-like structures and, versican mRNA in-situ results suggested that versican mRNA expression is devoid also in these tumour-like structures. Wild type in-situ experiments confirmed p450 side chain cleavage (*p450 SCC*) and *versican* mRNA to be expressed in the granulosa cells and matrix respectively (data not shown). In addition, wild type ovaries by immunohistochemistry demonstrated that FOXO1a protein was specifically expressed in the granulosa cells and oocytes of all follicles as expected. However within these abnormal follicle-like structures of the *K-ras* mutant ovaries both the granulosa cells and the oocytes were devoid of FOXO1a staining (*Fig 4.6*).

Fig.4.5- In –Situ hybridisation of *Lrh-1* in wild type and *k-ras* mutant mice ovaries

| 5X light Field | 5X dark field |

Immature wild type ovaries showing normal follicles with fluorescence in those mature enough to induce the expression of *Lrh* -1.

| 5X light Field | 5X dark field |

K-ras knock-in ovaries showing lack of fluorescence in the odd shaped granulosa cells and tumour like structures.
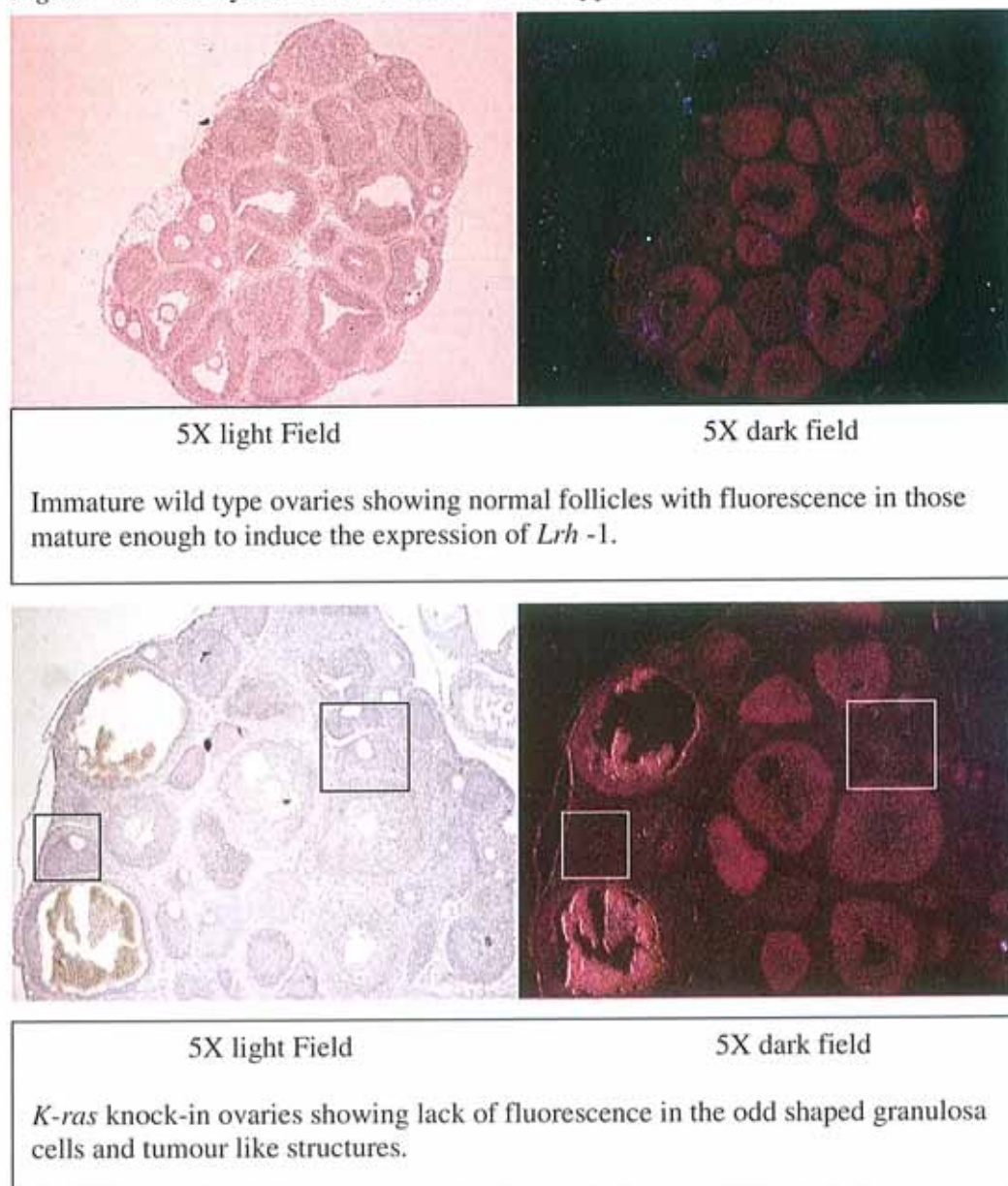
Fig.4.5 shows an in-situ hybridisation experiment for *Lhr-1* mRNA expression. (Top left) shows a 5X Wild type light field ovary section with black *Lhr-1* staining. This section is used to compare to the dark-field section. (Top left) shows the same section in dark field. It demonstrates fluorescence in follicles mature enough to induce the expression of *Lhr-1*. (Bottom left) shows a 5X light field *K-ras* mutant (*LSL-K-ras^{G12D};Amhr2-.Cre*) ovary section. It shows black *Lrh-1* staining in mature follicles. (Bottom right) shows the same picture as the latter in dark field and demonstrates the lack of *Lrh-1* expression in the aberrant follicles (highlighted in boxes).

Fig.4.6: FOXO 1 Immunohistochemistry staining in wild type and *K-ras* mutant ovaries

Wild Type
FOXO1a X10

FOXO1a staining in all normal ooytes and follicles

K-ras^{G12D}*Amhr2-Cre*
FOXO1 X10

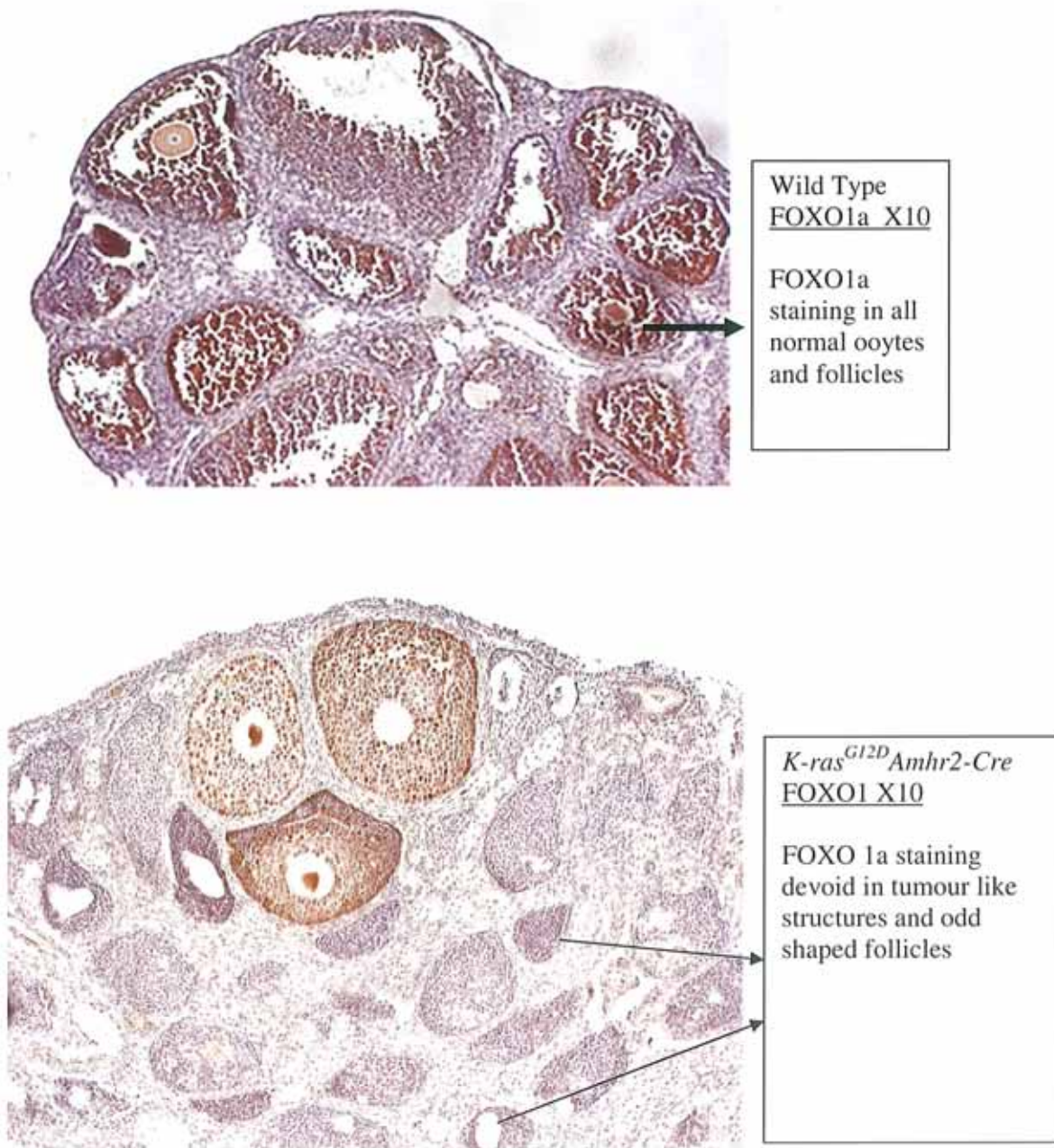FOXO 1a staining devoid in tumour like structures and odd shaped follicles

Fig.4.6 Shows an immunohistochemistry experiment for FOXO1a protein expression in the wild type (top) and *K-ras* mutant (bottom) ovaries at 10X magnification. FOXO1a is shown to be expressed in all granulosa cells and oocytes in the wild type ovary. In contrast the *K-ras* mutant (*LSL-K-ras*^{G12D}*; Amhr2-Cre*) ovary is devoid of FOXO1a staining in the aberrant follicles.

As these results demonstrated that there was aberrant protein and gene expression in the K-Ras mutant ovary the following objective was to study the effects of constitutively active *K-ras* on the gene expression of vital ovarian signalling genes- the *fshr*, *lhcgr* and *Mkp-3* genes.

An evaluation of constitutively active Ras expression on vital ovarian signalling genes- *fshr*, *lhcgr* and *Mkp-3* genes via RT-PCR.

The abnormal structure and function demonstrated in the *K-ras* mutant ovary indicated a possible malfunction in ovarian biochemical signalling. Thus, the following experiment attempted to gain insights into the signalling mechanisms of Ras and the possible causes of a signalling malfunction leading to abnormal structure and function. In this study three vital genes for ovarian signal transduction were chosen for study:

I) Follicle stimulating hormone receptor (*Fshr*) gene, vital for reaction with FSH to augment folliculargenesis.

2) Lutenising hormone receptor gene *(Lhcgr)*, vital for reaction with LH to augment ovulation

3) MAP kinase phosphatise (*Mkp-3*) gene, a dual specific phosphatase hypothesised to be vital for control of the Ras/Raf/MEK/ERK cascade.

As the FSHR and LHR are central to the processes of folliculargenesis and ovulation and as MKP-3 is a dual specific phosphatise hypothesised to dampen the effect of the Ras/Raf/MEK/ERK cascade, it was important to determine the effects of constitutively active *ras* on these genes. These genes were examined by RT-PCR using total ovarian RNA from both wild type and mutant constitutively active Ras mouse models. Total ovarian RNA was tested in both mouse models at days 15 and 23 without gonadotrophin treatment, at 48 hours post PMSG treatment and at 8 and 16 hours post hCG treatment to determine their expression dynamics.

1) *Fshr*

The FSH receptor was shown to be present at all stages and conditions studied i.e. at day 15 and 23 without gonadotrophin treatment, 48 hours post PMSG and at 8 and 16 hours post hCG treatments. The *Fshr* was demonstrated to be induced greatly by PMSG treatment and hCG treatments in the wild type mouse. However, in comparison the constitutively active mutant model (*LSL-K-Ras*^{G12D}*;Amhr2-Cre*) showed the *Fshr* receptor to be expressed at a lower level at all stages studied compared to the wild type *(Fig.4.7a)*. The control cyclophilin B was present under all conditions studied.

2) *Lhcgr*

The LH receptor was shown to be induced at 48 hours post PMSG treatment and at 16 hours post hCG treatment in the wild type mouse. However, in the K-ras mutant (*LSL- K-Ras* ^{G12D} *Amhr2-Cre*) mouse the *Lhcgr* is not induced under any of the conditions studied. In fact the receptor was shown to be down regulated *(Fig.4.7a)* The control cyclophilin B was present under all conditions studied.
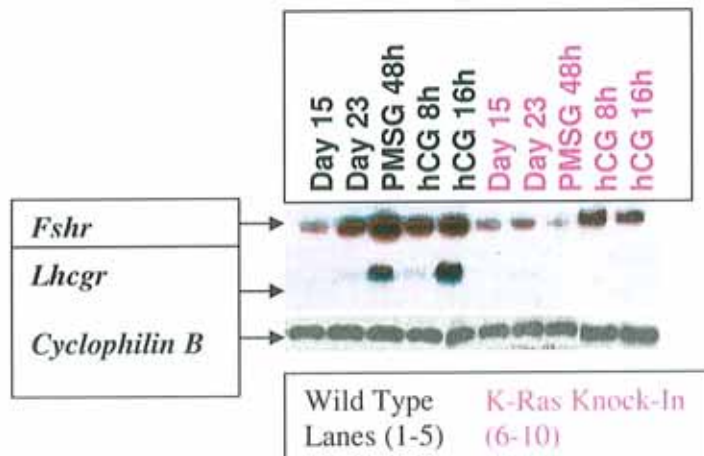
Fig.4.7a: RT-PCR of *Fshr* and *Lhcgr* genes

Fig.4.7a: Shows an RT-PCR experiment in the wild type versus the *K-ras* mutant (*LSL-K-ras*^{G12D}*;Amhr2-Cre*) knock-in mouse model. It demonstrates the expected up-regulation of the *Fshr* and *Lhcgr* receptor genes after gonadotrophin treatment in the wild type. It shows the down regulation of the *Fshr* and *Lhcgr* genes when the *K-ras* gene is made constitutively active in the knock-in model even on induction. Cyclophilin B is the control.

3) *Mkp-3*

Control of Ras regulated pathways holds the key for the prevention of excess proliferation and a propensity to oncogenesis. The MAP kinase phosphatases (MKPs) are a newly identified group of

MAPK inactivators that regulate the magnitude and duration of signalling. MKP-3 has been proposed as an important MKP controlling the Ras/Raf/MEK/ERK cascade. RT-PCR analysis was conducted to examine the effect of mutant constitutively active *K-ras* on the *Mkp-3* gene expression so as to hypothesise the mechanism and function of *Mkp-3* in the cascade.

RT-PCR revealed that *Mkp-3* is expressed in the ovaries of day 15 and 23 old *LSL-K-Ras* $^{G12D;}$ *Amhr2-Cre* mice even without gonadotrophin treatment, whereas it is expressed at much lower levels in wild type ovaries of the same age. Semi quantitative RT-PCR results show that *Mkp-3* expression is induced post 8 hour and 16 hour hCG treatments in both the wild type and K-ras mutant mice. However no great difference is seen in *Mkp-3* expression at 8 hours and 16 hours post hCG treatment between the wild type and *K-ras* mutant mice *(Fig.4.7b)*. An RNA-In-situ hybridisation experiment showed *Mkp-3* RNA to be significantly up regulated in wild type mouse granulosa cells 8 hours post hCG treatment (data not shown). The control cyclophilin B was control shown to be present under all time points and conditions tested.

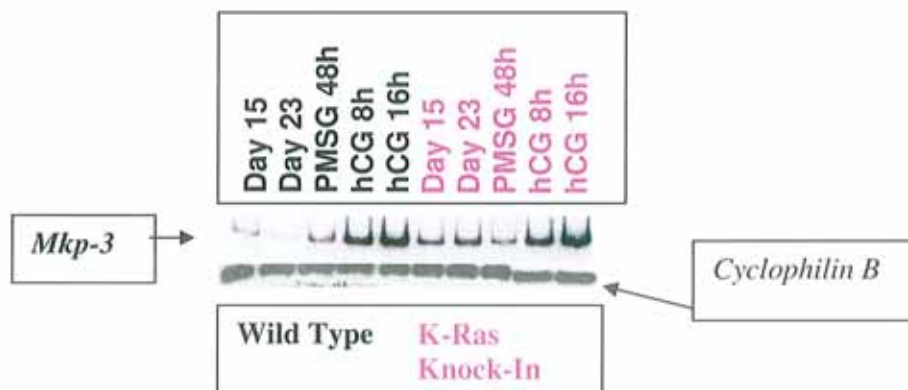*Fig. 4.7b*: RT-PCR of the *Mkp-3* gene

Fig.4.7b: Shows an RT-PCR experiment for *Mkp-3* expression in the wild type versus the *K-ras* mutant knock-in model (*LSL-K-ras^{G12D};Amhr2-Cre*). It demonstrates that constitutively active *ras* up-regulates the expression of *Mkp-3* without gonadotrophin. It shows no great upregulation of *Mkp-3* expression between the wild type and the *K-ras* knock-in mouse even on gonadotrophin induction possibly due to the hypothesised negative feedback action of MKP-3 on ERK1/2 a downstream effector of Ras.

These results showed aberrant expression of signal transduction genes. The following experiment aimed to determine the effects of constitutively active *ras* and thus the effects of these aberrant expressing genes on protein intermediates of the Ras/Raf/MEK/ERK and PI3K cascades. p-PKB and p-ERK are two such protein intermediates. They are important downstream effectors of Ras. Determination of their expression levels and their ovarian locality in the wild type and *K-ras* mutant mouse ovary is important to the study of Ras regulated signalling mechanisms and control that govern ovarian structure and function. Western blot was employed to determine the protein expression levels of p-ERK and p-PKB. p-ERK and p-PKB protein expression location was determined via immunofluorescence in gonadotrophin treated wild type and *K-Ras* mutant ovaries.

An evaluation of constitutively active Ras on the protein expression of the Ras cascade protein intermediate p-ERK and the PI3K cascade intermediate p-PKB via western blot and immunofluorescence.

P-ERK 1/2

The activated form of the external regulated kinase p-ERK1/2 of the Ras/Raf/MEK/ERK cascade showed that both ERK isoforms 1 and 2 were induced two hours post hCG treatment in the wild type mouse. Absent expression presented in the immature untreated, PMSG and the 12 and 16 hour post hCG treated wild type mice. At 4 and 8 hours post hCG treatment low expression was shown in the wild type mouse *(fig.4.8a)*. In the *ras* mutant (*LSL-K-Ras^{G12D};Cyp-19-Cre*) mouse p-ERK is still shown to be induced 2 hours post hCG treatment; however in comparison to the wild type mouse p-ERK expression it is down regulated *(Fig.4.8b)*. Immunofluorescence supported the western blot findings. immunofluorescence demonstrated that p-ERK expression was highest 2 hours post hCG treatment in the granulosa cells, especially in the mural granulosa cells and that expression had almost completely disappeared 16 hours post hCG treatment in the wild type mouse *(fig.4.8c)*. In the *K-Ras* mutant (*LSL-K-ras^{G12D};Cyp19-Cre*) mouse immunofluorescence confirmed the western blot findings where minimal to absent p-ERK expression was shown 2 hours post hCG treatment *(fig.4.8d)*. However in contrast immunofluorescence in the K-ras mutant (*LSL-K-ras^{G12D},Amhr2-Cre*) model p-ERK expression was still shown to exist 2 hours post hCG treatment *(fig.4.9b)*.

Fig 4.8a: Western blot of wild type whole mouse ovary lysate
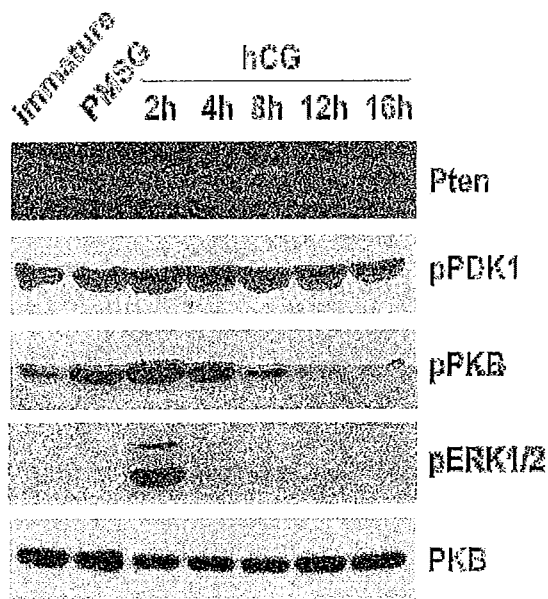

Fig.4.8a: Shows a western blot of wild type (WT) whole mouse ovary lysate for p-ERK (phosphorylated-Extracellular Related kinase-ERK), p-PKB (phophorylated Protein kinase B), PKB (unphosphorylated), PTEN (phosphate and tensin homologue (Protein) and pPDK1 (phosphoinositide dependant protein kinase 1) expression. Expression is shown for immature, pregnant mare serum gonadotrophin (PMSG) treated and hCG(human chorionic gonadotrophin) treated wild type mice at different time points(2,4,8,12 and 16 hours) post treatment.

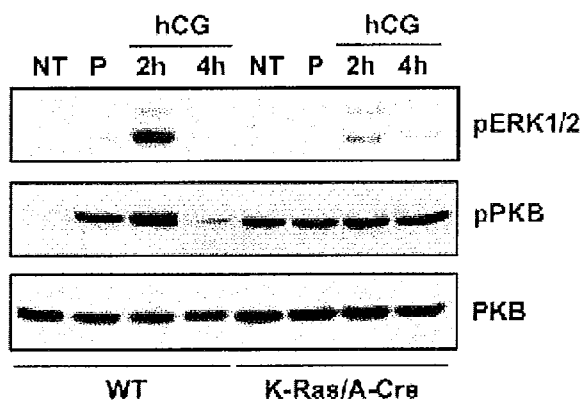*Fig.4.8b* Western blot of wild type versus *K-ras* mutant whole mouse ovary lysates

Fig.4.8b: Shows a western blot of wild type (WT) versus *K-ras* mutant (*LSL-K-Ras^{G12D} Cyp19-Cre*) ovary lysates for the protein expression of the Ras signalling down stream intermediates PKB, p-PKB, p-ERK (the phosphorylated and active forms of Protein kinase B-PKB and Extracellular related kinase-ERK), where PKB is a loading control. The mouse ovary lysates were extracted from untreated (NT), PMSG pregnant mare serum gonadotrophin (P) treated and hCG- human chorionic gonadotrophin treated WT and *K-ras* mutant mice 2 and 4 hours post hCG treatment.

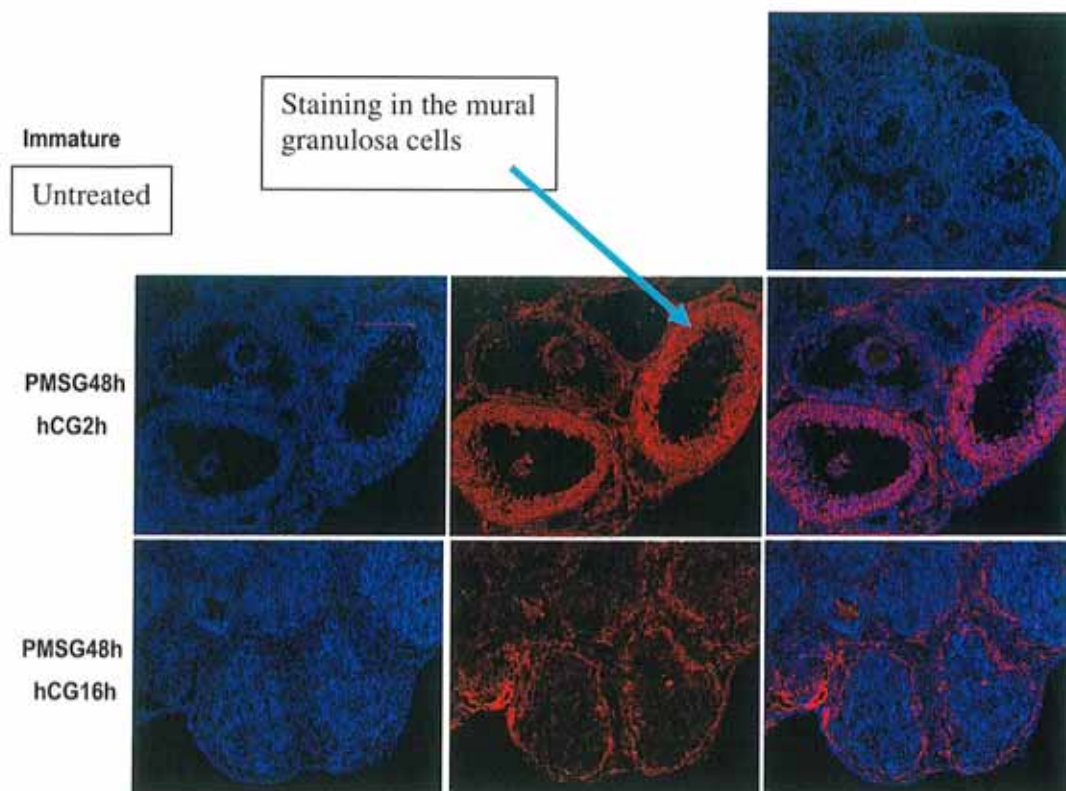*Fig. 4.8 c:* p-ERK immunofluorescence in the wild type mouse

Fig.4.8c: Showing p-ERK (active phosphorylated ERK) immunofluorescence staining within the granulosa cells of the ovary at 10x magnification. Expression is shown to be intense post PMSG and 2 hours post hCG treatments. After PMSG and 16 hours post hCG treatment expression is almost gone.

Fig.4.8d: p-ERK immunofluorescence in the wild type versus the *K-ras* mutant (*LSL-K-Ras* ^{*G12D*}*;Cyp19-Cre)-* 2 hours post hCG treatment.
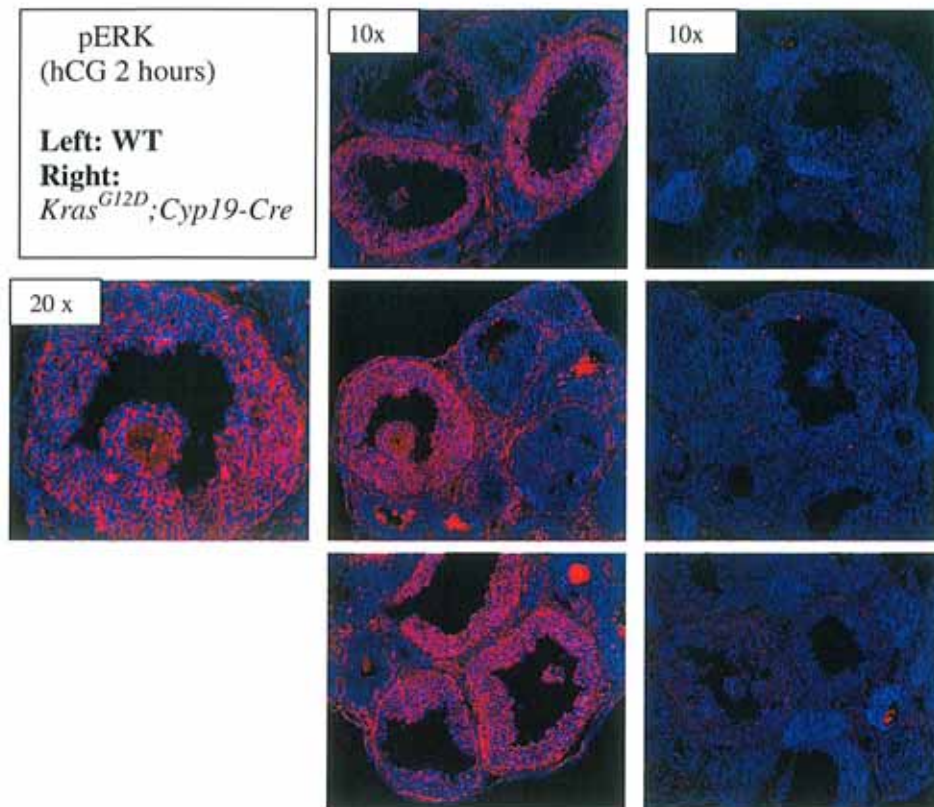
Note: mice were primed with PMSG for 48 hours first

Fig. 4.8d: Showing the high expression of p-ERK in the wild type mural granulosa cells post PMSG priming and 2 hours post hCG treatment in the wild type ovary at 10x and 20x magnification. In comparison the K-Ras mutant ovary (10x) shows no p-ERK expression under the same conditions as the latter.

p-PKB

The activated form of the protein kinase B intermediate, p-PKB of the PI3K cascade was induced by PMSG, 2 and 4 hours post hCG treatments in the wild type mouse. However, p-PKB expression was shown to be moderately induced by PMSG treatment, greatly induced two hours post hCG treatment and at 4 hours post hCG treatment induction was down regulated. Expression was therefore highest 2 hours post hCG treatment in the wild type. In the immature wild type untreated ovaries, expression was low to absent. At 8 hours and 16 hours post hCG treatment p-PKB expression decreased to almost absent levels in the wild type mouse (*fig.4.8a*). In the *K-ras* mutant mouse (*LSL-K-ras*^{*G12D*}*; Amhr2-Cre*) p-PKB was induced in the immature untreated, PMSG, 2 hours and 4 hours post hCG treatment and no significant difference was demonstrated in the level of expression between them (*fig.4.8b*).

These results were supported by immunofluorescence, where p-PKB expression was shown to be present in the oocytes and granulosa cells of the ovaries 2 hours post hCG treatment *(Fig.4.9a)*. In the other *K-ras* mutant (*LSL-K-ras^{G12D},Amhr2-Cre*) p-PKB expression is shown to be expressed in the same pattern *(Fig.4.9 b)*.

Fig.4.9a: p-PKB immunofluorescence in wild type versus *K-ras* mutant (*LSL-K-ras^{G12D};Cyp19-Cre*) ovaries.

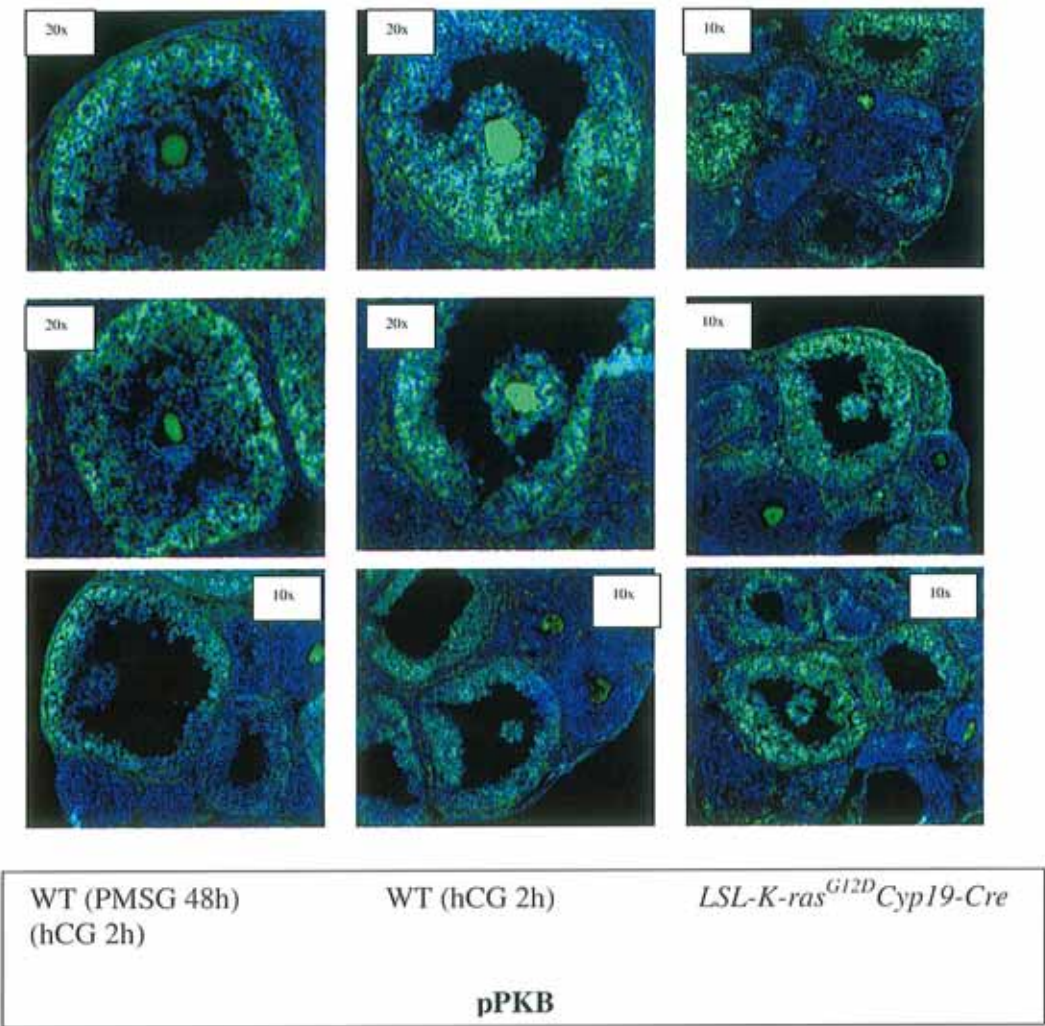| WT (PMSG 48h) (hCG 2h)	WT (hCG 2h)	*LSL-K-ras^{G12D}Cyp19-Cre*
	pPKB	

Fig.4.9a. Shows the phosphorylated form of protein kinase B (p-PKB) expression in the wild type (WT) pregnant mare serum gonadotrophin (PMSG) treated and 2 hours post human chorionic gonadotrophin (hCG) treated ovaries (10x and 20x). p-PKB is also shown in the PMSG primed and 2 hour post hCG treated *K-ras* mutant (*LSL-K-Ras^{G12D};Cyp19-Cre*) model (10x and 20x). Expression is shown in the granulosa cells and oocytes.

Fig.4.9b: Immunofluorescence of p-PKB versus p-ERK in the *K-ras* mutant (K-ras[G12D]Amhr2-*Cre*).

| pPKB 10x | p-ERK 10x |

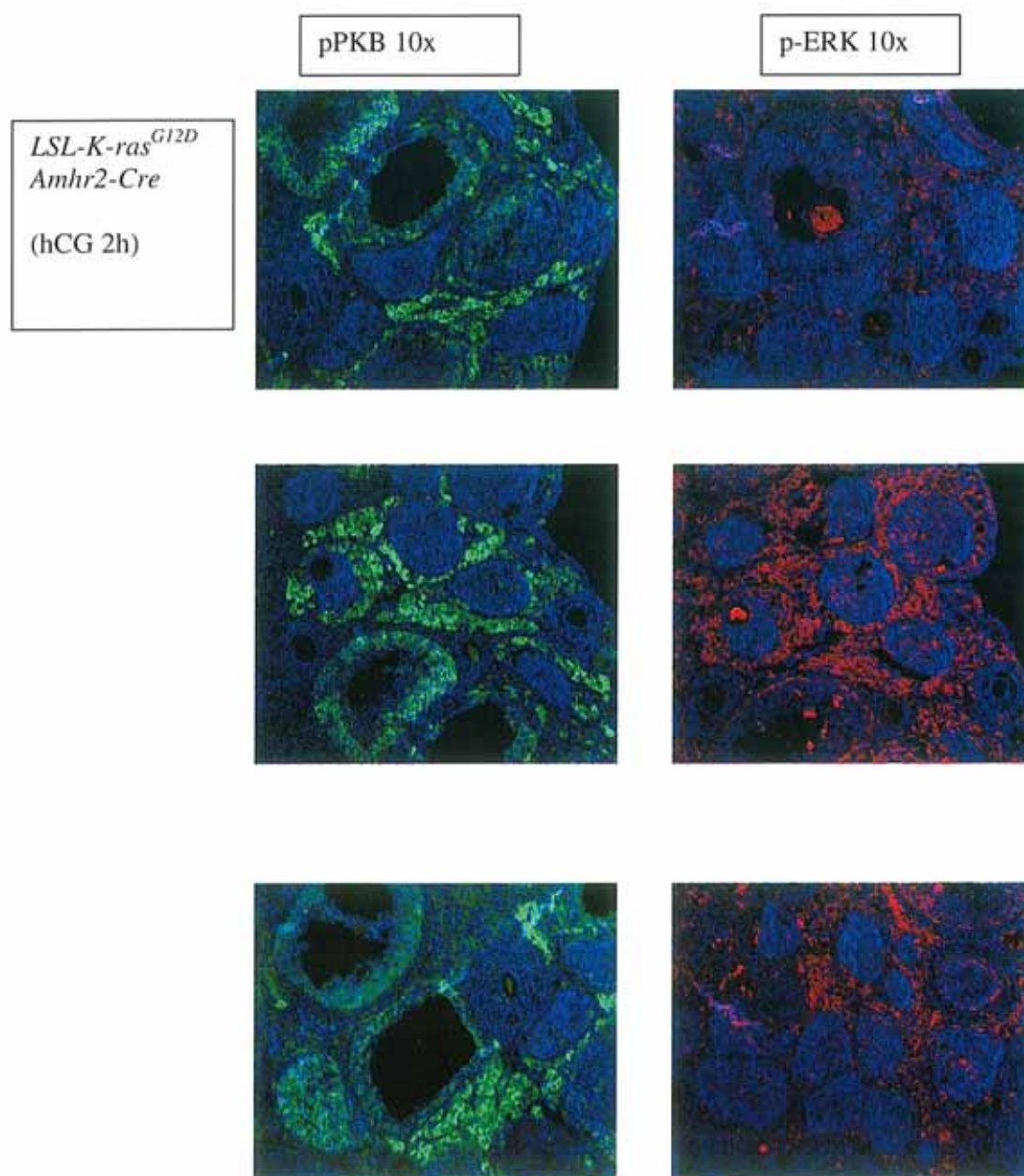*LSL-K-ras[G12D]*
Amhr2-Cre

(hCG 2h)

Fig.4.9b: Showing the expression of p-PKB (left green staining) and p-ERK (right red staining) in the ovaries of the *K-ras* mutant *LSL-K-ras[G12D];Amhr2-Cre* post PMSG priming and 2 hours post hCG treatment at 10x magnification.

The results have demonstrated that constitutively active *ras* alters ovarian structure and function. It causes the ovaries to become 4X larger compared to wild type ovaries. It causes the formation of aberrant shaped follicles and tumour-like follicles. It results in fertility problems where the *K-ras* mutant knock-in model (*LSL-K-ras^{G12D},Amhr2-Cre*) has shown an inability to ovulate even when induced. Constitutively active *ras* shows the aberrant expression of vital ovarian genes and signalling proteins. The *Fshr* and *Lchgr* genes are down regulated, the *Mkp-3* gene expression is dysregulated and Ras down stream signalling protein intermediates p-PKB and p-ERK expression is altered. These factors may all accumulate to account for the biochemical dyfunctions and aberrant morphology seen in these K-*ras* mutant mouse models. These results confirm that Ras plays a critical role in ovarian signalling.

SECONDARY AIM RESULTS

As Ras is known to support the activation of the PI3K cascade a vital survival and proliferative pathway, the following experiment was designed to test the objective of studying the histological effect on the ovary when PTEN the negative regulator of the PI3K cascade is removed. Additionally histological analysis was conducted to determine the morphological and functional consequences for the ovary when PTEN and K-Ras combined were removed so as to ascertain the importance of these signalling components in maintaining ovarian morphology. To ascertain the expression level and ovarian cell type in which PTEN is majoritively expressed, western blot analysis and immunofluorescence was conduced on the wild type gonadotrophin treated mouse ovary. In the wild type mouse the expression of PTEN was shown not to differ greatly over the hormone and time conditions studied in western blot analysis *(Fig.4.8a)*. In contrast immunofluorescence showed a difference in the level of fluorescent PTEN staining in the mural granulosa cells of the ovary. Levels of expression in the immature untreated and PMSG treated wild type mice were lower in comparison to those treated with hCG *(Fig.4.10a)*.

Fig.4.10a: PTEN Immunofluorescence in the wild type mouse ovary.

Immature untreated

PMSG 48 hours

PMSG 48hrs
2 Hrs hCG

Mural granulosa cells
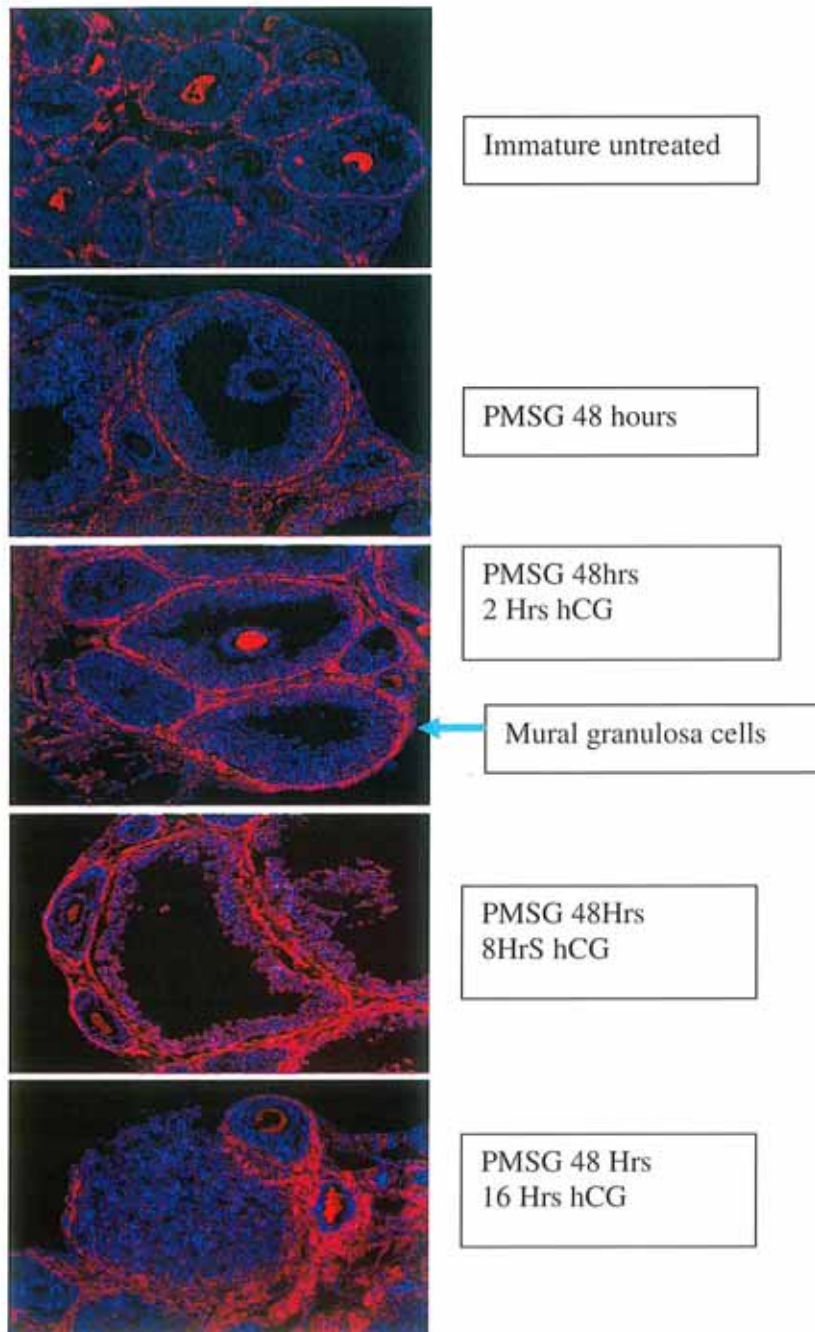
PMSG 48Hrs
8HrS hCG

PMSG 48 Hrs
16 Hrs hCG

Fig.4.10a: showing immunofluorescence on 10X wild type gonadotrophin treated ovary sections. Positve staining is denoted by red fluorescent staining shown in the mural granulosa cells at all time points studied.

As PTEN was shown to be majoritively expressed in the mural granulosa cells the following aim was to examine the controlling effect of PTEN on these mural granulosa cells by knocking out the Pten gene in appropriate mouse models and to examine the effect of PTEN knock out on ovarian histology via H&E staining.

H & E staining of 10 month old conditional knock out *Pten* ovaries demonstrated the granulosa cells morphing into a possible luteal cell pre- tumour phenotype (*Fig.4.10b*).

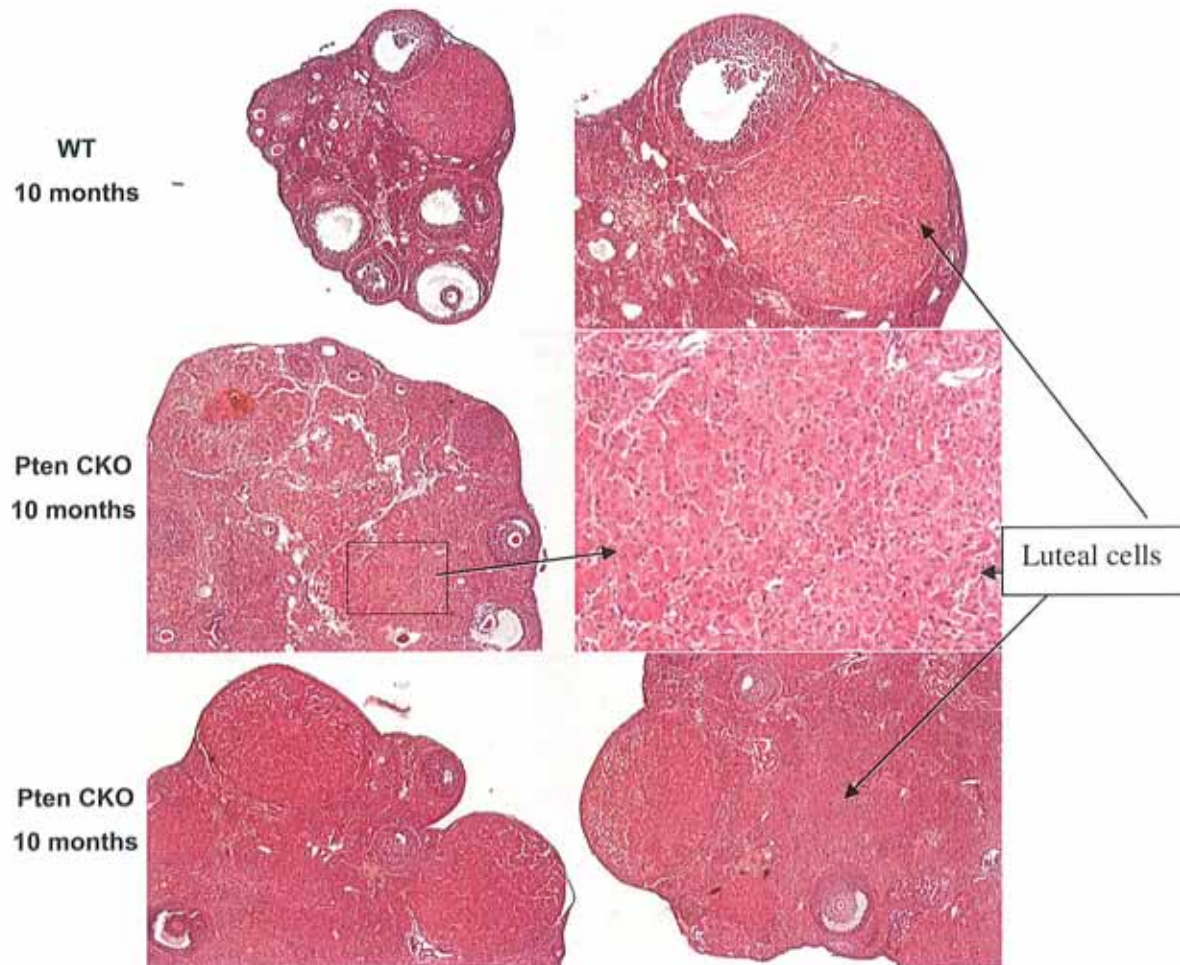*Fig.4.10b.* H&E of *Pten* Conditional Knock Out ovaries

Fig. 3.10b:(Top left & right)Showing a wild type (WT) 10 month old 5X (right) and 10X (left) H&E stained ovary sections with a normal amount of luteal cell differentiation.(Middle left & right) showing 10 month old *Pten* conditional knock out (Pten CKO) 5X(left) and 20X(right) ovary sections with extensive luteal differentiation and a luteal pre-tumour phenotype. (Bottom left and right) showing a different 10 month old *Pten* CKO ovary section at 10X with a luteal pre tumour like phenotype.

As H&E studies showed what looked like a luteal cell pre tumour phenotype the following aim was to prove the identity of these luteal cells using luteal cell markers via immunohistochemistry. Immunohistochemistry with luteal cell markers p21 and p450 SCC were shown to be strongly positive in the luteal cells and in cells destined to be eventually lutealised in the wild type ovaries.

In the *Pten* CKO ovaries the pre tumour luteal cell phenotype was confirmed with strong positive staining in the luteal cells (*Fig.4.10c*).

Fig.4.10c: p 21 Immunohistochemistry staining in the wild type versus *Pten* CKO ovary

p 21 staining in the wild type luteal cells (X10)

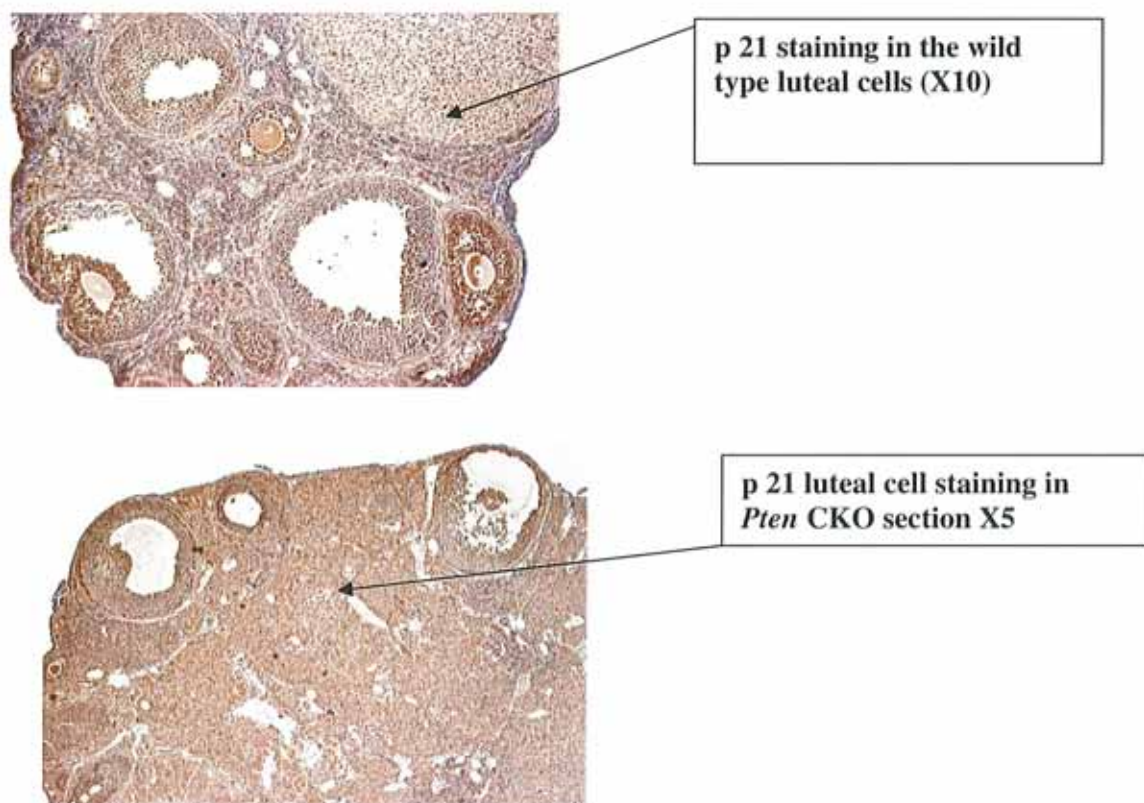**p 21 luteal cell staining in *Pten* CKO section X5**

Fig. 4.10c (Top) showing a 10X wild type ovary section displaying p21 brown staining mainly in the luteal cells and in granulosa cells that are preparing or destined to differentiate to luteal cells. (Bottom image) showing a 5X *Pten* Conditional knock out (CKO) ovary section with extensive brown p 21 staining denoting a more extensive luteal cell phenotype.

As Ras and the PI3K cascades are linked the following aim was to determine the histological effect on the ovary when both *K-Ras* and *Pten* were knocked out. On H&E staining it was demonstrated that the thecal cells of all follicles in the double knock out were substantially thickened i.e. they displayed multiple thecal cell layers that were approximately 4-5 times thicker than comparison to the wild type thecal cell layer number (*Fig.4.11*).

Fig.4.11: H&E staining of a wild type versus a *Pten/K-ras* conditional knock out ovary section

Thecal cell layers

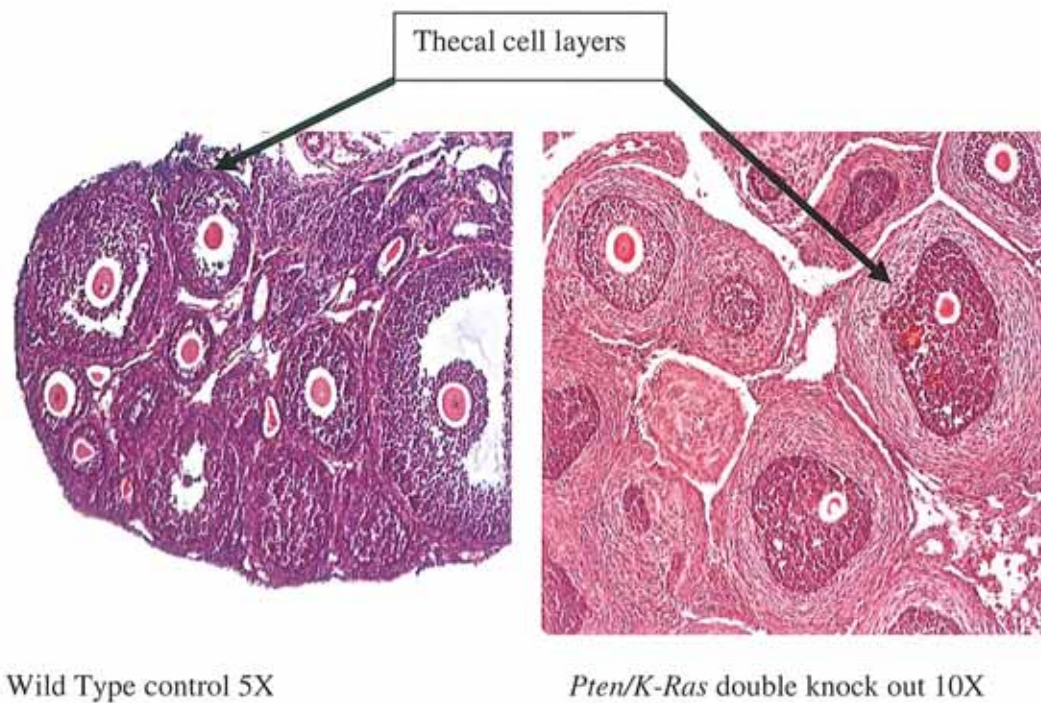Wild Type control 5X   *Pten/K-Ras* double knock out 10X

Fig.4.11 (left) Shows a wild type H&E 5X ovary section demonstrating the normal thecal cell width. (right) shows a *Pten/k-ras* double knock out 10X ovary section with thecal cell thickening.

5) DISCUSSION

This study aimed to examine the location and some of the effects of constitutively active *K-ras* on ovarian morphology and function. The ovarian location of constitutively active *K-ras* was assessed via the β-galactosidase assay and expression was found mainly in the granulosa cells. Ovarian morphology was assessed macroscopically and ovaries expressing constitutively active *K-ras* were shown to be considerably larger in size when compared to the wild type. Ovarian morphology was further examined microscopically via H&E staining and ovaries expressing constitutively active *K-ras* demonstrated aberrant tumour like follicles. Further immunohistochemistry and in-situ hybridization experiments demonstrated the lack of vital ovarian FOXO 1 protein expression and *Lrh-1* mRNA expression in these aberrant follicles. To hypothesise an explanation for the presence of such aberrant follicles in the *K-ras* mutant ovaries the effect of constitutively active *K-ras* on the expression of vital ovarian genes- *Fshr*, *Lhcgr* and *Mkp-3* was assessed by RT-PCR. In addition the effect of constitutively active *K-ras* on the expression of ovarian signaling protein intermediates- p-ERK and p-PKB was assessed via western blot and immunofluorescence. These studies were conducted to determine the functional role of *K-ras* in ovarian signaling and ovarian physiology/pathophysiology.

The results of the beta galactosidase/X-Gal assay indicated CYP-19 to be a more granulosa cell specific promoter and Amhr2 to be a dominant promoter in granulosa cells as blue X-gal staining was seen predominantly but not solely in the granuolsa cells. Thus these results confirmed that the previously reported *Amhr2-Cre* knock-in mouse (Jamin *et al* 2002) was a successful driver of *Cre* expression. In addition the results showed for the first time that the *Cyp-19-Cre* transgenic model was also a satisfactory *Cre* expression model to modify gene expression in granulosa cells (*Fig.4.2*). Thus, both models were deemed suitable models to implement the constitutively active *K-ras* gene in ovarian granulosa cells in this study. In addition *Cre* activity was found to be negative in the uterus of the *Amhr2-Cre* mouse.

The *K-ras* isoform was chosen as previous gene targeting studies by (Koera K *et al* 1997) determined the K-Ras isoform was essential for normal development in mice as opposed to the other H-Ras and N-Ras isoforms. Interestingly both the *LSL-K-Ras*^{G12D} *Amhr2-Cre* and *LSL-K-Ras*^{G12D};*Cyp19-Cre* mouse models demonstrated a compromised fertility. Previous unpublished studies by (Fan *et al* 2007) noted that the *LSL-K-ras*^{G12D};*Amhr2-Cre* females were infertile and that the *LSL-K-Ras*^{G12D};*Cyp19-Cre* females were sub fertile in that they were fertile up to two months and there after infertile.

The reasons for such infertility and sub-fertility shown in the *LSL-K-ras* ^{G12D}; *Amhr2-Cre* and *LSL-K-ras*^{G12D};*Cyp-19-Cre* models respectively may be due to one or many of the ovarian signaling pathways or any of their components that are influenced by Ras. However, this project has demonstrated a number of possible reasons that may result in the compromised fertility shown. The possibilities presented were an inability to ovulate due to the down regulation of *fshr* and *Lcghr*, the FSH and LH receptor genes (*Fig.4.7a*) and secondly the formation of ovarian tumours (*Fig.4.3, Fig.4.4*). Unpublished studies by (Fan *et al* 2007) reported a third possibility, a reduced oocyte number where the *LSL-K-Ras* $^{G12D;}$ *Cyp19-Cre* model demonstrated an oocyte number that represented only 60% of the average wild type oocyte number.

In this study a fourth possibility was shown on sectioning and H&E staining of the *LSL-K-ras* ^{G12D}; *Amhr2-Cre* model. It identified an inability to ovulate even when induced (16 hours post hCG treatment) (*Fig.4.4*). In these *K-ras* mutant ovaries the many fully mature un-ovulated follicles presented as structurally normal with well extended cumulus oocyte complexes. However, on induction to ovulate the oocyte remained trapped inside thus possibly suggesting an inability to ovulate. Histological studies on wild type control mice confirmed a normal ovarian physiology as most antral follicles had ovulated and lutealised on induction (16 hours post hCG treatment) as expected (*Fig.4.4*). The observation that these *K-ras* mutant ovaries showed some morphologically normal follicles amidst tumour-like follicles and that the only apparent fault of these morphologically

normal follicles was an inability to progress to the next stage to ovulation and lutenisation when induced indicated a possible hormone receptor complication.

RT-PCR analysis of the *Fshr* and *Lhcgr* genes demonstrated as expected the induction of both receptors after gonadotrophin treatment in the wild type ovary (*Fig.4.7a*). Interestingly, both receptors were down-regulated in the *K-ras* mutant mouse ovary even post induction with gonadotrophin treatment (*Fig.4.7a*). The results indicated that Ras itself or Ras regulated pathways may possibly work by a negative feedback control mechanism regulating the gonadotrophin receptors within the respective Ras regulated cascades. Thus, in this study as Ras was constitutively active in the Ras mutant mouse ovaries, it could be hypothesised that the over stimulatory effect of the constitutively active Ras could possibly account for the impact on receptor down regulation and thus the inability to ovulate even when induced to do so. The fact that the *Fshr* was down regulated to a lesser extent to the *Lhcgr* (*Fig.4.7a*) could account for the fact that the follicles in the mutant *K-ras* ovaries seemed structurally normal apart from the fact they couldn't ovulate on induction. As *Fshr* was still induced in the mutant *K-ras* ovaries, it could possibly bring about limited normal ovarian physiology and morphology, but not to the extent of the wild type. However small, the presence and induction of the *Fshr*, this still possibly could have accounted for the normal folliculargenesis seen in the mature un-ovulated follicles. FSH could activate its receptor to primarily govern folliculargenesis and then if allowed to mature further to a critical stage it could have acquired the LHR. As the *Lhcgr* gene was shown to be down regulated more in comparison to the *Fshr* gene in the *K-ras* mutant mouse ovaries it was hypothesised that the *Lhcgr* was possibly one of the main upstream targets of Ras. It could be hypothesised that Ras possibly works in a negative feedback manner to impinge on the *Lhcgr* first and then subsequently back on the *Fshr* representing the normal chain of events.

To hypothesise as to why the *LSL-K-ras* ^{G12D}*;Amhr2-Cre* mouse was infertile and in comparison *the LSL-K-Ras* ^{G12D}*;Cyp19-Cre* was sub-fertile may have possibly involved the fact that X-gal positivity and thus *Cre* activity was seen in the oocyte and granulosa cells of the *Amhr2-Cre* model ovaries opposed to X-gal staining exclusively demonstrated in the granulosa cells of the *Cyp19-Cre* model ovaries. As X-gal positivity represented the presence of *Cre* and as *Cre* allowed the expression of constitutively active Ras, wherever *Cre* was expressed constitutively active Ras was expressed. Thus, the fact that constitutively active Ras was expressed in both the granulosa cells and the oocytes of the *LSL-K-ras* ^{G12D}*; Amhr2-Cre* model opposed to only the granulosa cell of the *LSL-K-ras* ^{G12D} *Cyp-19-Cre* model possibly suggested that the expression and thus the effects of mutant *K-ras* on the oocyte in addition to the granulosa cells may have impinged on fertility and the efficiency of ovulation.

The H&E staining analysis on the *K-ras* Knock-in mice also showed them to have developed ovarian tumours (*Fig.4.4*). As these *K-ras* knock-in ovaries demonstrated tumour like follicles with highly condensed granulosa cells, absent follicle cavities and de-shaped oocytes pushed to the periphery, it was suggested that the abnormal structure identified translated into abnormal ovarian function and this then possibly related to a compromised fertility status. Further in-situ hybridisation analysis showed that *Lrh-1* mRNA, one of the granulosa cell marker genes, was not expressed in these tumour-like follicles (*Fig.4.5*). As LRH-1 was a known critical factor supporting organogenesis and steroidogenesis (Hinshelwood *et al* 2005), its lack of expression in these tumour like structures was one of the hypothesised reasons for the abnormal structure seen and resultant abnormal function. Similarly the lack of expression of the granulosa cell *p450 SCC* steroidogenic enzyme mRNA (Hadley M.E *et al* 2007) in these tumour-like follicles may support a possible abnormal steroidogenic function and thus a likely negative effect on ovarian function and fertility. As was revealed by immunohistochemistry, lack of the normal granulosa cell and oocyte maker FOXO 1A protein in the *K-ras* mutant ovaries again may suggest that these tumours display abnormal granulosa cell and oocyte functions with possible implications of a compromised fertility (*Fig.4.6*). As FOXO protein transcription factors are known to play a vital role in the transcription and activation of pro and anti

apoptotic factors (Richards *et al* 2002), the absence of FOXO may in part create an imbalance in cell growth favouring tumourigenesis and abnormal ovarian function. To further confirm these tumour like follicles as abnormal, little to no *versican* mRNA expression was demonstrated by in-situ hybridisation. Versican is a known vital matrix protein functioning in ovarian morphogenesis, matrix remodelling and corpus luteum vascularisation (Russell DL *et al* 2003), in order to properly augment ovulation and lutenisation. The lack of its expression in these follicle-like tumours again is suggested to create an abnormal follicle structure that in association with a number of other possible dysfunctioning factors ultimately impinged on ovarian dysfunction.

Ras and Ras activated/potentiated pathways are well known to induce cell cycle progression, mitogenesis, differentiation and oncogenenic transformation as evidenced herein and in other tissue studies. Control of such pathways holds the key for the prevention of over or under activation of pathways thus preventing excess proliferation with a propensity to oncogenesis or low levels of growth respectively. MAPK phosphatases (MKPs) act in direct opposition to MAPK kinases to dephosphorylate and inactivate the MAP kinase thus regulating the magnitude and duration of the activation and outcome of signalling (Karlsson *et al* 2004). As MKPs have been indicated as components of negative feedback loops and thus have been suggested as tumour suppressors (Karlsson *et al* 2004) it is vital to define a role for MKPs in MAPK cascade regulation. Previous unpublished micro-array data by (Fan *et al* 2007) indicated that *Mkp-3* is significantly up regulated in mouse granulosa cells and COCs by PMSG and hCG treatments as opposed to any other member of the MKP family. In this study RT-PCR analysis of the *Mkp-3* gene identified it as a possible downstream negative control factor and or possible tumour suppressor gene that may provide a possible control mechanism that governs the Ras/Raf/MEK/ERK cascade. The *Mkp-3* gene was expressed without gonadotrophin treatment in the knock-in model where *K-ras* was constitutively active unlike the wild type control (*Fig.4.7b*) This confirms that in the wild type ovary Ras switches between an on and off state and that it acts as a molecular switch becoming active in response to gonadotrophin. (Campbell SL *et al* 1998). However, when *K-ras* was constitutively active, as was the

case in the Knock-in model, it was predicted that the constitutively active Ras was constantly activating the down stream gene *Mkp-3* which was expressed without hormone treatment. In the wild type control and *K-ras* Knock-in model the *Mkp-3* gene demonstrated a significant induction to similar levels at 8 and 16 hours post hCG treatment but not post PMSG treatment *(Fig.4.7b)*. This suggested that *Mkp-3* was perhaps an LH induced gene. However there was no difference in induction levels demonstrated between the wild type and *K-ras* knock-in models given the same gonadotrophin treatment *(Fig.4.7b)*. It would be expected that if Ras was left constitutively active, *Mkp-3*, a downstream Ras target would also be continuously active and induced more in the knock-in model. However, *Mkp-3* was not induced more in the knock-in model. This lead to the hypothesis that *Mkp-3* on producing its protein MKP-3 and on reaching a precise threshold level, *Mkp-3* may work in a negative feedback manner on the upstream ERK component of the Ras cascade to switch it off and control the proliferative and differentiation effects of Ras. From this study it was hypothesised that possibly *Mkp-3* reaches its threshold quicker in the knock-in model opposed to the wild type. This suggested that even induction does not have time to catch up to this threshold level and thus has no effect as the threshold level has already been breached in the knock-in model before induction can have an effect.

Western blot displayed induction of the ERK 1 and 2 isoforms 2 hours post hCG treatment in both the wild type and *K-ras* mutant granulosa cells, however the level of induction in the *K-ras* mutant was reduced in comparison to the wild type *(Fig.4.8b)*. This showed ERK to be a protein of a very narrow expression range as it was not induced with PMSG or prolonged periods after hCG treatment. These results imply that ERK possibly works in a switch like manner which in connection with the MKP-3 hypothesis again suggests that MKP-3 works back in a negative feedback manner to switch off ERK. This suggests that ERK is activated under a tight time and hormone condition specific manner. Immunofluorescence confirmed p-ERK expression in the granulosa cells two hours post hCG treatment as expected in the wild type mouse*(Fig.4.8c)*. The absence of p-ERK expression in situ

within the *K-ras* mutant ovaries confirms that p-ERK expression is down regulated in the *K-ras* mutant; however the immunofluorescence technique may not be sensitive enough to detect it.

Western blot and immunofluorescence showed activation of PKB in the wild type to be induced moderately by PMSG treatment and greatly by 2 hours post hCG treatment and after which expression was reduced (*Fig.4.8 a&b, Fig.4.9a&b*). As expression dropped on prolonged hCG exposure i.e. (8-16 hours post hCG treatment on induction of ovulation) it was determined that activation of the PI3K cascade was restricted to the pre-ovulatory follicles. In the mutant model p-PKB was induced to a similar level in the immature, PMSG, 2 hours post hCG and 4 hour post hCG treated mouse and in other studies was still induced 8 hours post hCG. This suggests, as expected, that if Ras is left constitutively active it prolongs the stimulatory and activated state of the Ras down stream effector PKB as Ras supports and or facilitates PI3K activation and thus PKB activation. However, on comparing the wild type and *K-ras* mutant western blot, p-PKB expression was slightly more induced 2 hours post hCG in the wild type in comparison to the mutant, thus suggesting that p-PKB normally has a narrow range of expression and action that is time and hormone dependent. In the wild type case Ras would have been normally switched off at some stage. Finally p-PKB expression was demonstrated in the ovarian oocytes and granulosa cells thus deeming p-PKB to have an important role on cell signalling and morphology in these cells.

The results demonstrated that constitutively active Ras alters ovarian structure and function. It enlarges the ovary, causes the formation of aberrant shaped follicles and tumour-like follicles.

It causes fertility problems demonstrating an inability to ovulate even when induced. Constitutively active Ras displays the aberrant expression of vital ovarian genes and proteins. The *Fshr* and *Lchgr* genes are down regulated the *Mkp-3* gene expression is dysregulated and Ras down stream signalling protein intermediates p-PKB and p-ERK expression is altered. These factors may all contribute to the maintenance of ovarian morphology and biochemical function. Thus these results confirmed that Ras plays a critical role in ovarian signalling.

Both the Ras/Raf/MEK/ERK and PI3K cascades are vital to ovarian morphology and function and inter communicate to maintain ovarian function and cell homeostasis. The PI3K pathway is known to govern cell division, survival, size and apoptosis inhibition (Sulis M.L *et al* 2003). Without mural granulosa cell expression of "PTEN" the PI3K negative regulator and tumour suppressor, uncontrolled proliferation, evasion of apoptosis and possible tumourigenesis could prevail in the ovary. This in combination with the proliferative effects of Ras could further promote tumourigenesis.

On morphological examination, the *Pten* CKO presented with a luteal cell pre-tumour phenotype (*Fig.4.10b&c*). This could be accounted for by the over activation of the PI3K cascade. PTEN under normal circumstances was shown to be expressed intensely in the mural granulosa cells and thecal cells. This identifies PTEN to have an important role on cell signalling and morphology in these cells. In the wild type the PTEN expression level was relatively constant over all stages studied from the immature to the post ovulatory mouse, thus suggesting that PTEN does not work in a switch like manner.

Interestingly, unpublished studies by (Fan *et al* 2007) have demonstrated that *Pten* $^{flox/-}$ *Cyp-19-Cre* was fertile and *Pten* $^{flox/-}$ *Amhr2-Cre* models were infertile. However it was observed that the *Pten* conditional knock-out model did not overtly alter follicular development, ovulation or lutenisation. This may be explained by the fact that the normal chain of events and the pathway components of the PI3K involved were not dysfunctional only over activated and uncontrolled. Normally activation of the cascade by FSH, estradiol and IGF-1 has shown to have increased the expression of the pro-apoptotic factor FOXO 1a (Richards *et al* 2002). Activated PI3K then activated a downstream component PKB. Subsequent activation of downstream FOXO by activated PKB inactivated the activated FOXO by restricting its nuclear localization (Richards *et al* 2002). Therefore it could be hypothesised that FOXO, the transcription factor, could not transcriptionally activate the pro apoptotic factor gene Fas L, an inhibitor of the cell cycle p27kip and IGF protein 1 an inhibitor of the PI3K cascade peptide potentiator and initiator IGF-1. This therefore could have resulted in excess growth and proliferation of the ovarian cells; however the cells remained functional and allowed progression

to the next stage of ovulation and differentiation to luteal cells. At this stage the mouse would have naturally released LH and the LH caused the decrease in expression of the pro- apoptotic factor FOXO. Decreased levels of FOXO would have resulted in decreased activation of FOXO from the constitutively active PI3K cascade and thus decreased the levels of inhibition of the transactivation of pro-apoptotic factors. Eventually when the granulosa cells where induced to undergo lutenisation they possibly became resistant to apoptosis, and pro apoptotic factors were lost and lutenisation factors like p21 and Sgk acquired, thus possibly giving rise to a luteal cell pre-tumour phenotype and relative normal function. It could be predicted that eventually this phenotype will reach a tumourigenic stage that will impinge greatly on ovarian function. However as the *Pten*$^{floxl/-}$ *Amhr2-Cre* model was shown to be infertile and as ovarian function was shown to be not overtly compromised the reasons for infertility my lie somewhere else in the reproductive tract.

Histological studies on the *K-ras/Pten* double knock out demonstrated thecal cell thickening (*Fig.4.11*). The number of thecal cell layers doubled to tripled in number, in comparison to wild type controls. In the *Pten* CKO alone no thecal cell thickening was demonstrated, however no studies were conducted on a possible *K-ras* CKO model to confirm the extent to which knocking out *Pten* and or *K-ras* accounts for this phenotype. However the results hypothesised that as no thecal cell thickening was seen in the *Pten* CKO alone, other mechanisms in addition to the known K-Ras may work in collaboration with PTEN to control the PI3K cascade.

6) CONCLUSION

In conclusion, engineering ras to be constitutively active in the mouse ovary results in ovulation malfunction and fertility problems possibly due to one or more of the following possibilities. The formation of tumour like follicles, follicles with abnormally shaped oocytes with abnormal protein and mRNA expression, reduced oocyte number, the down regulation of gonadotrophin receptors and or the up regulation of the *Mkp-3 gene*, a newly suspected negative feedback component of the Ras/Raf/MEK/ERK pathway.

Secondly, the morphological effect of conditionally knocking out *Pten* results in a luteal cell pre tumour phenotype, one of the possible causes of fertility problems evidenced in the *Pten* knock out mice. Finally the effect of a *K-ras/Pten* double knock out on ovarian morphology presented thecal cell thickening suggesting both PTEN and K-Ras work together most likely in conjunction with other signalling pathways to augment signalling control and uphold a normal ovarian morphology and physiology.

7) BIBLIOGRAPHY

1. Bourne HR, Sanders DA, Mc Comack F. The GTPase superfamily: a conserved switch for diverse cell functions. *Nature* 1990; **348**:125-132.

2. Bos J. ras oncogenes in human cancer:a review. *Cancer Res* 1989,**49**:4682-4689

3. Breckwoldt M, Selvaraj N, Aharoni D, Barash A, Segal I, Insler V, Amsterdam A. Expression of Ad4-BP/ Cytochrome P450 side chain cleavage enzyme and induction of cell death in long-term cultures of human granulosa cells. *Molecular Human Reproduction* 1996; vol 2 No.**6**:391-393.

4. Campbell P.M, Groehler A.L, Kwang M.L, Ouellete M.M, Khazak V and Der C.J. K-ras promotes Growth transformation and Invasion of immortalized human pancreatic Cells by Raf and phosphatidylinositol 3-Kinase Signaling. *Cancer Research* 2007; **67**:2098-2106.

5. Campbell SL, Khosravi-Far R, Rossman KL, Clark GJ, Der CJ. Increasing complexity of Ras signaling. *Oncogene* 1998; **17**:395-1413.

6. Camps M, Nichols A, Arkinstall S. Dual specificity phosphatases: a gene family for control of MAP kinase function. *The Faseb J* 2000; **14**:6-16.

7. Camps M, Nichols A, Gilleroin C, Antonsson B, Muda M, Chabert C, Boschert U, Arkinstall S. Catalytic Activation of the phosphatase MKP-3 by ERK2 mitogen-activated protein kinase. *Science* 1998b; **280**:1262-1265.

8. Cespedes, M.V, Sancho FJ, Guerrero S, Parreno M, Casanova I, Pavon MA, Marcuello E, Trias M, Cascante M, Capella G and Mangues R. K-ras Asp12 mutant neither interacts with Raf nor signals through Erk and is less tumourigenic than K-ras val12. *Carcinogenesis* 2006; **27**(11): 2190-2200.

9. Colorado state University database. Retrieved April 21, 2007. www.vivo.colostate.edu/hbooks/pathway/endocrine/basics/steroiogensis/htm

10. de Rooij J, Rehmann H, van triestM, Cool RH, Witinghofer A, Bos JL. Mechanism of regulation of the Epac family of cAMP-dependent RapGEF's. *J. Biol Chem* 2000, **275**:20829-20836.

11. Falender A.E, Rainer L, Malenfant D, Belanger L, Richards J.S. Differential expression of Steroidogenic Factor-1 And FTF/LRH-1 in the rodent Ovary. *Endocrinology* 2003. Vol **144**: 3598-3610.

12. Fan H-Y *et al* unpublished- paper in progress

12. Figure 1.1a, University of Wisconsin-Madison database. Retrieved April 11, 2007. www.wisc.edu/ansci_repro/lec_11/menstrual.jpg

13. Figure 1.1b, University of Western Australia database. Retrieved May 12, 2007. www.embrology.med.unsw.edu.au/otherEmb/mouse2.htm

14. Gonzalez-Robayana I J, Alliston T.N, Buse P, Firestone Gary L, Richards J.S. Functional and Subcellular Changes in the A-Kinase-Signaling Pathway:Relation to Aromatase and Sgk Expression during the Transition of Granulosa Cells to Luteal Cells. *Molecular Endocrinology* 1999; **13**:1318-1337.

15. Gonzalez-Robayna I J, Falender AE, Ochsner S, Firestone GL, Richards JS. Follicle-Stimulating Hormone (FSH) Stimulates Phosphorylation and activation of Protein Kinase B (PKB/Akt) and serum and Glucocorticoid-Induced Kinase (Sgk): Evidence for A kinase-Independent Signaling by FSH in Granulosa Cells. *Molecular Endocrinology* 2000; **14**:1283-1300.

16. Hadley, Mac.E, Levine, J.E. Pitutitary Hormones. *In* Endocrinology. Pearson Education Inc, New Jersey 07458. sixth edition, 2007, chapter **5**; 102-104.

17. Hadley Mac.E, Levine J.E. Pitutitary Hormones. *In* Endocrinology. Pearson Education. Inc, New Jersey 07458. sixth edition, 2007, chapter **18**; 408-415.

18. Hinshelwood M.M, Shelton J.M, Richardson J.A, Mendelson C.R. Temporal and Spatial Expression of Liver Receptor Homologue-1 (LHR-1)uring Embrygenesis suggests a potential Role in Gonadal Development. *Developmental Dynamics* 2005; **234**:159-168.

19. Hunzicker-Dunn M, Maizels E.T. FSH signalling pathways in immature granulosa cells that regulate target gene expression: Branching out from protein kinase A. *Cellular Signaling* 2006; **18**:1351-1359.

20. Jackson E.L, Willis n, Mercer, K, Bronson R.T, Crowley D, Montoya R, Jacks T and Tuveson D.A. Analysis of lung tumour initiation and progression using conditional expression of oncogenic *K-ras. Genes Dev* 2001; **15**:3243-3248.

21. Jamin SP, Mishina Y, Hanks MC, Behringer RR. Requirement of Bmpr1 for mullerian duct regression during male sexual development. *Nat Genet* 2002; **32**(3):408-410.

22. Karlsson M, Mathers J, Dickinson RJ, Mandl M, Keyse SM. Both Nuclear-Cytoplasmic shuttling of the Dual Specificity phosphatase MKP-3 and Its Ability to Anchor MAP Kinase in the cytoplasm Are Mediated by a Conserved Nuclear Export Signal. *J. Biol. Chem* 2004; **vol.279**:41882-41891.

23. Kawasaki H, Springett GM, Mochizuki N, Toki S, Nakaya M, Matsuda M, Housman DE, Graybiel AM, A family of cAMP-binding proteins that directly activate Rap1. *Science* 1998; **282**:2275-2279.

24. Keyse SM. Protein phosphatases and the regulation of mitogen-activated protein kinase signalling. *Curr Opin Cell Biol* 2000; **12**:186-192.

25. Koera K, Nakamura K, Nakao K, Miyoshi J, Toyoshima K, hatta T, Otani H, aiba A and Katsuki M. *Oncogene* 1997; **15** :1151-1160.

26. Lesche R, Groszer M, Gao J, Wang Y, Messing A, Sun H, Liu X and Wu H. Cre.loxP-mediated inactivation of the murine Pten tumour suppressor gene. *Genesis* 2002; **32**(2):148-149.

27. Ochsner SA, Russell DL and Richards JS. Absence of TSG-6 expression in cumulus cells of the cyclooxygenase-2 knockout mouse. *In* Program & Abstracts of the 83rd Annual meeting of the Endocrine Society, 2001, Denver, Co; (Abstract pgs 2-237).

28. Park J-I, Strock CJ, Ball DW, Nelkin BD. The Ras/Raf MEK/ Extracellular Signal-Regulated Kinase Pathway Induces Autocrine-paracrine Growth Inhibition via the Leukemia Inhibitory Factor/ JAK/STAT Pathway. *Molecular and Cellular Biology* 3002; **23**(2):543-554.

29. Richards J.S, Russell D.L, Dajee M, Alliston T.N. Molecular mechanisms of ovulation and lutenization. *Mol Cell Endocrinol* 1998; **145**:47-54.

30. Richards J.S, Russell D.L, Ochsner S, Hseih M, Doyle K.H, Falender A.E, Lo Y.K and Sharma S.C. Novel Signaling Pathways That Control Follicular Development, Ovulation and Lutenization. *Recent Progress in Hormone Research* 2002b; **57**:195-220.

31. Richards J.S. New signalling pathways for hormones and Cyclic adenosine 3',5'-monophosphate action in endocrine cells. *Mol Endocrinol* 2001b; **15**:209-218.

32. Richards JS, Sharma SC, Falender AE, Lo YH. Expression of FKHR, FKHRL1 and AFX Genes in the Rodent Ovary: Evidence for regulation by IGF-1, Estrogen and the Gonadotrophins. *Molecular Endocrinology* 2002a; **16**(3):580-599.

33. Richards J.S. The Ovarian Follicle- A Persective in 2001*.*Endocrinology* 2001a; **142**(6):2184-2191.

34. Robker RL, Richards JS. Hormonal control of the cell cycle in ovarian cells: proliferation versus differentiation. *Bio Reprod* 1998a; **59**:476-482.

35. Robker RL, Richards JS. Hormone-induced proliferation and differentiation of granulosa cells: a coordinated balance of the cell cycle regulators cyclin D2 and p27KIP1. *Mol Endocrinol* 1998b; **12**:924-940.

36. Russell D.L, Ochsner S.A, Hsieh M, Mulders S, Richards J.S. Hormone-Regulated Expression and localisation of Versican in the Rodent Ovary. *Endocrinology* 2003; **144**:1020-1031.

37. Russell DL, Doyle KMH, Ochsner SA, Sandy JD and Richards JS. Procesing and Localisation of ADAMTS-1 and Proteolytic Cleavage of Versican during Cumulus Matrix Expansion and Ovulation. *The Journal of Biological Chemistry* 2003; **278**:42330-42339.

38. Soriano P. Generaliszed lac Z expression with the ROSA26 Cre reporter strain. *Nat Genet* 1999, **21**(1):70-71.

39. Sulis ML, Parsons R. PTEN: from pathology to biology. *Trends in Cell Biology* 2003. 13:478-483.

40. Tuveson DA, Shaw AT, Willis NA, Silver DP, Jackson EL, Chang S, Mercer KL, Grochow R, Hock H, Crowley D, Hingorani SR, Zaks T, King C, Jacobetz MA, Wang L Bronson RT, Orkin SH, DePinho RA, Jacks T. Endogenous oncogenic *K-ras* (G12D) stimulates proliferation and wide spread neoplastic and developmental defects. *Cancer cell* 2004 **5**:375-387

41. University of Western Australia database. Retrieved May12, 2007. www.lab.anhb.uwa.edu.au/mb140/corepages/femaleRepro/femaleRepro.htm

42. Wayne C.M, Fan HY, Cheng X, Richards JS. FSH-induces multiple signalling cascades: evidence that activation of SRC, RAS and the EGF receptor are critical for granulosa cell differentiation. *Mol Endocrinol* 2007;**21**:1940-1957.

43. Woods D.C, and Johnson A.L. Phosphatase activation by epidermal growth factor family ligands regulates extracellular regulated kinase signaling in undifferentiated hen granulose cells. *Endocrinology* 2006; **147**:4931-4940.

44. WOOMB-World ovulation organisation method billings database. Retrieved May 12, 2007.
www.billings.ovulation.method.org.au/act/physiol.shtml

45. Yamada KM, Araki M. Tumour suppressor PTEN: modulator of cell signalling growth, migration and apoptosis. *Journal of cell science* 2001; **114**:2375-2382.

Selective expression of $Kras^{G12D}$ in granulosa cells of the mouse ovary causes defects in follicle development and ovulation

Heng-Yu Fan[1], Masayuki Shimada[2], Zhilin Liu[1], Nicola Cahill[1], Noritaka Noma[2], Yun Wu[3], Jan Gossen[4] and JoAnne S. Richards[1,*]

Activation of the RAS family of small G-proteins is essential for follicle stimulating hormone-induced signaling events and the regulation of target genes in cultured granulosa cells. To analyze the functions of RAS protein in granulosa cells during ovarian follicular development in vivo, we generated conditional knock-in mouse models in which the granulosa cells express a constitutively active $Kras^{G12D}$. The $Kras^{G12D}$ mutant mice were subfertile and exhibited signs of premature ovarian failure. The mutant ovaries contained numerous abnormal follicle-like structures that were devoid of mitotic and apoptotic cells and cells expressing granulosa cell-specific marker genes. Follicles that proceeded to the antral stage failed to ovulate and expressed reduced levels of ovulation-related genes. The human chorionic gonadotropin-stimulated phosphorylation of ERK1/2 was markedly reduced in mutant cells. Reduced ERK1/2 phosphorylation was due, in part, to increased expression of MKP3, an ERK1/2-specific phosphatase. By contrast, elevated levels of phospho-AKT were evident in granulosa cells of immature $Kras^{G12D}$ mice, even in the absence of hormone treatments, and were associated with the progressive decline of FOXO1 in the abnormal follicle-like structures. Thus, inappropriate activation of KRAS in granulosa cells blocks the granulosa cell differentiation pathway, leading to the persistence of abnormal non-mitotic, non-apoptotic cells rather than tumorigenic cells. Moreover, those follicles that reach the antral stage exhibit impaired responses to hormones, leading to ovulation failure. Transient but not sustained activation of RAS in granulosa cells is therefore crucial for directing normal follicle development and initiating the ovulation process.

KEY WORDS: Ovary, Ovulation, Granulosa cell, $Kras$ (K-ras), Signal transduction, MKP3 (DUSP6)

INTRODUCTION

Activation of small G-proteins within the RAS superfamily impact multiple downstream signaling cascades, including RAF1/MEK/ERK1/2 and PI3K/AKT/FOXO, in many tissues in a cell- and context-specific manner (Campbell et al., 2007; Cespedes et al., 2006; Gupta et al., 2007; Rocks et al., 2006). In response to growth-regulatory molecules, transient activation of RAS can stimulate controlled proliferation as well as differentiation of cells. Uncontrolled activation of RAS is often associated with oncogenic transformation or senescence of cells (Jackson et al., 2001; Lin et al., 1998; Serrano et al., 1997; Shaw et al., 2007). Specifically, RAS family members become oncogenic by single-point mutations, mainly at codons 12 or 13 (Bourne et al., 1990), leading to constitutive signaling and cell transformation with changes in morphology, increased proliferation and/or inhibition of apoptosis. Tissue-specific activation of oncogenic $Kras^{G12D}$ causes mammary gland, lung and endometrioid ovarian carcinoma in mouse (Dinulescu et al., 2005; Jackson et al., 2001; Sarkisian et al., 2007). Mutations of $KRAS$ or $BRAF$ in non-invasive and invasive carcinomas of the ovary [involving the ovarian surface epithelium (OSE)] have been reported (Gemignani et al., 2003; Mayr et al., 2006).

In this study, we sought to determine the impact of RAS activation in granulosa cells in vivo. The constitutively active $Kras^{G12D}$ mutation (Johnson et al., 2001) was selectively expressed in mouse granulosa cells using a Cre-mediated DNA recombination approach. The inappropriate, premature expression of $Kras^{G12D}$ in granulosa cells blocked granulosa cell differentiation at an early stage, leading to the formation of abnormal follicle-like structures containing non-mitotic, non-apoptotic, non-differentiated and non-tumorigenic cells. Moreover, those follicles that reached the antral stage exhibited impaired responses to hormones, leading to ovulation failure. Thus, transient but not sustained activation of RAS in granulosa cells is crucial for normal follicle growth and successful completion of the ovulation process.

MATERIALS AND METHODS
Animals
LSL-$Kras^{G12D}$;$Amhr2$-Cre mice were derived from previously described $Amhr2$-Cre and LSL-$Kras^{G12D}$ parental strains (Jamin et al., 2002; Tuveson et al., 2004). Although $Amhr2$ is highly expressed in granulosa cells of growing follicles it is also known to be expressed in other reproductive tissues, including ovarian surface epithelial cells and the uterus (Arango et al., 2008) (our unpublished observations). Therefore, we sought to obtain a Cre-expressing mouse model that would be more highly specific for granulosa cells. $Cyp19$-Cre transgenic mice were generated by oocyte microinjection of a DNA fragment in which the 304 bp $Cyp19$ promoter (GenBank S85356, bp −278 to +26) was ligated to $iCre$ cDNA. To study ovarian responses to exogenous gonadotropins, 21-day-old immature females were analyzed to avoid the complexity of ovarian functions associated with estrous cycles and endogenous surges of gonadotropins. Specifically, immature mice were injected intraperitoneally (ip) with 4 IU eCG (equine chorionic gonadotropin;

[1]Department of Molecular and Cellular Biology, Baylor College of Medicine, Houston, TX77030, USA. [2]Department of Applied Animal Science, Graduate School of Biosphere Science, Hiroshima University, Higashi-Hiroshima, 739-8528, Japan. [3]Breast Cancer Center, Baylor College of Medicine, Houston, TX77030, USA. [4]NV Organon, part of the Schering-Plough Corporation, Target Discovery Oss, Molenstraat 110, 5340 BH Oss, The Netherlands.

*Author for correspondence (e-mail: joanner@bcm.edu)

Calbiochem) followed 48 hours later with 5 IU hCG (human chorionic gonadotropin; American Pharmaceutical Partners, Schaumburg, IL). Ovulated COCs were collected from oviducts 16 hours after hCG injection. Animals were treated in accordance with the NIH Guide for the Care and Use of Laboratory Animals.

Granulosa cell cultures
Undifferentiated granulosa cells were released from mouse antral follicles by puncturing with a 26.5-gauge needle. Cells were cultured at a density of 1×10^6 cells/ml in defined medium (DMEM:F12 containing penicillin and streptomycin) in 12-well culture dishes. Cells were cultured overnight to allow attachment to the culture dish and were infected with adenoviral vectors expressing Cre (Ad5-CMV-Cre, generated by the Vector Development Laboratory, Baylor College of Medicine) or GFP as the infection control. The infected cells were treated with or without FSH [NIH-FSH-16, National Hormone and Peptide Program (Al Parlow), Torrance, CA; 100 ng/ml] for time intervals designated in the figure legends.

BrdU incorporation and TUNEL assays
Mice were injected ip with 50 mg/kg of BrdU in PBS, and were killed 2 hours later. Ovaries were isolated and fixed with 4% paraformaldehyde (PFA) overnight. Incorporated BrdU was detected by immunohistochemistry using BrdU antibody according to manufacturer's instructions (Sigma, St Louis, MO). TUNEL assays were performed on PFA-fixed paraffin-embedded sections using the ApopTag Plus Peroxidase In Situ Apoptosis Detection Kit (Serologicals Corporation, Norcross, GA) according to manufacturer's instructions.

Immunohistochemistry and immunofluorescence
Immunohistochemistry was performed on 4% PFA-fixed paraffin-embedded 5-μm sections using the VectaStain Elite Avidin-Biotin Complex Kit as directed by the manufacturer (Vector Labs, Burlingame, CA). Sections were probed with primary antibodies against FOXO1 or PCNA (Cell Signaling, CA) and visualized using a 3,3V-Diaminobenzidine Peroxidase Substrate Kit (Vector Labs). For immunofluorescence, ovaries were PFA fixed, embedded in OCT compound (Sakura Finetek USA, Torrance, CA) and stored at –80°C before sectioning. Sections were probed with anti-KRAS (Santa Cruz

Biotechnology, Santa Cruz, CA), anti-phospho-AKT, anti-phospho-ERK1/2, anti-cleaved caspase 3, or anti-phospho-histone H3 (Cell Signaling Technology) antibodies and visualized with Alexa Fluor 594-conjugated goat anti-rabbit IgG (Molecular Probes, Eugene, OR). Digital images were captured using a Zeiss Axiphot microscope with 5-40× objectives. For all the experiments, exposure time was kept the same for control and *Kras* mutant samples.

In situ hybridization
Plasmids for *Nr5a2* and *Cyp11a1* probes were as described previously (Boerboom et al., 2005; Falender et al., 2003). A cDNA fragment of *Mkp3* was amplified by RT-PCR from mouse ovary total cDNA and subcloned into the pCR-TOPO4 vector (Invitrogen, Carlsbad, CA). In situ hybridization was performed as previously reported (Falender et al., 2003; Hsieh et al., 2005). Tissue histology and the radioactive probe were visualized under light- and dark-field illumination, respectively.

RT-PCR and real-time RT-PCR
Reverse transcription (RT)-PCR was performed using the SuperScript One-Step RT-PCR System with the Platinum Taq Kit (Invitrogen) and 100 ng samples of ovarian total RNA that had been isolated using the RNeasy Mini Kit (Qiagen, Germantown, MD). Approximately 0.625 μCi of [α-^{32}P]dCTP (3000 Ci/mmol; MP Biomedicals, Irvine, CA) were added to each reaction to generate radioactive signals. Primer sequences and amplification conditions used are available upon request. Samples were separated by electrophoresis on 5% PAGE gels, dried and exposed to Biomax XAR film (Eastman Kodak, Rochester, NY) to generate the presented images.

Quantitative (q) RT-PCR was performed using the Rotor-Gene 3000 thermocycler (Corbett Research, Sydney, Australia). Relative levels of gene expression were normalized to β-actin.

RAS activity assay
The RAS-binding domain (RBD) of the mouse PI3K p110α subunit (PIK3CA; aa 220-311) (Rodriguez-Viciana et al., 1996) and of mouse RAF1 (aa 55-131) (Campbell-Valois and Michnick, 2007) were PCR amplified from a mouse ovary cDNA pool and subcloned into pGEX 4T1 vector. Recombinant GST-PI3K RBD and GST-RAF1 RBD were expressed in the
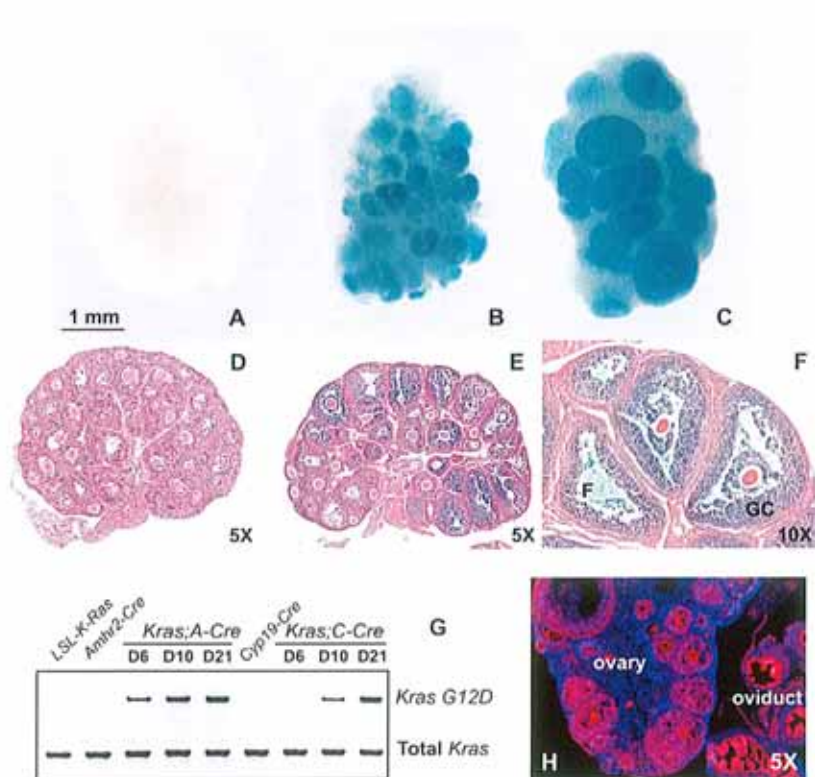

Fig. 1. Conditional knock-in of *Kras^G12D* in granulosa cells. (A-F) In vivo recombination of the *R26R* locus in ovaries by the *Cyp19-Cre* transgene. (A) *ROSA26*, (B) *ROSA26;Cyp19-Cre* and (C) *ROSA26;Cyp19-Cre*, 48 hours after eCG treatment. Images are of ovaries from 23-day-old mice showing β-gal staining (blue). (D) Day10 and (E) Day23 without eCG, and (F) Day23 with eCG treatment. Hematoxylin and Eosin staining of paraffin sections after β-gal staining showing the expression of β-gal in the ovaries of the *ROSA26;Cyp19-Cre* mouse. F, follicle; GC, granulosa cell. **(G)** RT-PCR detection of *Kras^G12D* and total *Kras* mRNAs in *LSL-Kras^G12D;Amhr2-Cre* and *LSL-L-ras^G12D;Cyp19-Cre* mouse ovaries. **(H)** Immunofluorescence of KRAS in the ovary of a 6-week-old cycling wild-type mouse.

Rosetta-pLysS *E. coli* strain (Novagen) and affinity purified using glutathione-agarose beads (Sigma). Ovaries were homogenized in lysis buffer (20 mM NaF, 10 mM MgCl₂, 100 mM NaCl, 10% glycerol, 0.5% Triton X-100, 20 mM HEPES, pH7.5). The lysates were incubated with agarose slurries linked with mouse RAF1 RBD or PI3K RBD to bind RAS-GTP. The agarose beads were washed and resuspended in Laemmli sample buffer prior to western blot analysis.

Western blot analysis

Western blots were performed utilizing 30 µg of lysate protein, 10% SDS-PAGE gels and transfer to Immobilin membrane (Millipore). Membranes were incubated with the following antibodies at 1:1000 dilutions: anti-phospho-FOXO1, anti-phospho-ERK1/2, anti-phospho-AKT, anti-AKT (all from Cell Signaling Technology) and anti-RAS (Upstate Biotechnology).

RNAi of *Mkp3*

Mkp3 siRNA (sc-39001) was purchased from Santa Cruz Biotechnology. Scrambled siRNA duplex (Ambion) was used as control. Transfection of siRNA (50 nM) into cultured granulosa cells was accomplished using the HVJ Envelope Vector Kit (Ishihara Sangyo, Tokyo, Japan) as previously reported (Shimada et al., 2007). The culture medium was replaced 5 hours after transfection and the cells were treated with 250 ng/ml amphiregulin (R&D Systems) for up to 4 hours.

RESULTS
Conditional knock-in of *Kras*^G12D in mouse ovarian granulosa cells

To induce the expression of KRAS^G12D in granulosa cells, the previously described *LSL-Kras*^G12D mice were crossed with either the *Amhr2-Cre* knock-in mice (*Amhr2*^cre/+) (Jamin et al., 2002) or with transgenic mice in which Cre expression is driven by the *Cyp19* promoter (*Cyp19-Cre*). The ovarian expression pattern of the *Amhr2-Cre* allele has been described previously (Jorgez et al., 2004; Pangas et al., 2006; Boerboom et al., 2006). The generation of the *Cyp19-Cre* mouse strain is described in Materials and methods. To monitor the Cre activity in the ovaries, the *Cyp19-Cre* mice were crossed to the *ROSA26* reporter mouse strain that expresses β-galactosidase (β-gal) only in Cre-expressing cells (Soriano, 1999). Ovaries were stained for β-gal activity using X-Gal substrate as previously reported (Jorgez et al., 2004). No β-gal activity was detected in ovaries of *ROSA26* mice lacking Cre (Fig. 1A). In the *ROSA26;Cyp19-Cre* mice, β-gal was detected at low levels in granulosa cells of small follicles at postnatal day 10 (Fig. 1D) and at increased levels in granulosa cells of all antral follicles (Fig. 1B,E). Injections of *ROSA26;Cyp19-Cre* mice with equine chorionic gonadotropin (eCG), a known inducer of endogenous *Cyp19* expression, stimulated follicle growth and increased Cre activity (Fig. 1C,F). Cre activity was not detected in theca cells or oocytes throughout postnatal development (Fig. 1D-F). These results indicate that the *Cyp19-Cre* mouse strain exhibits specific expression of Cre in the granulosa cells, with minimal leakage in other cell types.

Examination of *Kras*^G12D mRNA in immature *LSL-Kras*^G12D;*Amhr2-Cre* and *LSL-Kras*^G12D;*Cyp19-Cre* mice demonstrated that the *Kras*^G12D allele was efficiently recombined and expressed at levels comparable to the endogenous *Kras* gene (Fig. 1G). Since endogenous KRAS protein is highly expressed in granulosa cells of growing follicles, expression of the mutant allele is being induced in the same cell type as the endogenous gene (Fig. 1H).

Granulosa cell expression of *Kras*^G12D impairs ovulation and female fertility

For fertility tests, *LSL-Kras*^G12D;*Amhr2-Cre* and *LSL-Kras*^G12D;*Cyp19-Cre* females were bred to wild-type males continuously for 6 months. The average number of ~7-8 pups per

litter for the control mice (*LSL-Kras*^G12D) was not different from that of our C57BL/6J mouse colony. However, the *LSL-Kras*^G12D;*Amhr2-Cre* and *Kras*^G12D;*Cyp19-Cre* females (*n*=6, respectively) were subfertile over the 6-month period, with most pups being born in the first 2 months (Fig. 2A).

To determine the cause of reduced fertility in the *Kras*^G12D mutant mice, we tested their ability to ovulate by injecting immature mice with 4 IU of eCG and 46 hours later 5 IU of human chorionic gonadotropin (hCG). Whereas the control littermates ovulated many COCs at 16 hours after hCG injection, most *LSL-Kras*^G12D;*Amhr2-Cre* mice did not ovulate at all, and only a few COCs were observed in the oviducts of *LSL-Kras*^G12D;*Cyp19-Cre* mice (Fig. 2B). The
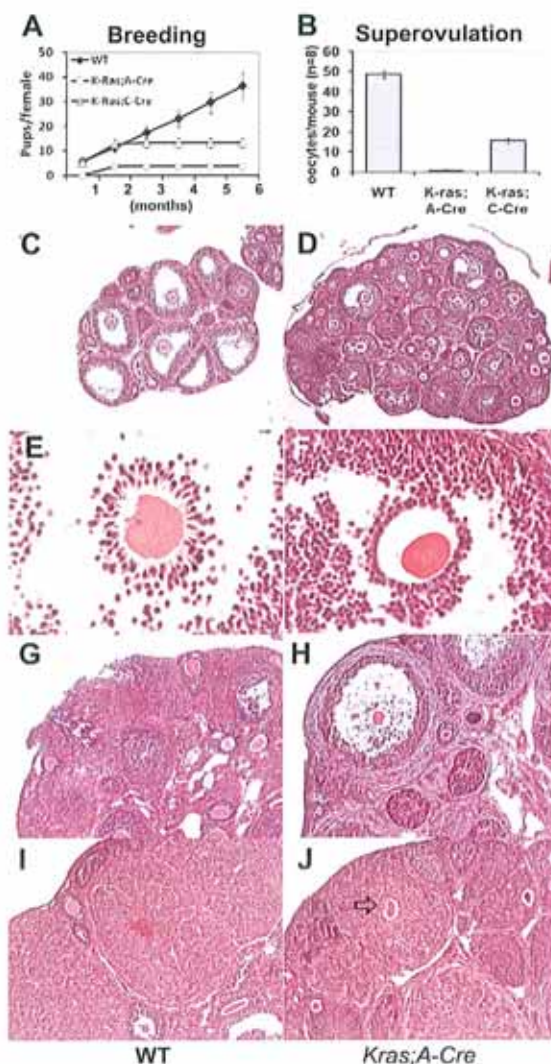

Fig. 2. Expression of KRAS^G12D in granulosa cells causes multiple reproductive defects. (A) Continuous breeding assay showing the cumulative number of progeny per female. The *LSL-Kras*^G12D;*Amhr2-Cre* and *LSL-Kras*^G12D;*Cyp19-Cre* females (*n*=6) were subfertile. (B) Superovulation experiments showing that the ovulation rate in response to gonadotropins was reduced in *Kras* mutant mice (*n*=10) as compared with the wild type (WT). (C-J) Histology of WT (C,E,G,I) and *LSL-Kras*^G12D;*Amhr2-Cre* (D,F,H,J) ovaries at 8 (C-F), 16 (G,H) and 48 (I,J) hours after hCG treatment. Histology of WT (I) and *LSL-Kras*^G12D;*Amhr2-Cre* (J) ovaries 48 hours after hCG treatment shows that an oocyte is trapped in the corpus luteum of the *Kras* mutant ovary (arrow).
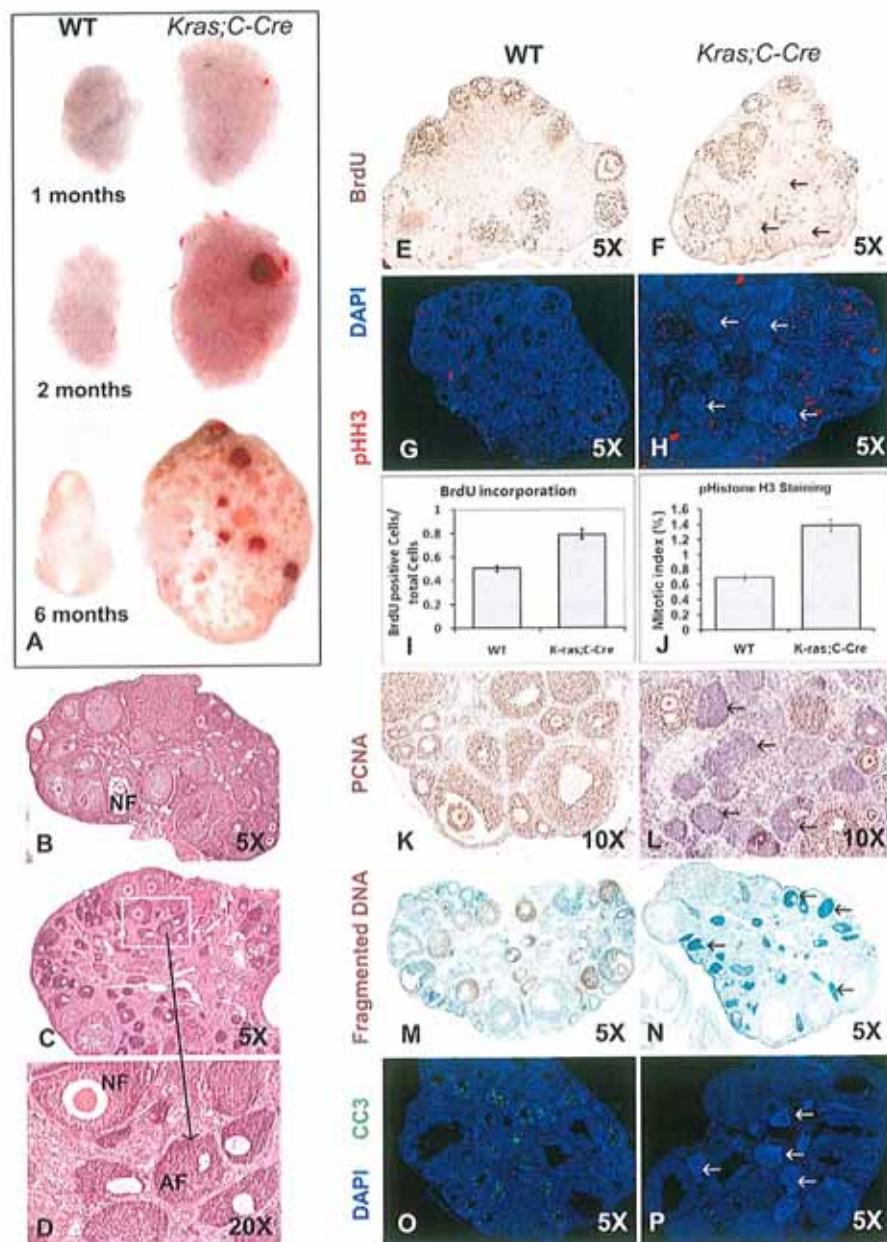
Fig. 3. *Kras*^{G12D} conditional knock-in mice develop ovarian lesions with altered granulosa cell proliferation, differentiation and apoptosis. (**A**) Size differences in wild-type (WT) and *LSL-Kras*^{G12D}*;Cyp19-Cre* ovaries at various ages. (**B-D**) Histology of WT (B) and *LSL-Kras*^{G12D}*;Cyp19-Cre* (C,D) ovaries at 6 months of age. NF, normal follicle; AF, abnormal follicle. (**E,F**) BrdU incorporation assay in 12-week-old WT (E) and *LSL-Kras*^{G12D}*;Cyp19-Cre* (F) ovaries. Abnormal follicle-like structures are indicated by arrows (as below). (**G,H**) Immunofluorescent detection of phospho-histone H3 (pHH3, red) in 12-week-old WT (G) and *LSL-Kras*^{G12D}*;Cyp19-Cre* (H) ovaries. (**I,J**) BrdU incorporation (I) and immunofluorescence for the mitosis marker phospho-histone H3 (J) indicate slightly increased levels of proliferation in *Kras*^{G12D}-expressing granulosa cells of antral follicles, as compared with wild type. (**K,L**) Immunohistochemical detection of PCNA in 12-week-old WT (K) and *LSL-Kras*^{G12D}*;Cyp19-Cre* (L) ovaries. (**M,N**) Apoptosis assays in 4-week-old WT (M) and *LSL-Kras*^{G12D}*;Cyp19-Cre* (N) ovaries, 2 hours after hCG treatment. (**O,P**) Immunofluorescent detection of cleaved caspase 3 (CC3) in 12-week-old WT (O) and *LSL-Kras*^{G12D}*;Cyp19-Cre* (P) ovaries.

histological data from the *LSL-Kras*^{G12D}*;Amhr2-Cre* mice are presented because the block of ovulation was more complete in this strain. However, the overall histological patterns in the two mutant strains were similar. Specifically, ovulation failure in the mutant mice was associated with defects of COC expansion and with the germinal vesicle breakdown of oocytes (Fig. 2D,F), whereas expanded COCs and meiotic oocytes with condensed chromosomes were present in the preovulatory follicles of control mice, at 8 hours post-hCG (Fig. 2C,E). In control mice, most large antral follicles ovulated by 16 hours after hCG (Fig. 2G) and had well developed corpora lutea (CLs) at 48 hours post-hCG (Fig. 2I). By contrast, antral follicles containing unovulated COCs remained in the mutant mouse ovaries at 16 hours post-hCG (Fig. 2H) and unovulated oocytes were trapped at the center of the CL at 48 hours post-hCG (Fig. 2J). More than 40 sections of *Kras*^{G12D} mutant ovaries (*n*=4) were examined, and trapped oocytes were present in 80-90% of the newly formed CLs. Because comparative analyses of the two mutant

mouse strains revealed similar phenotypes and because expression of the *Cyp19-Cre* transgene is more specific for granulosa cells than is *Amhr2-Cre*, data from the *Kras*^{G12D}*;Cyp19-Cre* mice (C-Cre) mice are presented.

Kras^{G12D} conditional knock-in mice develop abnormal follicle-like structures with altered granulosa cell proliferation and apoptosis

Ovaries from *LSL-Kras*^{G12D}*;Amhr2-Cre* and *LSL-Kras*^{G12D}*;Cyp19-Cre* mice were consistently larger and increased progressively in size, as compared with control littermates (Fig. 3A). Histological sections of the *Kras* mutant ovaries revealed multiple abnormal small 'follicle-like' structures compared with controls (Fig. 3, C and D compared with B). These small follicle-like structures lacked an antrum and consisted of nests of disorganized, pleiomorphic granulosa cells. Many of these structures contained an oocyte of abnormal appearance that was

displaced to the periphery of the 'follicle' rather than being central (Fig. 3D). Cells within these abnormal follicle-like structures failed to express the granulosa cell marker genes *Nr5a1* (see Fig. S1A-D in the supplementary material), *Cyp11a1* (see Fig. S1E-H in the supplementary material) and *Foxo1* (data not shown), indicating that normal granulosa cell differentiation had been blocked at an early stage of follicle growth.

To characterize the *Kras* mutant ovaries at the cellular level, we examined the proliferative rate of the developing follicles. In antral follicles, $Kras^{G12D}$-expressing granulosa cells demonstrated slightly increased levels of proliferation, based on BrdU incorporation (Fig. 3E,F,I) and immunofluorescence for the mitosis marker phospho-histone H3 (pHH3) (Fig. 3G,H,J). By contrast, only a limited number of cells within the abnormal follicle-like structures were positive for these proliferation markers. Immunohistochemical staining for proliferating cell nuclear antigen (PCNA) further proved that these abnormal structures are negative for proliferation markers (Fig. 3K,L).

Since the cells in the aberrant ovarian lesions were non-mitotic, the progressive enlargement of *Kras* mutant ovaries and the increased number of abnormal follicle-like structures might be caused by repression of apoptosis, a common feature in the mammalian ovary that serves to eliminate atretic follicles (Wang et al., 2006). Both the TUNEL assay and immunostaining for cleaved caspase 3 (CC3) were analyzed in the *Kras* mutant ovaries. Immature control and *Kras* mutant mice were primed with eCG and hCG to stimulate increased follicle growth. At 2 hours after hCG, DNA fragmentation (Fig. 3M) and caspase 3 cleavage (Fig. 3O) were detected in multiple pre- and early-antral follicles in control ovaries. By contrast, these apoptosis markers were markedly reduced in the *Kras* mutant ovaries, where the abnormal follicle-like structures were completely devoid of fragmented DNA and cleaved caspase 3 (Fig. 3N,P). These results show that apoptosis was repressed by the $Kras^{G12D}$ mutation in granulosa cells.

$Kras^{G12D}$ downregulates genes essential for granulosa cell differentiation and ovulation

Because the $Kras^{G12D}$ knock-in mice failed to ovulate, the expression of genes crucial for granulosa/cumulus cell differentiation and ovulation was analyzed in wild-type and mutant ovaries. As shown in Fig. 4A, *Fshr* mRNA was readily detected in ovaries of immature control mice and increased ~2.5-fold in response to eCG and was associated with the growth of preovulatory follicles. Other genes highly induced by eCG were *Lhcgr*, a marker of differentiated granulosa cells in preovulatory follicles, *Areg*, which encodes an EGF-like factor, and *Cyp11a1*, which encodes the steroidogenic enzyme leading to progesterone biosynthesis. Whereas expression of *Fshr* and *Lhcgr* was selectively reduced by the ovulatory stimulus of hCG, genes associated with ovulation (*Areg*, *Ptgs2* and *Tnfaip6*) and luteinization (*Cyp11a1*) were upregulated markedly by hCG (Fig. 4A). By contrast, the induced expression of these genes was reduced/altered in ovaries of the $Kras^{G12D}$ mutant mice. Notably, levels of *Fshr* mRNA were reduced in the ovaries of immature (untreated) *Kras* mutant mice indicating that constitutively active KRAS impairs the expression of this gene at an early stage of granulosa cell differentiation.

To determine whether the decreased levels of *Fshr* and *Lhcgr* mRNAs were the direct effect of mutant $Kras^{G12D}$ expression, we isolated undifferentiated granulosa cells from immature *LSL-$Kras^{G12D}$* mice and cultured them in serum-free medium followed by infection with an adenoviral vector expressing Cre recombinase driven by the CMV promoter (Ad-CMV-Cre). In control cells,
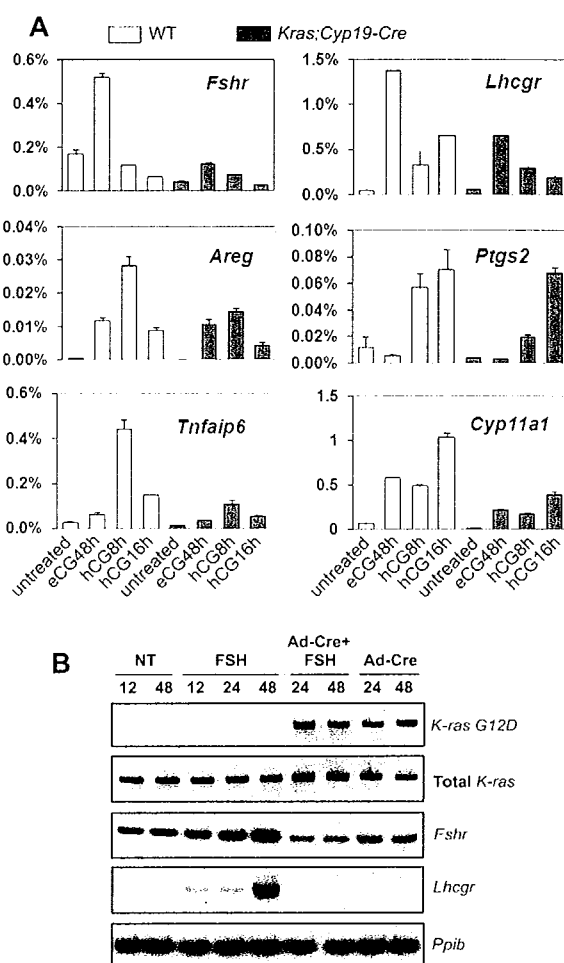

Fig. 4. $Kras^{G12D}$ **downregulates genes essential for granulosa cell differentiation and ovulation. (A)** qRT-PCR of ovulation-related genes from mouse whole ovary mRNAs. Six ovaries from different animals were analyzed. **(B)** $Kras^{G12D}$ downregulated the expression of *Fshr* and prevented the FSH-induced expression of *Lhcgr* in cultured granulosa cells. Expression of $Kras^{G12D}$ was induced by infecting the cells with an adenoviral vector encoding Cre recombinase (Ad-Cre). FSH (100 ng/ml) was added to the medium of cells infected, or not, with Ad-Cre. NT, non-treated. *Ppib* was amplified by RT-PCR in the same samples, as loading control.

addition of FSH to the medium upregulated *Fshr* and induced the expression of *Lhcgr* mRNAs. However, the *Fshr* mRNA level decreased in the granulosa cells expressing $Kras^{G12D}$, and the inductive effect of FSH on *Lhcgr* mRNA was totally abolished (Fig. 4B). This experiment confirmed our observations in vivo (Fig. 4A) and provided direct evidence that KRAS^{G12D} reduces *Fshr* mRNA levels and blocks FSH-mediated induction of luteinizing hormone (LH) receptors in granulosa cells.

KRAS^{G12D} activates both RAF1/MAPK and PI3K/AKT pathways in granulosa cells

FSH and LH transiently activate ERK1/2 and PI3K pathways in granulosa cells (Cottom et al., 2003; Gonzalez-Robayna et al., 2000). Recently, FSH has been shown to activate RAS, indicating that granulosa cells have factors that mediate G-protein receptor coupling to RAS (Wayne et al., 2007). Therefore, we analyzed components of the RAF1/MEK1/ERK1/2 and PI3K/AKT cascades
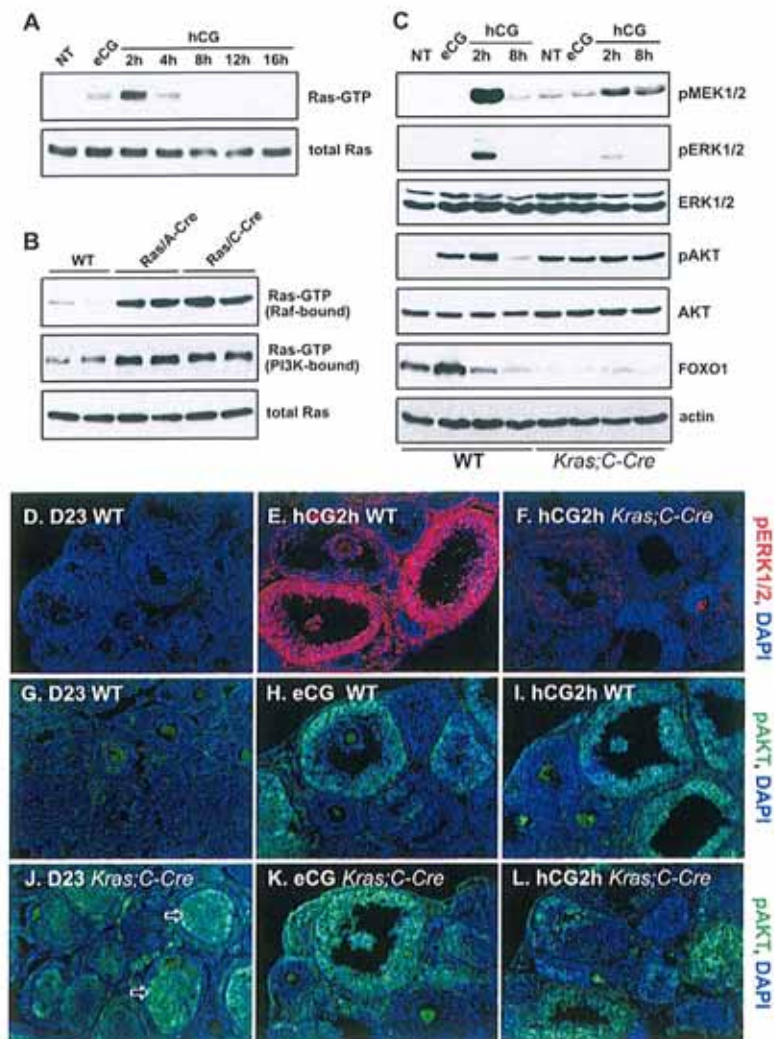
Fig. 5. KRAS^{G12D} activates the RAF1/MEK/ERK1/2 and PI3K/AKT pathways in granulosa cells. (A) RAS activity in wild-type ovaries during ovulation, as measured by a GST pull-down assay using RAF1 RAS-binding domain (RBD) as the bait. NT, non-treated. (B) RAS-GTP levels increased in immature *LSL-Kras^{G12D};Amhr2-Cre* and *LSL-Kras^{G12D};Cyp19-Cre* ovaries, as measured by the GST pull-down assay using both RAF1 RBD and p110α RBD. (C) Phosphorylation of MEK1/2, ERK1/2 and AKT in wild-type and *LSL-Kras^{G12D};Cyp19-Cre* ovaries after eCG/hCG treatment. Total ERK1/2 and AKT are shown as loading controls. (D-F) Localization of phospho-ERK1/2 in ovaries. The level of phospho-ERK1/2 was low in immature wild-type mouse ovaries (D), but was increased in the large antral follicles 2 hours after hCG injection (E). By contrast, the phospho-ERK1/2 level remained low in *LSL-Kras^{G12D};Cyp19-Cre* ovaries after the same treatment (F). (G-I) Immunofluorescence of phospho-AKT in wild-type ovaries. (G) Immature ovary; (H) 48 hours after eCG; (I) 2 hours after hCG. (J-L) Immunofluorescence of phospho-AKT in *LSL-Kras^{G12D};Cyp19-Cre* ovaries. (J) Immature ovary before eCG treatment (abnormal follicle-like structures indicated by arrows); (K) 48 hours after eCG treatment; (L) 2 hours after hCG treatment. Three to six ovaries from different animals of each genotype were analyzed in each of these experiments.

in both control and *Kras^{G12D}* mutant ovaries. First, we measured RAS activity by RAS-GTP pull-down assay. Whereas levels of total RAS did not change throughout the ovulation period, levels of active, GTP-bound RAS were undetectable in ovaries at postnatal day 23, increased slightly in response to eCG (48 hours) and then increased markedly (but transiently) 2 hours after hCG (Fig. 5A). When RAS-GTP was measured by GST-RAF1 and GST-p110α pull-down assays in *Kras* mutant ovaries, high levels of RAS-GTP were present compared with control mice (Fig. 5B). These results indicate that *Kras^{G12D}* mutant protein interacts with both PI3K and RAF1 in ovaries.

The phosphorylation status of selected RAS downstream kinases was also analyzed. Levels of phospho-MEK1/2 (MAP2K1/2 – Mouse Genome Informatics) and phospho-ERK1/2 were negligible in ovaries of immature mice prior to and 48 hours after eCG treatment (Fig. 5C; NT and eCG, respectively), increased dramatically 2 hours post-hCG and declined by 4 hours (see Fig. S2A in the supplementary material). Levels of phospho-AKT were low in ovaries of immature mice but increased markedly after eCG treatment. Phospho-AKT was further increased 2 hours post-hCG stimulation, was maintained at 4 hours (Fig. 5C and see Fig. S2A in the supplementary material) and returned to a basal level 8 hours post-hCG, a pattern similar to that of PDK1 (see Fig. S2A in the supplementary material). In addition, the total amount of the known

AKT target, FOXO1, was reduced in *Kras* mutant ovaries compared with controls. The total amounts of ERK1/2 and AKT, as well as of actin (loading control), were not altered by gonadotropin treatment (Fig. 5C).

In comparison to their phosphorylation patterns in wild-type mice, elevated levels of phospho-MEK1/2 and phospho-AKT were observed in ovaries of *Kras* mutant mice even without hormonal stimulation (Fig. 5C, NT), and were only marginally increased in response to hCG, indicating that KRAS^{G12D} exerted stimulatory effects on these pathways (Fig. 5C). By contrast, the levels of phospho-ERK1/2 were undetectable in the same *Kras* mutant ovaries and increased only marginally after hCG treatment. These data suggested that potent inhibitory factors selectively reduced ERK1/2 phosphorylation.

To determine the cell-specific pattern of phospho-ERK1/2 and phospho-AKT in ovaries, immunofluorescent staining was performed using phospho-specific antibodies. In wild-type ovaries, phospho-ERK1/2 was only detected in the large antral follicles 2 hours after hCG (Fig. 5E and see Fig. S2B in the supplementary material). By contrast, levels of phospho-ERK1/2 were markedly reduced in *Kras* mutant ovaries treated in the same manner (Fig. 5F). In control ovaries, phospho-AKT was first detected after eCG stimulation in the mural layer of granulosa cells in the large antral follicles, whereas the signal was weak in the cumulus cells (Fig. 5H

and see Fig. S1C in the supplementary material). However, within 2 hours of hCG treatment, phospho-AKT was present in all granulosa/cumulus cells (Fig. 5I and see Fig. S1D in the supplementary material). By comparison, the phospho-AKT signal was already high in granulosa cells of the 23-day-old *Kras* mutant mice before eCG treatment. Phospho-AKT was also detected in some of the abnormal follicle-like structures (Fig. 5J, arrows). The progressive pattern of AKT phosphorylation was not seen in *Kras* mutant follicles. Rather, all granulosa/cumulus cells were positive for phospho-AKT after eCG treatment alone (Fig. 5K) or eCG/hCG treatment (2 hours) (Fig. 5L).

Acute effect of *Kras*^{G12D} expression in cultured granulosa cells

That KRAS^{G12D} interacts with RAF1 and activates MEK1/2 in granulosa cells but failed to increase ERK1/2 phosphorylation suggested that potent negative-feedback mechanisms were operative in these cells. To test this, granulosa cells isolated from 21-day-old *LSL-Kras*^{G12D} mouse ovaries were infected with Ad-CMV-Cre. Expression of *Kras*^{G12D} mRNA was detected by RT-PCR after adenoviral infection (Fig. 6A). Phospho-ERK1/2 increased gradually from 8 to 24 hours post-infection, but decreased to a basal level at 48 hours (Fig. 6B). Phospho-AKT also increased post-infection, but remained elevated at 48 hours, a time when the phospho-ERK1/2 level decreased, indicating that both the ERK1/2 and PI3K pathways in granulosa cells were transiently activated by KRAS^{G12D} but that negative-feedback mechanisms were induced to selectively block the ERK1/2 pathway in response to constitutively active KRAS^{G12D}. Additional *LSL-Kras*^{G12D} granulosa cells were infected with Ad-CMV-Cre or Ad-CMV-GFP (as control) for 48 hours and then stimulated with FSH, forskolin (Fo) or AREG for 20 minutes. As shown in Fig. 6C, each agonist induced ERK1/2 phosphorylation in control cells. However, in the cells expressing KRAS^{G12D}, the responses to agonists were markedly reduced indicating that KRAS^{G12D} activates a negative-feedback mechanism that represses ERK1/2 phosphorylation.

Mkp3 is upregulated by *Kras*^{G12D} in granulosa cells and negatively regulates ERK1/2 activity

To elucidate specific changes in ovarian gene expression associated with the *Kras*^{G12D} mutation, microarray analyses were undertaken using RNA prepared from ovaries of *LSL-Kras*^{G12D};*Amhr2-Cre* versus *LSL-Kras*^{G12D} mice at 26 days of age. The microarray data showed that the *Mkp3* (*Dusp6*) gene was upregulated in the *Kras* mutant ovaries, and this was confirmed by RT-PCR (Fig. 7A). This gene encodes MAPK phosphatase 3 (MKP3), which is an ERK1/2-specific protein phosphatase (Camps et al., 2000; Keyse, 2000; Li et al., 2007; Urness et al., 2007; Woods and Johnson, 2006). Expression of *Mkp3* was induced in granulosa cells both in vivo (2-4 hours) and in vitro (1-2 hours) by hCG and AREG stimulation, respectively (Fig. 7B,J). In situ hybridization showed that *Mkp3* mRNA is highly expressed in pre-ovulatory follicles 4 hours after hCG treatment (Fig. 7C,D), but is undetectable in 23-day-old ovaries (Fig. 7E,F). Ovaries of *LSL-Kras*^{G12D};*Amhr2-Cre* mice (23 days old) exhibited elevated expression of *Mkp3* mRNA in growing follicles, as compared with wild type (Fig. 7G,H, arrows).

To provide further evidence that MKP3 is functionally involved in the negative regulation of ERK1/2 activity, *Mkp3* mRNA was depleted in cultured granulosa cells by RNAi. *Mkp3* siRNA (50 nM) efficiently decreased *Mkp3* mRNA in unstimulated cells or those exposed to AREG, the most potent stimulator of ERK1/2 in granulosa cells (Fig. 7I). AREG induced rapid but transient
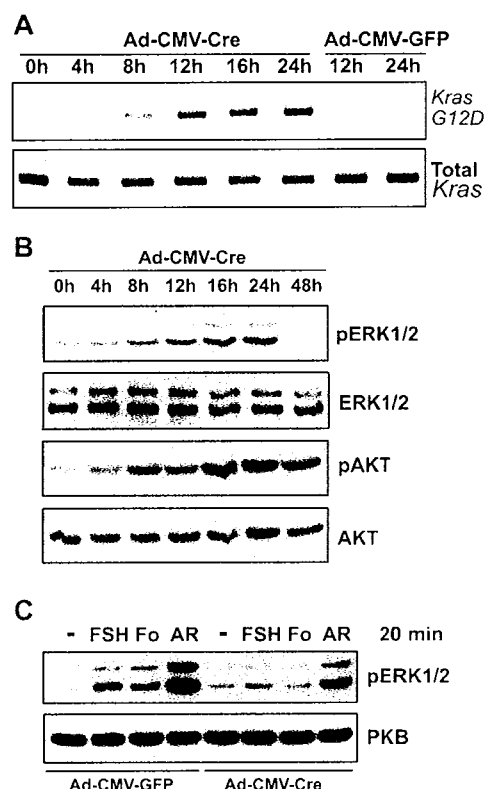

Fig. 6. Acute effect of *Kras*^{G12D} expression in cultured granulosa cells. (A) Expression of *Kras*^{G12D} mRNA in *LSL-Kras*^{G12D} granulosa cells after infection with Ad-CMV-Cre. (B) Levels of phospho-ERK1/2 and phospho-AKT post-infection. (C) *LSL-Kras*^{G12D} granulosa cells infected with Ad-CMV-Cre and control vectors (Ad-CMV-GFP) for 48 hours were stimulated with FSH, forskolin (Fo) or amphiregulin (AR) for 20 minutes. Each agonist induced ERK1/2 phosphorylation in control granulosa cells, but the responses were reduced in the cells expressing KRAS^{G12D}.

phosphorylation of ERK1/2 in control granulosa cells. However, in cells treated with *Mkp3* siRNA, the dephosphorylation of ERK1/2 was significantly delayed (Fig. 7J,K). Lastly, ERK1/2 activity is required for the induction of *Mkp3*, because the MEK1/2 inhibitor PD98059 blocked the AREG-induced *Mkp3* expression in cultured granulosa cells (Fig. 7M,N).

DISCUSSION

Activation of the RAS small G-protein family is crucial for FSH and EGF-like factor-induced signaling events in cultured granulosa cells via stimulation of downstream kinases such as ERK1/2 and AKT (Wayne et al., 2007). Based on in vitro studies, the ERK1/2 pathway is presumed to be essential for COC expansion and meiotic resumption of oocytes (Diaz et al., 2006; Fan et al., 2003; Shimada et al., 2006; Su et al., 2002). FSH-mediated stimulation of the PI3K pathway is also presumed to impact follicular development (Alam et al., 2004; Alliston et al., 2000; Park et al., 2005; Richards et al., 2002; Zeleznik et al., 2003). By analyzing the effects of expressing a constitutively active form of KRAS (KRAS^{G12D}) selectively in granulosa cells of two mouse models, we report the first detailed investigation of the consequences of mutant KRAS activation during mammalian follicle development and ovulation. In both models, we observed two distinct follicular phenotypes, suggesting that the impact of *Kras*^{G12D} is dependent on the stage of granulosa cell
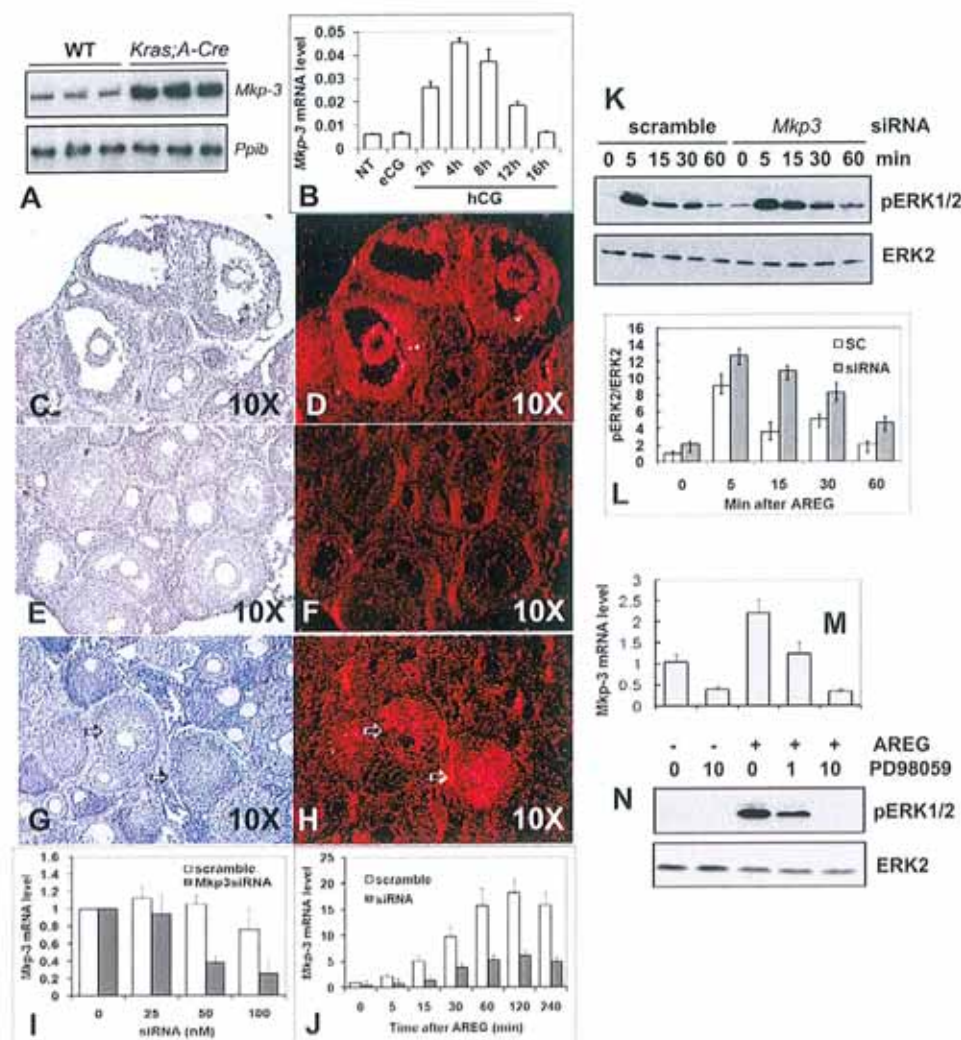
Fig. 7. Mkp3 is a KRAS[G12D]-induced gene involved in normal and abnormal granulosa cell development. (A) Semi-quantitive RT-PCR shows that *Mkp3* mRNA levels were elevated in *LSL-Kras[G12D];Amhr2-Cre* ovaries as compared with those of wild-type mice (*n*=3 for each genotype). (B) *Mkp3* mRNA expression was induced in wild-type granulosa cells by eCG/hCG treatment. (C-H) In situ hybridization for *Mkp3* in wild-type and *Kras* mutant ovaries. Bright-field images show ovarian histology (C,E,G), whereas dark-field images show the signals of *Mkp3* antisense probe (D,F,H). *Mkp3* mRNA was detected in granulosa/cumulus cells at 4 hours after hCG (D), but not in immature wild-type ovaries (F). By contrast, *Mkp3* mRNA was detected in some preantral follicles (H, arrows) in *Kras* mutant ovaries of the same age. (I,J) *Mkp3* siRNA decreased the *Mkp3* mRNA levels in unstimulated granulosa cells (I) or those stimulated with AREG (J). (K,L) AREG induced transient phosphorylation of ERK1/2 in control granulosa cells; however, in the granulosa cells treated with *Mkp3* siRNA, levels of phospho-ERK1/2 remained elevated for longer (K). (L) Intensity comparison of phospho-ERK2/total ERK2. (M,N) PD98059 blocked AREG-induced *Mkp3* expression (M), when the ERK1/2 activation is blocked (N).

differentiation. If recombination occurred at early stages of follicle development, many abnormal follicle-like structures were observed, whereas if recombination occurred later, events associated with ovulation were impaired (Fig. 8). These changes in ovarian function caused the *Kras[G12D]* mutant mice to be subfertile and to exhibit premature ovarian failure. Because *Amhr2-Cre* is expressed earlier in follicular development than *Cyp19-Cre* (our unpublished observations), the *Kras[G12D];Amhr2-Cre* mice exhibited more-severe ovulation defects. The expression of the *Cyp19-Cre* transgene is highly specific for granulosa cells. Although *Cyp19-Cre* is expressed in follicles at slightly later stages of growth than *Amhr2-Cre*, the *Kras[G12D];Cyp19-Cre* and *Kras[G12D];Amhr2-Cre* phenotypes are very similar, verifying that mutant KRAS[G12D] impacts granulosa cell function in a stage-specific manner.

Because granulosa cells are highly proliferative and KRAS[G12D] can induce tumorigenic transformation of several cell types (Campbell et al., 2007; Sarkisian et al., 2007; Shaw et al., 2007; Tuveson et al., 2004), we anticipated that expression of KRAS[G12D] in granulosa cells might lead to enhanced proliferation and oncogenic transformation of these cells. Oncogenic transformation was not observed and alterations in proliferation were critically dependent on when recombination and expression of KRAS[G12D] were initiated. In the abnormal follicle-like structures, no evidence for proliferation was observed. However, in the large antral

follicles, proliferation was increased, indicating that the effects of mutant KRAS were dependent on the stage of granulosa cell differentiation. Furthermore, expression of KRAS[G12D] led to impaired apoptosis of granulosa cells in the abnormal follicle-like structures, whose growth appeared to be self-limiting. Expression of KRAS[G12D] also profoundly altered the fate and differentiation of granulosa cells. Specifically, expression of mutant KRAS[G12D] in granulosa cells of small growing follicles completely disrupted normal follicular development and granulosa cell differentiation, as known markers of granulosa cell function (*Fshr* and *Nr5a2*) (Richards, 1994) were not detected. This altered cell fate led to a novel and unexpected ovarian phenotype, with follicle-like structures that were devoid of mitotic, apoptotic and differentiated cells (Fig. 8). The behavior of the granulosa cells in these abnormal follicle-like structures appears to be similar to the premature senescence observed in primary cells in culture expressing mutant forms of HRAS (Lin et al., 1998).

Follicles in which granulosa cells escaped the recombination events at an early stage of development continued to grow to the antral stage. However, follicles with granulosa cells expressing KRAS[G12D] at this stage also exhibited impaired function. Specifically, most antral follicles failed to ovulate even if exposed to exogenous hormones. Ovulation failure was associated with impairments in expansion of cumulus cells, in meiotic maturation of
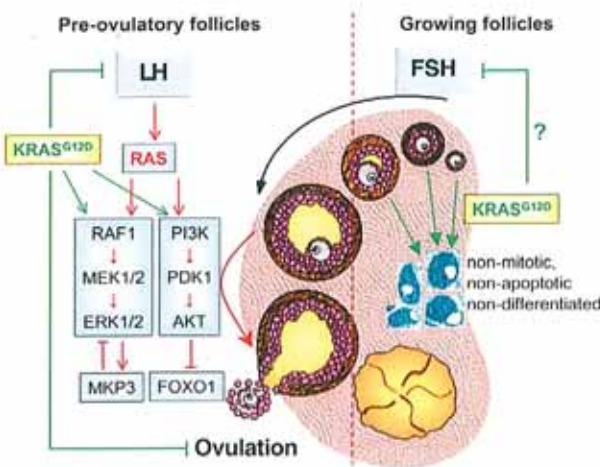
Fig. 8. Schematic of the ovarian defects caused by the expression of KRAS^{G12D} in developing follicles. In ovaries of wild-type mice, the LH/hCG surge transiently activates RAS and its downstream effecters, the ERK1/2 pathway and the PI3K pathway, which impact granulosa cell differentiation and ovulation by regulating the expression of numerous genes. ERK1/2 induces the expression of MKP3, which negatively regulates ERK1/2 activity in ovulating follicles as well as in cells expressing mutant *Kras*^{G12D}. PI3K regulates the phosphorylation of AKT and FOXO1. When KRAS^{G12D} is expressed in the granulosa cells, it interacts with both RAF1 and PI3K, activates ERK1/2 and AKT, respectively, and leads to two major ovarian phenotypes. In small follicles, the granulosa cells fail to differentiate and are devoid of their marker genes such as the FSH receptor. Moreover, these granulosa cells are non-mitotic, non-apoptotic and reside in abnormal follicle-like structures that accumulate in the ovaries of the mutant mice. Those follicles that escape this senescent fate develop to the antral stage but fail to ovulate because of the impaired expression of genes associated with ovulation. In addition, the mutant antral follicles exhibit reduced levels of phospho-ERK1/2 related to abnormally elevated levels of *Mkp3*. Red lines, RAS-related events in normal ovaries; green lines, KRAS^{G12D}-related events in mutant ovaries.

the oocytes and in expression of ovulation-related genes. This phenotype is similar to that of the mutant mouse model with an EGFR signaling defect (Hsieh et al., 2007). The altered response of KRAS^{G12D}-expressing granulosa cells to LH/hCG appears to be related to low levels of *Fshr* and the inability of FSH to induce expression of *Lhcgr* mRNA, and therefore to the loss of the crucial LH-ERK1/2 signaling pathways. This conclusion is supported by the reduced expression of specific genes known to be essential for COC expansion and ovulation (Richards, 2005), including *Ptgs2*, *Has2* and *Tnfaip6*.

The mechanisms by which KRAS^{G12D} alters granulosa cell functions and fate appear to be mediated by both the ERK1/2 pathway and the PI3K pathway. Specifically, our results show for the first time that treatment of mice in vivo with exogenous hormones, eCG and hCG, leads to transient activation of RAS and that this is associated with the transient phosphorylation of ERK1/2 and AKT in granulosa cells. By contrast, granulosa cells expressing KRAS^{G12D} exhibit elevated levels of RAS-GTP, as would be expected. In these cells, KRAS^{G12D} interacts with RAF1 and initially leads to increased phosphorylation of ERK1/2. These results support our recent study showing that RAS-GTP in rat granulosa cells interacts with RAF1 directly (Wayne et al., 2007), as well as the studies of others who have shown that KRAS^{G12D} selectively activates RAF1 and/or PI3K in a cell- and context-specific manner

(Campbell et al., 2007; Cespedes et al., 2006; Gupta et al., 2007; Tuveson et al., 2004). However, KRAS^{G12D}-mediated ERK1/2 phosphorylation is transient and becomes markedly reduced in the mutant granulosa cells in vivo and in culture. This transient activation of ERK1/2 is mediated, at least in part, by the upregulation of MKP3, a specific ERK1/2 phosphatase (Camps et al., 2000; Keyse, 2000; Li et al., 2007; Urness et al., 2007; Woods and Johnson, 2006). *Mkp3* mRNA was rapidly induced in granulosa cells of wild-type mice in response to hCG and was elevated in *Kras*^{G12D} mutant ovaries (Fig. 7) and cultured granulosa cells expressing KRAS^{G12D} (data not shown). Because induction of *Mkp3* mRNA by AREG in granulosa cells was blocked by the MEK1/2 inhibitor PD98059, these results reinforce the notion that ERK1/2 induces expression of this negative-regulatory factor in granulosa cells. Conversely, reducing *Mkp3* expression by a siRNA approach prolonged the presence of phospho-ERK1/2 in response to AREG by up to 60 minutes. Collectively, these results provide evidence that MKP3 is regulated in murine ovarian granulosa cells and controls the duration of ERK1/2 phosphorylation.

Although *Mkp3* is induced in granulosa cells of preovulatory follicles and is initially elevated in these cells in the *Kras*^{G12D} mutant ovaries, *Mkp3* mRNA was not expressed in the granulosa cells contained within the abnormal follicle-like structures. Thus, the absence of phospho-ERK1/2 in these cells also indicates that other potent mechanisms impact and reduce ERK1/2 signaling in these mutant cells. For example, RAS can mediate the epigenetic silencing of genes via its ability to induce CpG methylation at promoter regions of certain genes (Gazin et al., 2007). Moreover, the mediators of RAS epigenetic silencing include *Mapk1* (*Erk2*), *Pdpk1* (*Pdk1*) and *Dnmt1* (Gazin et al., 2007). Thus, it is tempting to speculate that the cells within the abnormal follicle-like structures have undergone specific epigenetic changes to prevent their proliferation, apoptosis and differentiation.

In contrast to ERK1/2, phosphorylation of AKT in granulosa cells of growing and large antral follicles was enhanced by the presence of KRAS^{G12D} in vivo and in KRAS^{G12D}-expressing granulosa cells in culture. Since our GST pull-down assays showed that KRAS^{G12D} interacts directly with the p110α subunit of PI3K as previously reported (Rodriguez-Viciana et al., 1994; Rodriguez-Viciana et al., 1996), it is likely that KRAS^{G12D} stimulates the PI3K pathway directly, leading to the prolonged activation of AKT in granulosa cells. KRAS^{G12D} also impairs the expression of FOXO1 that may be mediated by prolonged activation of AKT. Since FOXO1 has been shown to impair granulosa cell differentiation (Park et al., 2005; Rudd et al., 2007), one might have predicted that the mutant cells would exhibit increased responsiveness to FSH, which is not the case. Rather, the PI3K pathway appears to regulate additional functions in granulosa cells. Because *Pdpk1* is a factor implicated in RAS-mediated epigenetic gene silencing (Gazin et al., 2007), it is possible that the PI3K pathway is crucial for dictating the fate of granulosa cells in small follicles.

In summary, transient activation of RAS and the phosphorylation of downstream targets, such as the RAF1/MEK1/ERK1/2 and PI3K/AKT cascades, appear to be crucial for mediating appropriate responses of granulosa cells to the gonadotropic hormones FSH and LH, leading to progressive follicular development and ovulation. Conversely, persistent expression of a constitutively active form of KRAS (KRAS^{G12D}) impairs ovulation and the expression of ovulation-related genes. Moreover, if expressed at an early stage in follicle development, KRAS^{G12D} dramatically alters granulosa cell fate by precluding granulosa cell differentiation, proliferation and apoptosis, thus impairing granulosa cell responses to gonadotropins

and leading to premature ovarian failure (Fig. 8). This marked divergence in granulosa cell function suggests that the potent epigenetic silencing of the promoters of specific genes might provide the basis of how activation of RAS alone can cause quiescence/senescence, rather than transformation, of these cells. These results also provide novel evidence that granulosa cells in vivo possess mechanisms that make them extremely impervious to tumorous transformation and that instead lead to premature ovarian failure.

Supplementary material

Supplementary material for this article is available at
http://dev.biologists.org/cgi/content/full/135/12/2127/DC1

References

Alam, H., Maizels, E. T., Park, Y., Ghaey, S., Feiger, Z. J., Chandel, N. S. and Hunzicker-Dunn, M. (2004). Follicle-stimulating hormone activation of hypoxia-inducible factor-1 by the phosphatidylinositol 3-kinase/AKT/Ras homolog enriched in brain (Rheb)/mammalian target of rapamycin (mTOR) pathway is necessary for induction of select protein markers of follicular differentiation. *J. Biol. Chem.* **279**, 19431-19440.

Alliston, T. N., Gonzalez-Robayna, I. J., Buse, P., Firestone, G. L. and Richards, J. S. (2000). Expression and localization of serum/glucocorticoid-induced kinase in the rat ovary: relation to follicular growth and differentiation. *Endocrinology* **141**, 385-395.

Arango, N. A., Kobayashi, A., Wang, Y., Jamin, S. P., Lee, H. H., Orvis, G. D. and Behringer, R. R. (2008). A mesenchymal perspective of mullerian duct differentiation and regression in Amhr2-lacZ mice. *Mol. Reprod. Dev.* **75**, 1154-1162.

Boerboom, D., Paquet, M., Hsieh, M., Liu, J., Jamin, S. P., Behringer, R. R., Sirois, J., Taketo, M. M. and Richards, J. S. (2005). Misregulated Wnt/beta-catenin signaling leads to ovarian granulosa cell tumor development. *Cancer Res.* **65**, 9206-9215.

Boerboom, D., White, L. D., Dalle, S., Courty, J. and Richards, J. S. (2006). Dominant-stable beta-catenin expression causes cell fate alterations and Wnt signaling antagonist expression in a murine granulosa cell tumor model. *Cancer Res.* **66**, 1964-1973.

Bourne, H. R., Sanders, D. A. and McCormick, F. (1990). The GTPase superfamily: a conserved switch for diverse cell functions. *Nature* **348**, 125-132.

Campbell, P. M., Groehler, A. L., Lee, K. M., Ouellette, M. M., Khazak, V. and Der, C. J. (2007). K-Ras promotes growth transformation and invasion of immortalized human pancreatic cells by Raf and phosphatidylinositol 3-kinase signaling. *Cancer Res.* **67**, 2098-2106.

Campbell-Valois, F. X. and Michnick, S. W. (2007). The transition state of the ras binding domain of Raf is structurally polarized based on Phi-values but is energetically diffuse. *J. Mol. Biol.* **365**, 1559-1577.

Camps, M., Nichols, A. and Arkinstall, S. (2000). Dual specificity phosphatases: a gene family for control of MAP kinase function. *FASEB J.* **14**, 6-16.

Cespedes, M. V., Sancho, F. J., Guerrero, S., Parreno, M., Casanova, I., Pavon, M. A., Marcuello, E., Trias, M., Cascante, M., Capella, G. et al. (2006). K-ras Asp12 mutant neither interacts with Raf, nor signals through Erk and is less tumorigenic than K-ras Val12. *Carcinogenesis* **27**, 2190-2200.

Cottom, J., Salvador, L. M., Maizels, E. T., Reierstad, S., Park, Y., Carr, D. W., Davare, M. A., Hell, J. W., Palmer, S. S., Dent, P. et al. (2003). Follicle-stimulating hormone activates extracellular signal-regulated kinase but not extracellular signal-regulated kinase kinase through a 100-kDa phosphotyrosine phosphatase. *J. Biol. Chem.* **278**, 7167-7179.

Diaz, F. J., O'Brien, M. J., Wigglesworth, K. and Eppig, J. J. (2006). The preantral granulosa cell to cumulus cell transition in the mouse ovary: development of competence to undergo expansion. *Dev. Biol.* **299**, 91-104.

Dinulescu, D. M., Ince, T. A., Quade, B. J., Shafer, S. A., Crowley, D. and Jacks, T. (2005). Role of K-ras and Pten in the development of mouse models of endometriosis and endometrioid ovarian cancer. *Nat. Med.* **11**, 63-70.

Falender, A. E., Lanz, R., Malenfant, D., Belanger, L. and Richards, J. S. (2003). Differential expression of steroidogenic factor-1 and FTF/LRH-1 in the rodent ovary. *Endocrinology* **144**, 3598-3610.

Fan, H. Y. and Sun, Q. Y. (2004). Involvement of mitogen-activated protein kinase cascade during oocyte maturation and fertilization in mammals. *Biol. Reprod.* **70**, 535-547.

Fan, H. Y., Tong, C., Lian, L., Li, S. W., Gao, W. X., Cheng, Y., Chen, D. Y., Schatten, H. and Sun, Q. Y. (2003). Characterization of ribosomal S6 protein kinase p90rsk during meiotic maturation and fertilization in pig oocytes: mitogen-activated protein kinase-associated activation and localization. *Biol. Reprod.* **68**, 968-977.

Gazin, C., Wajapeyee, N., Gobeil, S., Virbasius, C. M. and Green, M. R. (2007). An elaborate pathway required for Ras-mediated epigenetic silencing. *Nature* **449**, 1073-1077.

Gemignani, M. L., Schlaerth, A. C., Bogomolniy, F., Barakat, R. R., Lin, O., Soslow, R., Venkatraman, E. and Boyd, J. (2003). Role of KRAS and BRAF gene mutations in mucinous ovarian carcinoma. *Gynecol. Oncol.* **90**, 378-381.

Gonzalez-Robayna, I. J., Falender, A. E., Ochsner, S., Firestone, G. L. and Richards, J. S. (2000). Follicle-Stimulating hormone (FSH) stimulates phosphorylation and activation of protein kinase B (PKB/Akt) and serum and glucocorticoid-Induced kinase (Sgk): evidence for A kinase-independent signaling by FSH in granulosa cells. *Mol. Endocrinol.* **14**, 1283-1300.

Gupta, S., Ramjaun, A. R., Haiko, P., Wang, Y., Warne, P. H., Nicke, B., Nye, E., Stamp, G., Alitalo, K. and Downward, J. (2007). Binding of Ras to phosphoinositide 3-kinase p110alpha is required for Ras-driven tumorigenesis in mice. *Cell* **129**, 957-968.

Hsieh, M., Boerboom, D., Shimada, M., Lo, Y., Parlow, A. F., Luhmann, U. F., Berger, W. and Richards, J. S. (2005). Mice null for Frizzled4 (Fzd4-/-) are infertile and exhibit impaired corpora lutea formation and function. *Biol. Reprod.* **73**, 1135-1146.

Hsieh, M., Lee, D., Panigone, S., Horner, K., Chen, R., Theologis, A., Lee, D. C., Threadgill, D. W. and Conti, M. (2007). Luteinizing hormone-dependent activation of the epidermal growth factor network is essential for ovulation. *Mol. Cell. Biol.* **27**, 1914-1924.

Jackson, E. L., Willis, N., Mercer, K., Bronson, R. T., Crowley, D., Montoya, R., Jacks, T. and Tuveson, D. A. (2001). Analysis of lung tumor initiation and progression using conditional expression of oncogenic K-ras. *Genes Dev.* **15**, 3243-3248.

Jamin, S. P., Arango, N. A., Mishina, Y., Hanks, M. C. and Behringer, R. R. (2002). Requirement of Bmpr1a for Mullerian duct regression during male sexual development. *Nat. Genet.* **32**, 408-410.

Johnson, L., Mercer, K., Greenbaum, D., Bronson, R. T., Crowley, D., Tuveson, D. A. and Jacks, T. (2001). Somatic activation of the K-ras oncogene causes early onset lung cancer in mice. *Nature* **410**, 1111-1116.

Jorgez, C. J., Klysik, M., Jamin, S. P., Behringer, R. R. and Matzuk, M. M. (2004). Granulosa cell-specific inactivation of follistatin causes female fertility defects. *Mol. Endocrinol.* **18**, 953-967.

Keyse, S. M. (2000). Protein phosphatases and the regulation of mitogen-activated protein kinase signalling. *Curr. Opin. Cell Biol.* **12**, 186-192.

Li, C., Scott, D. A., Hatch, E., Tian, X. and Mansour, S. L. (2007). Dusp6 (Mkp3) is a negative feedback regulator of FGF-stimulated ERK signaling during mouse development. *Development* **134**, 167-176.

Lin, A. W., Barradas, M., Stone, J. C., van Aelst, L., Serrano, M. and Lowe, S. W. (1998). Premature senescence involving p53 and p16 is activated in response to constitutive MEK/MAPK mitogenic signaling. *Genes Dev.* **12**, 3008-3019.

Mayr, D., Hirschmann, A., Lohrs, U. and Diebold, J. (2006). KRAS and BRAF mutations in ovarian tumors: a comprehensive study of invasive carcinomas, borderline tumors and extraovarian implants. *Gynecol. Oncol.* **103**, 883-887.

Pangas, S. A., Li, X., Robertson, E. J. and Matzuk, M. M. (2006). Premature luteinization and cumulus cell defects in ovarian-specific smad4 knockout mice. *Mol. Endocrinol.* **20**, 1406-1422.

Park, J. Y., Su, Y. Q., Ariga, M., Law, E., Jin, S. L. and Conti, M. (2004). EGF-like growth factors as mediators of LH action in the ovulatory follicle. *Science* **303**, 682-684.

Park, Y., Maizels, E. T., Feiger, Z. J., Alam, H., Peters, C. A., Woodruff, T. K., Unterman, T. G., Lee, E. J., Jameson, J. L. and Hunzicker-Dunn, M. (2005). Induction of cyclin D2 in rat granulosa cells requires FSH-dependent relief from FOXO1 repression coupled with positive signals from Smad. *J. Biol. Chem.* **280**, 9135-9148.

Richards, J. S. (1994). Hormonal control of gene expression in the ovary. *Endocr. Rev.* **15**, 725-751.

Richards, J. S. (2005). Ovulation: new factors that prepare the oocyte for fertilization. *Mol. Cell. Endocrinol.* **234**, 75-79.

Richards, J. S., Sharma, S. C., Falender, A. E. and Lo, Y. H. (2002). Expression of FKHR, FKHRL1, and AFX genes in the rodent ovary: evidence for regulation by IGF-I, estrogen, and the gonadotropins. *Mol. Endocrinol.* **16**, 580-599.

Rocks, O., Peyker, A. and Bastiaens, P. I. (2006). Spatio-temporal segregation of Ras signals: one ship, three anchors, many harbors. *Curr. Opin. Cell Biol.* **18**, 351-357.

Rodriguez-Viciana, P., Warne, P. H., Dhand, R., Vanhaesebroeck, B., Gout, I., Fry, M. J., Waterfield, M. D. and Downward, J. (1994). Phosphatidylinositol-3-OH kinase as a direct target of Ras. *Nature* **370**, 527-532.

Rodriguez-Viciana, P., Warne, P. H., Vanhaesebroeck, B., Waterfield, M. D. and Downward, J. (1996). Activation of phosphoinositide 3-kinase by interaction with Ras and by point mutation. *EMBO J.* **15**, 2442-2451.

Rudd, M. D., Gonzalez-Robayna, I., Hernandez-Gonzalez, I., Weigel, N. L., Bingman, W. E., 3rd and Richards, J. S. (2007). Constitutively active FOXO1a and a DNA-binding domain mutant exhibit distinct co-regulatory functions to enhance progesterone receptor A activity. *J. Mol. Endocrinol.* **38**, 673-690.

Sarkisian, C. J., Keister, B. A., Stairs, D. B., Boxer, R. B., Moody, S. E. and Chodosh, L. A. (2007). Dose-dependent oncogene-induced senescence in vivo and its evasion during mammary tumorigenesis. *Nat. Cell Biol.* **9**, 493-505.

Serrano, M., Lin, A. W., McCurrach, M. E., Beach, D. and Lowe, S. W. (1997). Oncogenic ras provokes premature cell senescence associated with accumulation of p53 and p16INK4a. *Cell* **88**, 593-602.

Shaw, A. T., Meissner, A., Dowdle, J. A., Crowley, D., Magendantz, M., Ouyang, C., Parisi, T., Rajagopal, J., Blank, L. J., Bronson, R. T. et al. (2007). Sprouty-2 regulates oncogenic K-ras in lung development and tumorigenesis. *Genes Dev.* **21**, 694-707.

Shimada, M., Hernandez-Gonzalez, I., Gonzalez-Robayna, I. and Richards, J. S. (2006). Paracrine and autocrine regulation of epidermal growth factor-like factors in cumulus oocyte complexes and granulosa cells: key roles for prostaglandin synthase 2 and progesterone receptor. *Mol. Endocrinol.* **20**, 1352-1365.

Shimada, M., Yanai, Y., Okazaki, T., Yamashita, Y., Sriraman, V., Wilson, M. C. and Richards, J. S. (2007). Synaptosomal-associated protein 25 gene expression is hormonally regulated during ovulation and is involved in cytokine/chemokine exocytosis from granulosa cells. *Mol. Endocrinol.* **21**, 2487-2502.

Soriano, P. (1999). Generalized lacZ expression with the ROSA26 Cre reporter strain. *Nat. Genet.* **21**, 70-71.

Su, Y. Q., Wigglesworth, K., Pendola, F. L., O'Brien, M. J. and Eppig, J. J. (2002). Mitogen-activated protein kinase activity in cumulus cells is essential for gonadotropin-induced oocyte meiotic resumption and cumulus expansion in the mouse. *Endocrinology* **143**, 2221-2232.

Tuveson, D. A., Shaw, A. T., Willis, N. A., Silver, D. P., Jackson, E. L., Chang, S., Mercer, K. L., Grochow, R., Hock, H., Crowley, D. et al. (2004). Endogenous oncogenic K-ras(G12D) stimulates proliferation and widespread neoplastic and developmental defects. *Cancer Cell* **5**, 375-387.

Urness, L. D., Li, C., Wang, X. and Mansour, S. L. (2007). Expression of ERK signaling inhibitors Dusp6, Dusp7, and Dusp9 during mouse ear development. *Dev. Dyn.* **237**, 163-169.

Wang, H., Jiang, J. Y., Zhu, C., Peng, C. and Tsang, B. K. (2006). Role and regulation of nodal/activin receptor-like kinase 7 signaling pathway in the control of ovarian follicular atresia. *Mol. Endocrinol.* **20**, 2469-2482.

Wayne, C. M., Fan, H. Y., Cheng, X. and Richards, J. S. (2007). Follicle-stimulating hormone induces multiple signaling cascades: evidence that activation of Rous sarcoma oncogene, RAS, and the epidermal growth factor receptor are critical for granulosa cell differentiation. *Mol. Endocrinol.* **21**, 1940-1957.

Woods, D. C. and Johnson, A. L. (2006). Phosphatase activation by epidermal growth factor family ligands regulates extracellular regulated kinase signaling in undifferentiated hen granulosa cells. *Endocrinology* **147**, 4931-4940.

Zeleznik, A. J., Saxena, D. and Little-Ihrig, L. (2003). Protein kinase B is obligatory for follicle-stimulating hormone-induced granulosa cell differentiation. *Endocrinology* **144**, 3985-3994.

Targeted Disruption of *Pten* in Ovarian Granulosa Cells Enhances Ovulation and Extends the Life Span of Luteal Cells

Heng-Yu Fan, Zhilin Liu, Nicola Cahill, and JoAnne S. Richards

Department of Molecular and Cellular Biology, Baylor College of Medicine, Houston, Texas 77030

FSH activates the phosphatidylinositol-3 kinase (PI3K)/acute transforming retrovirus thymoma protein kinase pathway and thereby enhances granulosa cell differentiation in culture. To identify the physiological role of the PI3K pathway *in vivo* we disrupted the PI3K suppressor, *Pten,* in developing ovarian follicles. To selectively disrupt *Pten* expression in granulosa cells, *Pten^{fl/fl}* mice were mated with transgenic mice expressing cAMP response element recombinase driven by *Cyp19* promoter (*Cyp19-Cre*). The resultant *Pten* mutant mice were fertile, ovulated more oocytes, and produced moderately more pups than control mice. These physiological differences in the *Pten* mutant mice were associated with hyperactivation of the PI3K/ acute transforming retrovirus thymoma protein kinase pathway, decreased susceptibility to apoptosis, and increased proliferation of mutant granulosa cells. Strikingly, corpora lutea of the *Pten* mutant mice persisted longer than those of control mice. Although the follicular and luteal cell steroidogenesis in *Pten^{fl/fl};Cyp19-Cre* mice was similar to controls, viable nonsteroidogenic luteal cells escaped structural luteolysis. These findings provide the novel evidence that *Pten* impacts the survival/ life span of granulosa/luteal cells and that its loss not only results in the facilitated ovulation but also in the persistence of nonsteroidogenic luteal structures in the adult mouse ovary. (*Molecular Endocrinology* 22: 2128–2140, 2008)

IN MAMMALS, OVARIAN follicular growth, ovulation, and luteinization are tightly regulated by FSH and LH. FSH is obligatory for supporting the development of follicles to the preovulatory stage. The LH surge rapidly initiates terminal differentiation of granulosa/ cumulus cells, leading to meiotic maturation of oocytes and expansion of cumulus oophorus. Granulosa cells (GCs) luteinize to form the corpus lutea (CL) after ovulation (1). FSH and LH mediate these effects by inducing a complex pattern of gene expression in the GCs that is regulated by the coordinate input from different signaling cascades such as the cAMP/protein kinase A, ERK1/2, and phosphatidylinositol-3 kinase (PI3K) cascades (2).

FSH promotes rapid activation of the PI3K pathway in GCs, resulting in the phosphorylation of the downstream branch-point kinase AKT (acute transforming retrovirus

thymoma protein kinase) (3, 4). This pathway is known to regulate many aspects of cell function including cell cycle progression/arrest, DNA repair, and apoptosis (5, 6). Targets of AKT include FOXO1 (Forkhead winged helix box O1) and FOXO3 (Forkhead winged helix box O3), transcription factors that are expressed abundantly in GCs and are presumed to regulate GC responsiveness to FSH (2, 7, 8). The critical roles of the PI3K pathway in gonadotropin-mediated GC differentiation, cumulus expansion, and oocyte maturation have been demonstrated in culture (3, 4, 7–11). Moreover, depletion of *Foxo3a* or *Pten* in mouse oocytes resulted in premature ovarian failure due to the global exit of follicles from the primordial pool (12, 13). However, the impact of PI3K pathway components in regulating functions of ovarian somatic cells during follicle development, ovulation, and/or luteinization has not been determined *in vivo*.

The PI3K pathway is negatively regulated by phosphatase and tensin homolog (PTEN) that dephosphorylates PIP3 (phosphatidylinositol 3,4,5-triphosphate), the lipid product of PI3K. *Pten* was originally cloned as a tumor suppressor, and its importance is further noted because *Pten*-null mice are embryonic lethal. *Pten* mutations in human and mice present tumors in selected tissues suggesting that PTEN acts in a tissue-specific manner to regulate PI3K pathway (14, 15).

In view of the potential importance of the PI3K pathway in the differentiation of GCs and luteal cells, we sought to identify the physiological role of *Pten* in developing follicles and its regulation of the PI3K pathway. *Pten^{fl/fl}* mice have been generated (16) and were used in these studies to obtain a conditional knockout mouse strain in which *Pten* is
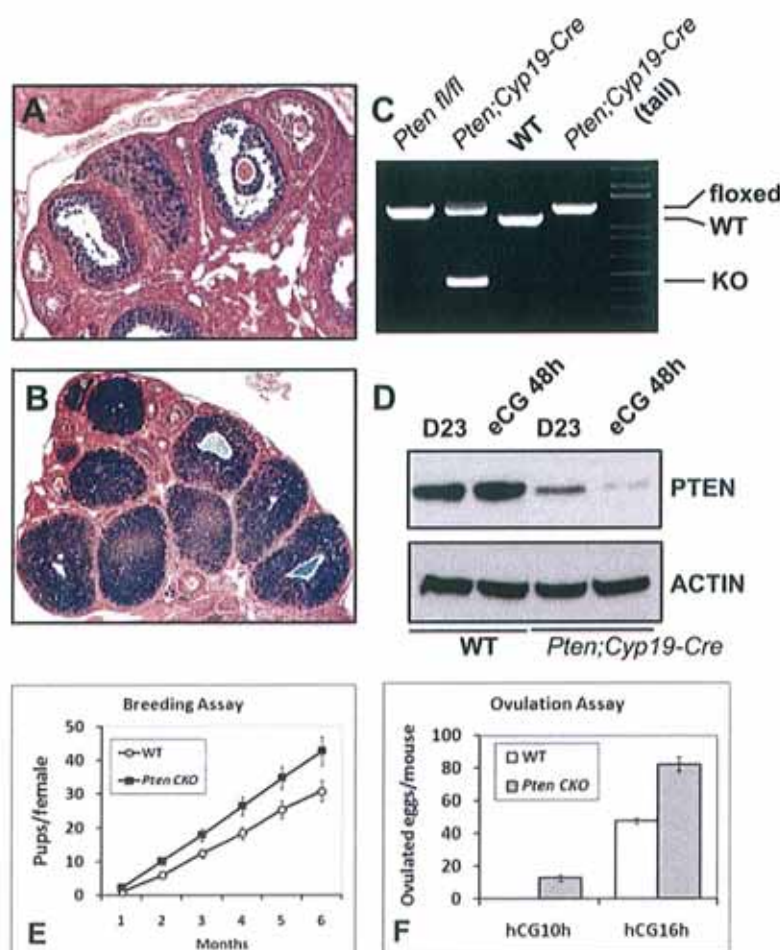
Fig. 1. Generation and Evaluation of Reproductive Functions of *Pten^{fl/fl};Cyp19-Cre* Mice

Shown in *ROSA26* reporter mouse strain, CRE activity was present in GCs of most antral follicles (A) and LCs (B). PCR analysis showed that recombination occurred exclusively in ovaries of *Pten^{fl/fl};Cyp19-Cre* progeny (C). PTEN protein levels were reduced in the GCs of the *Pten^{fl/fl};Cyp19-Cre* mice compared with wild-type mice (D). The *Pten^{fl/fl};Cyp19-Cre* females gave birth to more pups than wild type (E). In superovulation assay, *Pten^{fl/fl};Cyp19-Cre* mice ovulated more oocytes than do wild type at 16 h after hCG. At 10 h after hCG, 10–15 oocytes were ovulated by *Pten^{fl/fl};Cyp19-Cre* mice, but not the control littermates (F). KO, Knockout; WT, wild type.

specifically depleted in GCs of antral follicles and luteal cells (LCs). Strikingly, mice with *Pten* deletion in GCs do not develop ovarian tumors but demonstrated increases in ovary volume due to the accumulation of CLs. The *Pten* mutant mice ovulate more oocytes in response to a super-ovulatory regimen of equine (e) chorionic gonadotropin (CG)/human (h) CG than do control mice. GCs of the mutant mice demonstrated increased proliferation whereas GCs and LCs exhibited decreased apoptosis. These findings provide *in vivo* evidence that activation of the PI3K pathway promotes granulosa/luteal cell survival, in part by regulating FOXO1 and other mediators of cell cycle arrest and cell survival (7).

RESULTS

Granulosa/Luteal Cell-Specific Disruption of the *Pten* Gene

The *Pten^{fl/fl}* mouse strain (16) was crossed with transgenic mice in which the *Cyp19* promoter drives expression of Cre

recombinase (*Cyp19-Cre*). To monitor the cAMP response element (CRE)-mediated recombination in ovaries, the *Cyp19-Cre* mice were crossed to the *ROSA26* reporter mouse strain that expresses β-galactosidase only in cells that have CRE activity (17). As shown in Fig. 1, A and B, CRE activity was present in GCs of all antral follicles and most LCs, but was low/undetectable in GCs of primordial/primary follicles, theca cells, and oocytes. PCR analysis of ovarian and tail DNA templates confirmed that CRE-mediated recombination occurred exclusively in ovarian tissue of *Pten^{fl/fl};Cyp19-Cre* (*Pten* CKO; conditional knockout) progeny (Fig. 1C).

To determine the levels of PTEN protein in the mutant cells, GCs were isolated from immature mice at d 23 with or without treatment with eCG to stimulate follicle growth. Western blot showed that the levels of the PTEN protein were reduced dramatically in the GC extracts prepared from the *Pten* CKO mice compared with *Pten^{fl/fl}* control mice (Fig. 1D). More than three animals were analyzed in each experiment with similar results.
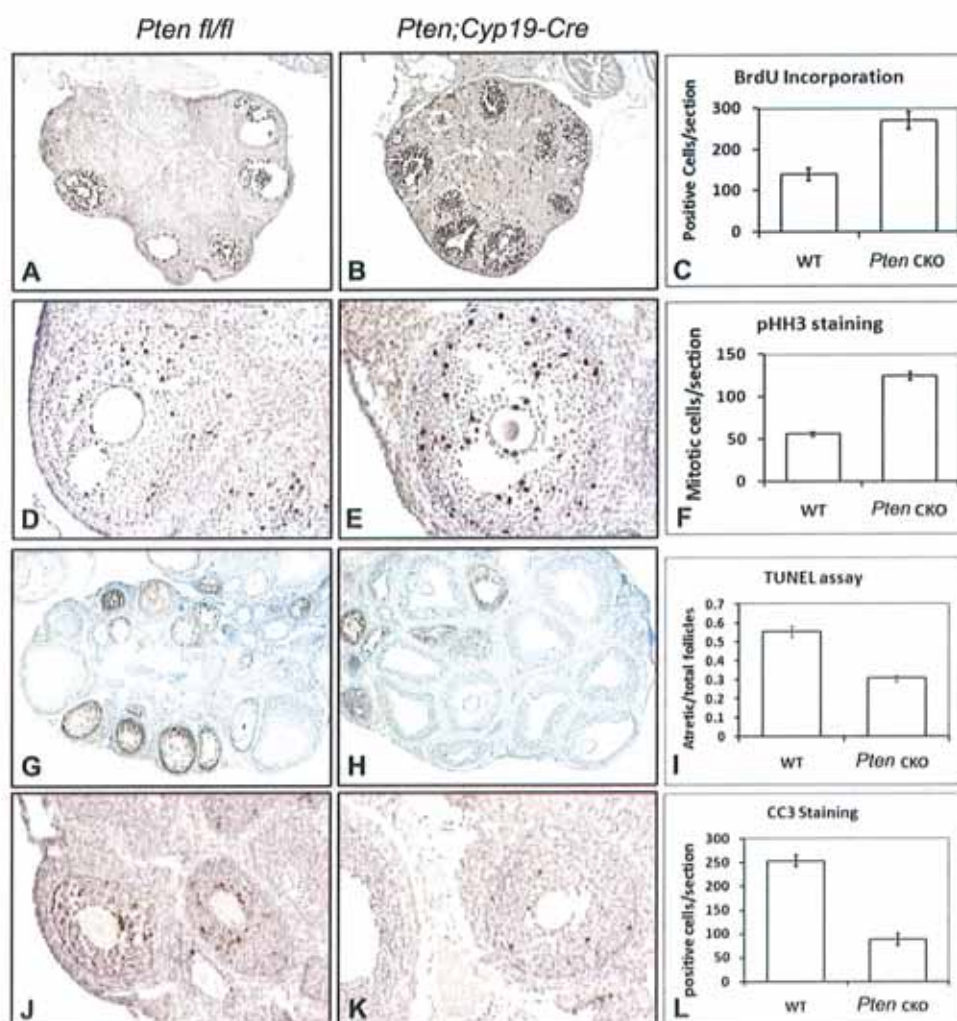
Fig. 2. GC Proliferation and Apoptosis with or without *Pten* Depletion

Pten-depleted GCs demonstrated increased levels of proliferation, based on BrdU incorporation (A, control ovary; B, *Pten* CKO ovary; C, quantification of BrdU-positive cells) and immune staining for pHH3 (D, control ovary; E, *Pten* CKO ovary; F, quantification of pHH3-positive cells). According to TUNEL assay (G, control ovary; H, *Pten* CKO ovary; I, quantification of atretic follicles) and immunostaining of CC3 (J, control ovary; K, *Pten* CKO ovary; L, quantification of CC3-positive cells), the numbers of apoptotic follicles were decreased in the eCG-primed *Pten* knockout ovaries. WT, Wild type.

The low levels of PTEN protein that were detected in the GCs collected from *Pten* CKO mice likely come from GCs in which recombination is not complete as well as from non-GC ovarian cell components (theca, oocytes, endothelial cells, and interstitial cells) where PTEN expression is higher than that in GCs (see Fig. 4K). More efficient PTEN depletion in GCs after eCG treatment may contribute to the decrease in PTEN in these cells compared with untreated mice because *Cyp19-Cre* expression is increased by eCG treatment (35).

Increased Follicle Growth and Ovulation in *Pten* Conditional Knockout Mice

Although *Pten* mutations often lead to cell transformation and tumor development in different tissues, the conditional knockout of *Pten* in GCs does not lead to

ovarian tumor formation even at 12 months of age (data not shown). Moreover, the *Pten* CKO mice are fertile and give birth to approximately 20% more pups than *Pten^{fl/fl}* control mice during a 6-month breeding period (Fig. 1E) (n = 6 per genotype). The increased number of pups born appears to be related to increased ovulation potential because immature *Pten* CKO mice primed with a superovulatory regimen of eCG (an FSH equivalent) followed by hCG (an LH equivalent) ovulate more oocytes than do control mice as determined by oviductal inspection at 16 h after hCG (Fig. 1F) (n = 8 per genotype). Even at 10 h after hCG, on average 10–15 oocytes were recovered from the oviducts of *Pten* CKO mice, whereas no oocytes had been ovulated in controls (Fig. 1F) (n = 6 per genotype). Thus, ovulation rate is advanced and increased in the mutant mice.
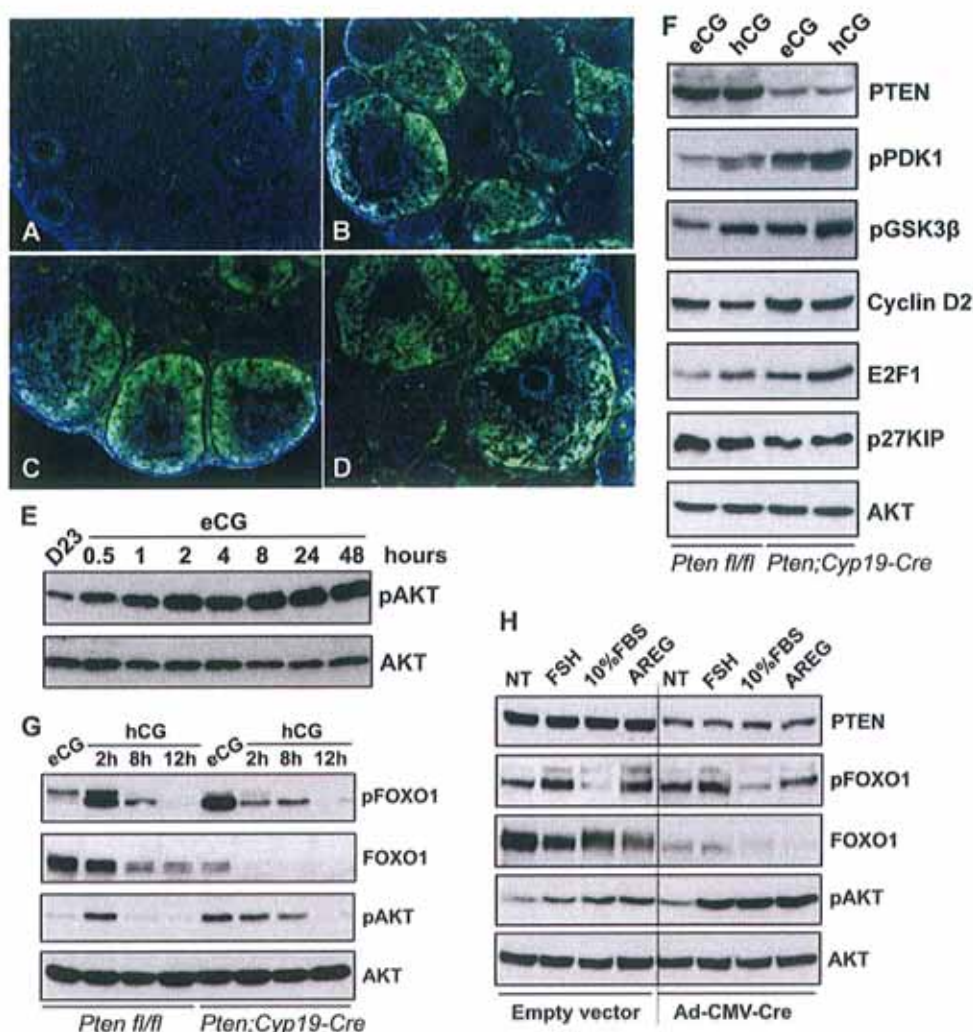
Fig. 3. Activation of PI3K Pathway in Ovaries with or without *Pten* Depletion

Phospho-AKT was absent in untreated immature ovaries (A) but was stimulated in GCs of growing follicles (B–D: 1, 8, and 24 h after eCG, respectively). These results were confirmed by Western blots (E). The levels of phospho-PDK1, -AKT, -GSK3β, and -FOXO1 were increased in *Pten* mutant GCs. Cyclin D2 and E2F1 levels were up-regulated whereas FOXO1 and p27^{KIP} levels were down-regulated, in *Pten* CKO cells (F and G). In cultured *Pten*$^{fl/fl}$ GCs, PTEN levels were decreased after infection with an adenoviral vector expressing Cre (Ad-CMV-Cre). FSH, FBS, and AREG induced more robust AKT phosphorylation in PTEN-depleted cells than in the PTEN-intact cells. FOXO1 levels decreased markedly in *Pten*-depleted cells (H). NT, No treatment.

To characterize the observed changes of *Pten* knockout ovaries at the cellular level, we first examined the proliferative rate of GCs in the developing follicles. GCs of *Pten* CKO mice demonstrated increased proliferation based on bromodeoxyuridine (BrdU) incorporation (Fig. 2, A–C) and immunostaining for the mitosis marker phosphohistone H3 (pHH3) (Fig. 2, D–F). Apoptosis is a common feature of growing follicles in the mammalian ovary and serves to eliminate those follicles that do not become competent to ovulate. Because the *Pten*$^{fl/fl}$;*Cyp19-Cre* mice ovulate more oocytes than wild type, reduced apoptosis could permit more follicles to develop to the preovulatory stage. To test this, the TUNEL (terminal deoxynucleotide transferase-mediated deoxyuridine triphosphate nick end labeling) assay and immunostaining for cleaved caspase 3 (CC3) were performed. The numbers of both apoptotic follicles (Fig. 2,

G–I) and CC3-positive GCs (Fig. 2, J–L) were decreased in the eCG-primed *Pten* mutant ovaries. Ovaries from more than four animals were analyzed in each experiment. These results suggest that *Pten* negatively impacts GC proliferation *in vivo* and promotes conditions favoring atresia/apoptosis of growing follicles, therefore constraining the number of oocytes to be ovulated in normal ovaries. Thus, follicle growth and ovulation were enhanced by disrupting of *Pten* in GCs.

The PI3K/Protein Kinase B Pathway Is Hyperactivated in *Pten*-Depleted GCs

Based on these results and the well-established role of PTEN in regulating the PI3K/AKT pathway, we hypothesized that activation of this pathway by FSH, in the
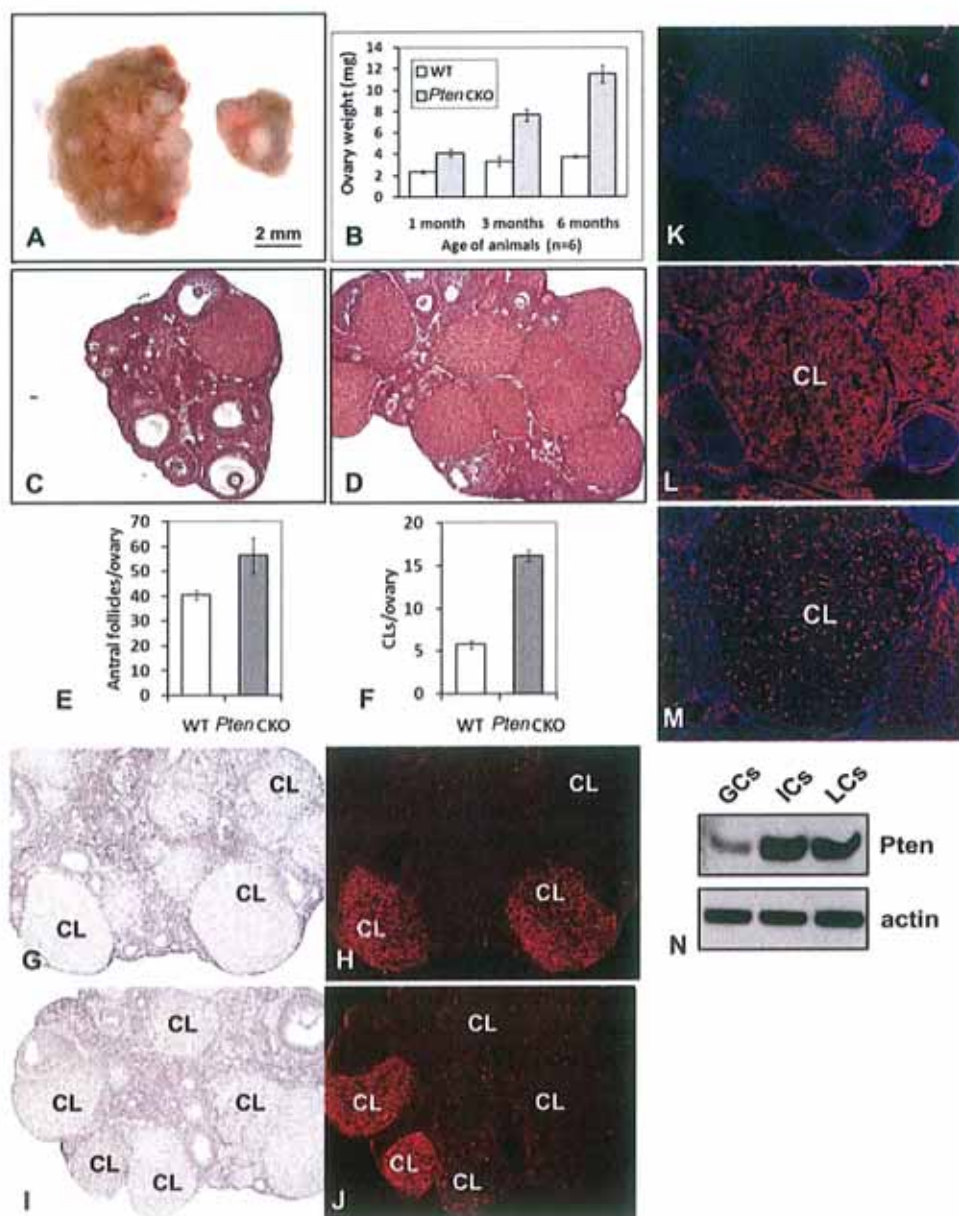
Fig. 4. Progressive Accumulation of CL in *Pten* CKO Mice

Ovaries of the *Pten* CKO mice are larger and heavier than wild-type mice (A and B). Hematoxylin and eosin staining (C and D) followed by quantification showed that the *Pten* CKO ovaries contained more antral follicles and CL than controls (E and F). *In situ* hybridization showed that whereas the fully developed, healthy CL in wild-type ovaries expressed *Lhcgr* (G and H), only some of the CL in *Pten* CKO ovaries expressed *Lhcgr* (I and J). Immunofluorescence showed that PTEN protein is highly expressed in wild-type CL (K and L), was markedly reduced in *Pten* mutant LCs, but remained in the endothelial cells (M). The protein levels of PTEN were higher in LCs and RT than in GCs (N). ICs, Interstitial cells; WT, wild type.

absence of PTEN, would increase AKT activation leading to increased follicular growth. To test whether this pathway was activated *in vivo* in response to eCG, wild-type mice were injected with eCG, and the phosphorylation of AKT was evaluated by immunofluorescence at 1, 8, and 48 h after eCG treatment. As shown in Fig. 3, A–D, phosphorylation of AKT was increased in GCs as early as 1 h after eCG treatment, and persisted in the mural GCs of fast growing antral follicles thereafter. These results were confirmed by Western

blot analyses (Fig. 3E). At each time point, protein samples were collected by homogenizing the ovaries from three different animals; protein concentrations were determined by Bradford assay.

We next compared the phosphorylation status of key components within the PI3K pathway and levels of AKT targets in GCs isolated from hormone-primed control and *Pten* CKO ovaries. As shown in Fig. 3, F and G, the levels of PTEN were reduced in the *Pten* mutant cells whereas levels of phospho-phosphoinositide-

dependent protein kinase (PDK)1, -AKT, -glycogen synthase kinase 3 (GSK3)β were all increased in eCG- and hCG-primed *Pten* mutant GCs compared with controls. Moreover, levels of phospho-FOXO1 were increased whereas total FOXO1 protein was decreased in eCG-primed *Pten* mutant cells (Fig. 3G) providing additional evidence that hyperactivation of the PI3K pathway occurred in response to the loss of endogenous PTEN. Known targets of the PI3K pathway were also altered: cyclin D2 and E2F1 levels were up-regulated whereas p27^{KIP} levels were down-regulated in *Pten* CKO cells compared with controls. Levels of total AKT showed no change. These results are consistent with the pattern of increased proliferation observed in the *Pten*-depleted GCs (Fig. 2).

We also tested the basal activity of the PI3K pathway in ovaries of 23-d-old females without hormonal stimulation. In these ovaries, there was little difference between wild-type and *Pten* CKO mice (data not shown), primarily because endogenous hormone levels appear too low to activate the PI3K pathway at this time. In addition, because *Cyp19-Cre* is preferentially expressed in antral follicles after eCG treatment (Fan *et al.*, Development, in press), recombination is enhanced in antral, preovulatory follicles. Similar results were observed in cultured cells (Fig. 3H).

To study the synchronized and acute responses of GCs to *Pten* depletion, we isolated GCs from 21-d-old *Pten*$^{fl/fl}$ mice and infected these cells with an adenoviral vector expressing CRE recombinase (Ad-CMV-Cre) or control vector. As shown in Fig. 3H, PTEN protein levels decreased dramatically in Ad-CMV-Cre-infected *Pten*$^{fl/fl}$ cells. Although the basal level (NT, no treatment) of phospho-AKT in these cells increased only slightly when compared with cells infected with the control vector (similar to *in vivo* results; Fig. 3, F and G), addition of FSH, fetal bovine serum (FBS), and amphiregulin (AREG, a known intrafollicular effect of LH) to the culture medium induced more robust AKT phosphorylation in PTEN-depleted cells than in the PTEN-intact cells. Moreover, the levels of FOXO1 decreased markedly in PTEN-depleted cells causing the relative ratio of phospho-FOXO1 to total FOXO1 to increase in these cells. These *in vitro* experiments indicate that activation of the PI3K pathway by ligands is enhanced in GCs in which endogenous PTEN levels are reduced.

Structural But Not Functional (Steroidogenic) Luteolysis Is Repressed in *Pten*-Deficient CLs

One of the most dramatic differences in the *Pten* CKO mouse ovaries compared with control ovaries is the extraordinary abundance of corpora lutea (CL) present in the ovaries of the *Pten* mutant mice. Specifically, after 3 months of age the ovaries of *Pten* CKO mice were larger and visually appeared to contain more CL than control mice (Fig. 4, A and B). Histological analyses of ovaries from 6-month-old *Pten* mutant mice confirmed the abundance of CL (Fig. 4, C and D). Total

numbers of antral follicles and CL in ovaries of control and *Pten* CKO mice were counted in serial ovarian sections. Whereas the *Pten* CKO ovaries contained slightly more antral follicles than controls (Fig. 4E), they had 3 times more CL than normal cycling ovaries (Fig. 4F). *In situ* hybridization results showed that the fully developed CL in wild-type ovaries expressed *Lhcgr* (Fig. 4, G and H), which encodes the LH receptor and is a marker of newly formed, healthy CL. But only some of the CL in *Pten* CKO ovaries expressed *Lhcgr*. However, other persistent CL did not express *Lhcgr* (Fig. 4, I and J). These results suggested that the numerous CL observed in *Pten* CKO ovaries were at different stages of differentiation, and that some of them might be nonfunctional [a fact that has been conformed (see Fig. 6)]. Furthermore, immunofluorescent staining of wild-type ovaries revealed that PTEN protein was highly expressed in CL of control mice (Fig. 4, K and L) but was markedly reduced in the endocrine LCs of *Pten* CKO ovaries (Fig. 4M). In contrast, PTEN remained highly expressed in the vascular endothelial cells present in corpora lutea (Fig. 4M). The relative abundance of PTEN protein levels in GCs, LCs, residual tissue (RT, stromal/interstitial cells, and remaining small follicles), were compared by Western blot analysis. GCs were collected from preovulatory follicles by needle puncture of ovaries isolated from eCG-primed control mice whereas LCs were collected by needle disruption of ovaries isolated from eCG-primed mice 48 h after hCG. RT was collected as that remaining after removal of LCs. As shown in Fig. 4N, the levels of PTEN were higher in LCs and RT than in GCs.

To determine the extent to which the life span of CL in the *Pten* mutant ovaries was extended, immature *Pten* CKO and control mice were injected with a superovulatory regimen of eCG/hCG, and the ovaries were examined on selected days thereafter. In control mice, CL that were present in ovaries on d 2 after hCG, began to regress by d 4 and disappeared by d 7 [Fig. 5A (hCG D2), B (hCG D5), C (hCG D7)]. In contrast, ovaries of the *Pten* mutant mice contained many large CL on d 5 and d 7 (four of eight mice) (Fig. 5, D–F) and even until d 15 (two of eight mice) (data not shown). TUNEL assays showed many apoptotic LCs in ovaries of control mice on d 4–5 after hCG (Fig. 5G), whereas no apoptotic cells were observed in LCs of the mutant mice at any time point examined after ovulation (Fig. 5, H and I), indicating that luteolysis was dramatically impaired and delayed.

Because PTEN is highly expressed in LCs and the *Pten*-depleted CL exhibit a prolonged life span, additional analyses were done to determine the relative levels of PI3K pathway components in ovaries of *Pten* CKO mice compared with controls. Western blots of ovaries obtained from eCG/hCG-primed mice (n = 3 per genotype at each time point) showed that phospho-AKT and FOXO3 were dramatically up-regulated in *Pten* CKO ovaries compared with controls at d 2 and d 5 after hCG injection when many CL were present
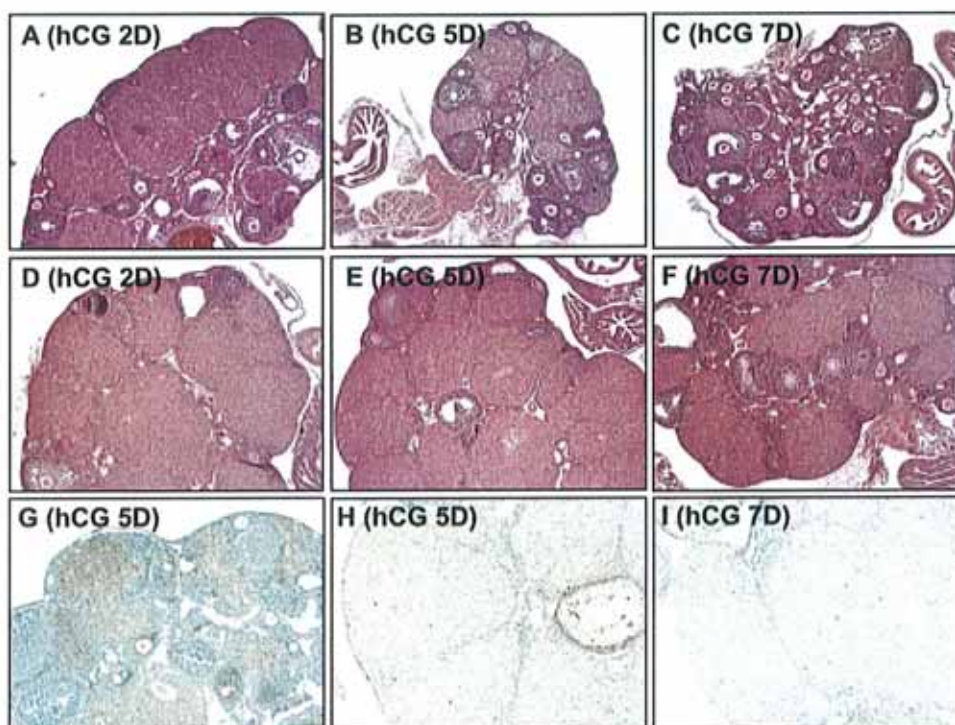
Fig. 5. Luteal Regression after hCG Injection

In wild-type mice, CL began to regress by d 4 after hCG and disappeared by d 7 (A–C: hCG d 2, d 5, and d 7, respectively), whereas the *Pten* CKO ovaries retained many CL at d 2, d 5, and d 7 (D–F). Apoptosis of LCs culminated at d 4–5 after hCG in wild type (G), but not in *Pten* mutant CL at the hCG d 5 (H) or d 7 (I).

(Fig. 6A). Immunofluorescent staining documented elevated levels of phospho-AKT and FOXO3 in CL of the *Pten* mutant mice on d 2 (Fig. 6, panels B, C, F, and G). However, the known AKT targets, FOXO1 and p27^{KIP}, were differentially regulated during luteinization. FOXO1 levels were dramatically down-regulated by LH/hCG (Fig. 3G). In contrast to the Western blot results, FOXO1 was undetectable in fully developed CL at d 2 after hCG, in both control (Fig. 6D) and *Pten* CKO (Fig. 6E) ovaries. In contrast, p27^{KIP} (Fig. 6, H and I) was highly expressed in the CL, regardless of the genotype. Both the Western blots and immunostaining were performed at least twice with similar results.

Steroidogenically Inactive LCs Accumulate in *Pten*-Deficient CL

To evaluate the endocrine function of *Pten*-depleted GCs and LCs, we analyzed levels of serum estradiol and progesterone in control and *Pten* CKO mice. In mice of both genotypes (n = 3 per genotype at each time point), estradiol increased in association with the growth of preovulatory follicles in response to eCG and dropped precipitously in response to hCG (Fig. 7A). Progesterone peaked on d 2 after hCG, when CL have formed and declined precipitously thereafter (Fig. 7B). These observations indicated that steroid biosynthesis was similar in mice of each genotype even though CL structures persist longer in the

Pten CKO mice. To assess the molecular basis for these endocrine events, we compared the expression patterns of key enzymes of progesterone metabolism in LCs of control and *Pten* CKO mice. At d 2 after hCG, cytochrome P450 (CYP)11A1, a key enzyme of progesterone biosynthesis and a marker of LC function, was expressed at high levels in CL of both control (Fig. 7C) and *Pten* CKO ovaries (Fig. 7D) but declined at d 5 after hCG regardless of genotype (Fig. 7, G and H). Moreover, 20α-hydroxysteroid dehydrogenase (20α-HSD), which catalyzes the inactivation of progesterone, and is a marker of functionally regressing LCs, was expressed in a reciprocal manner to CYP11A1, in both control (Fig. 7, E and I) and *Pten* CKO ovaries (Fig. 7, F and J). Thus, despite the extension of their life span, the CL in *Pten* CKO mice did not remain steroidogenically active. These observations clearly separate functional (endocrine) luteolysis from structural luteolysis.

DISCUSSION

The pituitary gonadotropin FSH controls follicular development by regulating granulosa cell proliferation and differentiation (18, 19). LH, in turn, initiates ovulation, terminates granulosa cell proliferation, and mediates the genetic transition of GCs to LCs (20). Both
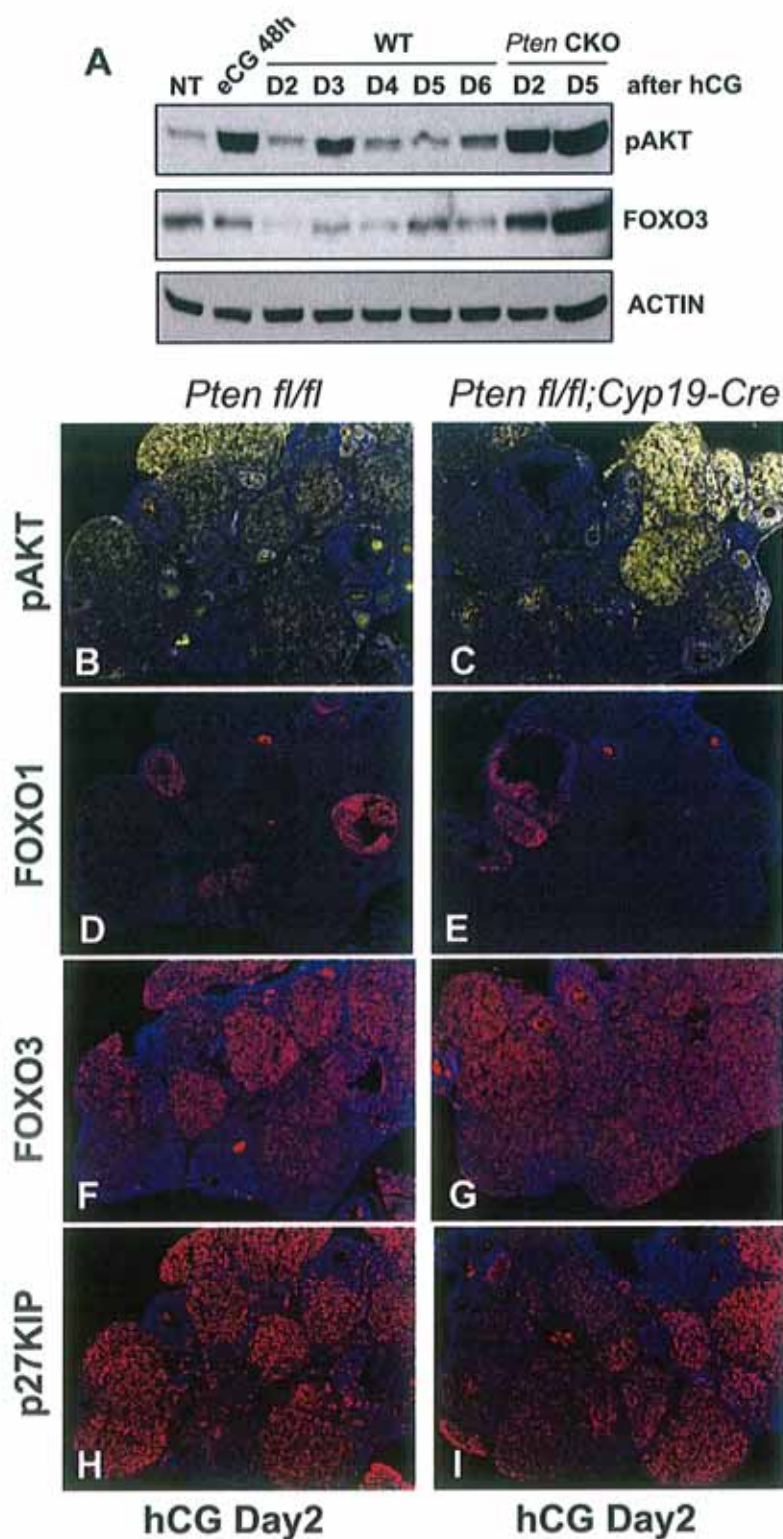
Fig. 6. Expression of PI3K Pathway Components in Fully Developed CLs

Western blots showed that AKT activity and FOXO3 were up-regulated in *Pten* CKO ovaries after CL formation (A). Immunofluorsecent staining showed higher levels of phospho-AKT in CL of the *Pten* mutant mice (C) than control mice (B) on d 2. Among the known targets of AKT, FOXO1 was undetectable in fully developed CLs, in both control (D) and *Pten* CKO (E) ovaries. In contrast, FOXO3 (F and G) and p27^KIP (H and I) were highly expressed in the CLs, regardless of the genotypes. WT, Wild type; NT, no treatment.
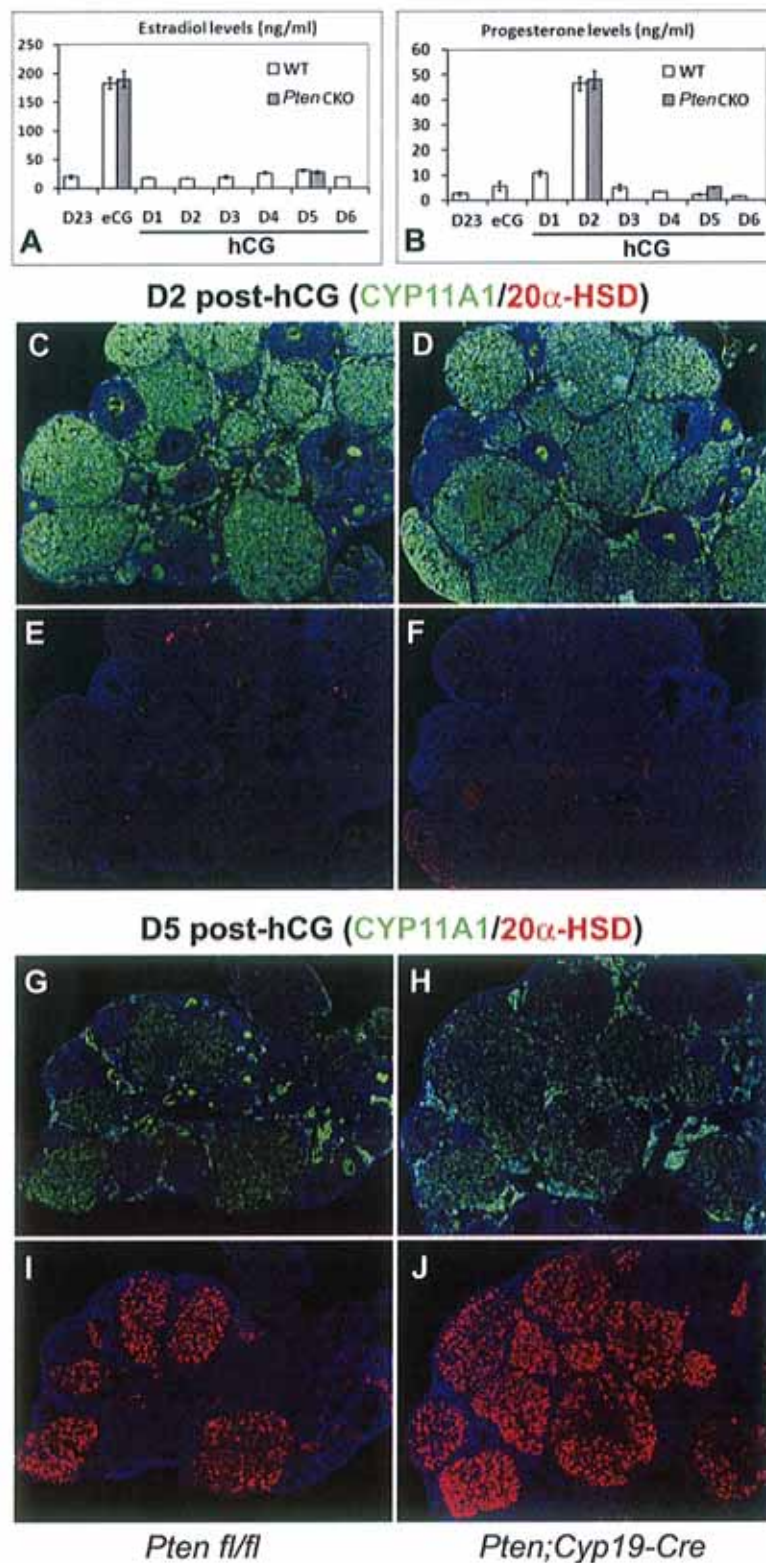
D2 post-hCG (CYP11A1**/**20α-HSD**)**

D5 post-hCG (CYP11A1**/**20α-HSD**)**

Pten fl/fl   *Pten;Cyp19-Cre*

Fig. 7. Endocrine Functions of CL in *Pten* CKO Mice

Levels of serum estradiol (A) and progesterone (B) were not different between control and *Pten* CKO mice after eCG/hCG treatments. At d 2 after hCG, CYP11A1 was expressed at high level in CL (C and D) but declined at d 5 regardless of genotype (E and F). Conversely, 20α-HSD was expressed in a reciprocal manner to CYP11A1, in both wild (G and I) and *Pten* CKO ovaries (H and J). WT, Wild type.

hormones bind cognate G-protein coupled receptors and activate adenylyl cyclase leading to increased levels of cAMP and protein kinase A (2, 21). However, recent studies show that FSH and LH activate additional signaling cascades, independently of protein kinase A, that impact follicular development, ovulation, and oocyte maturation. Specifically, FSH and LH activate RAS and the downstream targets RAF1, MEK, and ERK1/2 (22) (35) as well as PI3K and the downstream targets AKT and the transcription factor FOXO1 (4, 7). Phosphorylation of FOXO1 excludes its transport to the nucleus and leads to its degradation in the cytoplasm (23, 24). FSH and LH also act to turn off expression of the *Foxo1* gene in GCs in culture and preovulatory follicles, respectively, suggesting that FOXO1 may antagonize GC proliferation and/or differentiation (7, 8, 25).

One well-characterized negative regulator of the PI3K/AKT pathway is the tumor suppressor PTEN, which when mutated frequently leads to tumorigenesis (14, 26). Based on the critical role of this pathway in cell proliferation and survival and because the physiological roles of the PI3K, AKT, and FOXO pathway during follicular development and luteinization have not been characterized, we hypothesized that selective disruption of the PI3K repressor, PTEN, in GCs using a novel, GC-specific *Cyp19-Cre*-mouse model would alter GC proliferation and differentiation and thereby impact follicular development, ovulation, and/or luteinization.

In agreement with our hypothesis, we show that disruption of the *Pten* gene in GCs altered both FSH regulation of follicular development and that this was related to increased phosphorylation of the PI3K components, PDK1, AKT, and FOXO1. Increased phosphorylation of FOXO1 was also associated with a dramatic reduction of FOXO1 protein in the mutant cells. These biochemical changes in GCs were associated with an enhanced number of follicles ovulating and the rate at which they ovulated. This enhancement of ovulation was mediated, in part, by increased proliferation of GCs that was associated with higher levels of the cell cycle activators cyclin D2 and E2F1 and reduced levels of the cell cycle inhibitor p27^{KIP}. Enhanced follicular growth and the increased number of ovulating follicles were also related to a reduced number of follicles exhibiting apoptotic GCs. These results indicate that the increased phosphorylation and activation of AKT and the premature decrease in FOXO1 *in vivo* are associated with the promotion of GC survival and an increased number of follicles reaching the preovulatory stage.

The effects of *Pten* loss in GCs are much less dramatic than the loss of *Pten* in oocytes where disruption of this gene leads to premature follicle growth, depletion of the follicle reserve, and premature ovarian failure (13). The apparent lack of a more dramatic effect of *Pten* disruption in GCs on the number of follicles growing and ovulating may be due to the relatively low levels of PTEN protein present in GCs compared with other ovarian cell types, including oocytes. Therefore, we hypothesize that negative regulatory factors, in addition to PTEN, impact the PI3K pathway in GCs. The expression levels of PTEN in GCs may vary among different mammalian species. It is noteworthy that mouse is a polyovulatory species in which multiple oocytes are ovulated in each estrous cycle. In mono-ovulatory mammals PTEN might play more critical roles in restraining the activity of PI3K pathway and controlling the single follicle that reaches the ovulation stage. In support of this possibility, a recent study indicated that levels of PTEN increased in ovine GCs during terminal follicular growth, and that PTEN regulated the expression of p27^{KIP} and E2F in these cells (27).

Because the *Pten* CKO mice were fertile and gave birth to live pups, the loss of *Pten* in GCs did not impair LH-induced ovulation, block the terminal differentiation of GCs to LCs, or disrupt the maintenance of functional CL during pregnancy. These results clearly indicate that responses to FSH and LH were not impaired. Moreover, the endocrine profiles of serum estradiol and progesterone and the expression of enzymes controlling progesterone biosynthesis were identical in hormonally primed *Pten* CKO mice and control mice. However, despite the normal pattern of endocrine functions in the LCs of the *Pten* CKO mice, the CL exhibited a prolonged existence that was not associated with prolonged steroidogenic activity. PTEN is expressed at low levels in GCs but is increased in LCs. These results support recent immunohistochemical localization of PTEN in human CL (28). Although the cell cycle repressor p27^{KIP} is highly expressed in LCs is required for CL formation (29, 30), p27^{KIP} levels were not altered dramatically in the *Pten*-deficient cells and therefore do not appear to be the primary mediator of the *Pten*-null phenotype (Fig. 6).

Rather, the biochemical basis for the extended life span of the *Pten*-deficient LCs appears to be associated with enhanced phosphorylation and activation of AKT and the expression of a distinct set of PI3K pathway components, including FOXO3. Whereas levels of FOXO1 protein are rapidly decreased during luteinization, expression of FOXO3 continues in LCs (Fig. 6). These results support our previous *in situ* hybridization analyses and clearly indicate that each FOXO factor is expressed in a cell-specific manner and differentially regulated by specific hormones (7). Moreover, the levels of FOXO3 are elevated in the *Pten*-deficient LCs, indicating that activated AKT may exert a positive regulatory role on this factor. These results indicate that FOXO3 may also exert functions that are distinct from those of FOXO1, as has been observed in other cell types (31). Again it is important to note that PTEN, AKT, and FOXO3 are present at high levels in oocytes, and depletion of either *Pten* or *Foxo3* causes premature ovarian failure (12, 13, 32). Thus, it is clear that the consequences of disrupting *Pten* in LCs are distinct from those in oocytes. Because apoptosis was decreased and delayed in the *Pten* mutant LCs, as de-

termined by TUNEL assays and activated caspase 3 staining, it is possible that components of the apoptic pathway are targets of AKT and FOXO3. However, because caspase 3-null mice do not exhibit the marked accumulation of CL as observed in the *Pten* CKO mice (33, 34), factors in addition to caspase 3 appear to be involved in regulating the extended life span of *Pten*-null LCs. The identification of these factors will provide important information on targets of the PI3K pathway that may be specific for LCs compared with GCs.

Collectively, these data provide evidence that PTEN is expressed in a cell-specific manner in the ovary and appears to exert cell-specific functions to regulate GC proliferation and apoptosis as well as LC longevity. That PTEN is expressed at higher levels in LCs than GCs was somewhat unexpected given the high levels of FOXO1 in GCs. Therefore, additional regulators of the PI3K pathway in GCs are likely to be operative. That the loss of PTEN leads to a dramatic extension of LC longevity and to the accumulation of CL in the adult *Pten* mutant ovaries indicates that this regulator of the PI3K pathway plays an important role in LC survival. Because FOXO3 is preferentially expressed in LCs suggests that this factor may play a specific role in these cells as well. Importantly, loss of PTEN and changes in activation of the PI3K pathway did not exert pronounced effects of GC differentiation or luteinization, indicating that factors controlling cell survival operate by mechanisms distinct from those controlling cell differentiation and steroidogenesis. Thus, repression of the AKT pathway by PTEN appears to be required to favor GC and LC apoptosis as well as structural regression of the CL but does not markedly impact the endocrine functions of these cells.

MATERIALS AND METHODS

Animals

Immature C57BL/6 mice were obtained from Harlan, Sprague Dawley, Inc. (Indianapolis, IN). Mice lacking *Pten* in GCs were generated by crossing *Cyp19-Cre* mice with previously reported *Pten^{fl/fl}* mice (16). The *Cyp19-Cre* transgenic mice were generated by oocyte microinjection of a DNA fragment in which the *Cyp19* promoter (304 bp) is followed by *iCre* cDNA. On d 23 of age, female mice were injected ip with 4 IU of eCG (Pregnyl; Organon, West Orange, NJ) followed 48 h later with 5 IU hCG (Gestyl; Diosynth, Oss, The Netherlands) to promote synchronized follicle growth and ovulation. Animals were housed under a 16-h light, 8-h dark schedule, provided food and water *ad libitum*, and treated in accordance with the National Institutes of Health Guide for the Care and Use of Laboratory Animals.

Serum Analysis

Mice were anesthetized and blood was collected by cardiac puncture. FSH, LH, progesterone, and estradiol measurements were made by the University of Virginia Ligand Core Facility (Specialized Cooperative Center Program in Reproduction and Infertility Research: NIH U54 HD28934).

Immunohistochemistry

Tissues were fixed in 4% paraformaldehyde and embedded in paraffin. Immunohistochemistry was performed on 5-μm sections using the Vectastain ABC kit (Vector Laboratories, Burlingame, CA). Rabbit antiphosphohistone H3 (Upstate Laboratories, Lake Placid, NY), and rabbit anticleaved caspase-3 (Cell Signaling Technology, Beverly, MA) were used to evaluate cell proliferation and apoptosis in follicles. For direct comparison, wild-type and *Pten* CKO ovary sections from four individual females were processed together. Phospho-HH3 or CC3-positive cell numbers were quantified in 10 high-power fields per section, and four individual sections were quantified per specimen.

TUNEL Assay

Analysis of apoptosis in ovarian follicles was carried out by TUNEL assay using the ApopTag Plus *in situ* apoptosis detection kit (Chemicon International, Temecula, CA). At least four different specimens from *Pten* CKO and *Pten^{fl/fl}* mice were analyzed in parallel. Total and TUNEL-positive follicles were quantified per section, and three individual sections were quantified per specimen.

BrdU Incorporation Assay

Mice received an ip injection of 50 mg/kg of BrdU and were killed 2 h after treatment. Incorporated BrdU was detected by immunohistochemistry using BrdU antibody (Sigma Chemical Co., St. Louis, MO) according to manufacturer's instruction.

GC Culture

GCs were harvested from 23-d-old *Pten^{fl/fl}* mice and cultured at a density of 1×10^6 cells in serum-free medium (DMEM/F12) in 12-well culture dishes. After 4 h culture, cells were infected with adenoviral vectors expressing Cre recombinase (Vector Development Laboratory, Baylor College of Medicine) at a multiplicity of infection of 4:1. At 20 h after infection, GCs were stimulated with FSH (100 ng/ml), FBS (10%), or AREG (100 ng/ml).

Western Blot Analysis

Cell extracts containing 30 μg protein were resolved by SDS-PAGE and transferred to polyvinylidine difluoride membranes (Millipore Corp., Bedford, MA). The primary antibodies used were: p27^{KIP} and E2F1 (Santa Cruz Biotechnology, Inc., Santa Cruz, CA), cyclin D2 (Lab Vision Corp., Fremont, CA), FOXO1, phospho-FOXO1, AKT, phospho-AKT, phospho-ERK1/2, phospho-PDK1, phospho-GSK3β, PTEN (Cell Signaling Technology).

REFERENCES

1. Stocco C, Telleria C, Gibori G 2007 The molecular control of corpus luteum formation, function, and regression. Endocr Rev 28:117–149
2. Hunzicker-Dunn M, Maizels ET 2006 FSH signaling pathways in immature granulosa cells that regulate target gene expression: branching out from protein kinase A. Cell Signal 18:1351–1359
3. Gonzalez-Robayna IJ, Falender AE, Ochsner S, Firestone GL, Richards JS 2000 Follicle-Stimulating hormone (FSH) stimulates phosphorylation and activation of protein kinase B (PKB/Akt) and serum and glucocorticoid-induced kinase (Sgk): evidence for A kinase-independent signaling by FSH in granulosa cells. Mol Endocrinol 14:1283–1300
4. Alam H, Maizels ET, Park Y, Ghaey S, Feiger ZJ, Chandel NS, Hunzicker-Dunn M 2004 Follicle-stimulating hormone activation of hypoxia-inducible factor-1 by the phosphatidylinositol 3-kinase/AKT/Ras homolog enriched in brain (Rheb)/mammalian target of rapamycin (mTOR) pathway is necessary for induction of select protein markers of follicular differentiation. J Biol Chem 279:19431–19440
5. Rodriguez-Viciana P, Marte BM, Warne PH, Downward J 1996 Phosphatidylinositol 3' kinase: one of the effectors of Ras. Philos Trans R Soc Lond B Biol Sci 351:225–231; discussion 231–222
6. Gupta S, Ramjaun AR, Haiko P, Wang Y, Warne PH, Nicke B, Nye E, Stamp G, Alitalo K, Downward J 2007 Binding of Ras to phosphoinositide 3-kinase p110α is required for Ras-driven tumorigenesis in mice. Cell 129:957–968
7. Richards JS, Sharma SC, Falender AE, Lo YH 2002 Expression of FKHR, FKHRL1, and AFX genes in the rodent ovary: evidence for regulation by IGF-I, estrogen, and the gonadotropins. Mol Endocrinol 16:580–599
8. Park Y, Maizels ET, Feiger ZJ, Alam H, Peters CA, Woodruff TK, Unterman TG, Lee EJ, Jameson JL, Hunzicker-Dunn M 2005 Induction of cyclin D2 in rat granulosa cells requires FSH-dependent relief from FOXO1 repression coupled with positive signals from Smad. J Biol Chem 280:9135–9148
9. Shimada M, Ito J, Yamashita Y, Okazaki T, Isobe N 2003 Phosphatidylinositol 3-kinase in cumulus cells is responsible for both suppression of spontaneous maturation and induction of gonadotropin-stimulated maturation of porcine oocytes. J Endocrinol 179:25–34
10. Zeleznik AJ, Saxena D, Little-Ihrig L 2003 Protein kinase B is obligatory for follicle-stimulating hormone-induced granulosa cell differentiation. Endocrinology 144:3985–3994
11. Hoshino Y, Yokoo M, Yoshida N, Sasada H, Matsumoto H, Sato E 2004 Phosphatidylinositol 3-kinase and Akt participate in the FSH-induced meiotic maturation of mouse oocytes. Mol Reprod Dev 69:77–86
12. Castrillon DH, Miao L, Kollipara R, Horner JW, DePinho RA 2003 Suppression of ovarian follicle activation in mice by the transcription factor Foxo3a. Science 301:215–218
13. Reddy P, Liu L, Adhikari D, Jagarlamudi K, Rajareddy S, Shen Y, Du C, Tang W, Hamalainen T, Peng SL, Lan ZJ, Cooney AJ, Huhtaniemi I, Liu K 2008 Oocyte-specific deletion of Pten causes premature activation of the primordial follicle pool. Science 319:611–613
14. Cantley LC, Neel BG 1999 New insights into tumor suppression: PTEN suppresses tumor formation by restraining the phosphoinositide 3-kinase/AKT pathway. Proc Natl Acad Sci USA 96:4240–4245
15. Sansal I, Sellers WR 2004 The biology and clinical relevance of the PTEN tumor suppressor pathway. J Clin Oncol 22:2954–2963
16. Lesche R, Groszer M, Gao J, Wang Y, Messing A, Sun H, Liu X, Wu H 2002 Cre/loxP-mediated inactivation of the murine Pten tumor suppressor gene. Genesis 32:148–149
17. Soriano P 1999 Generalized lacZ expression with the ROSA26 Cre reporter strain. Nat Genet 21:70–71
18. Rao MC, Midgley Jr AR, Richards JS 1978 Hormonal regulation of ovarian cellular proliferation. Cell 14:71–78
19. Richards JS, Fitzpatrick SL, Clemens JW, Morris JK, Alliston T, Sirois J 1995 Ovarian cell differentiation: a cascade of multiple hormones, cellular signals, and regulated genes. Recent Prog Horm Res 50:223–254
20. Robker RL, Richards JS 1998 Hormonal control of the cell cycle in ovarian cells: proliferation versus differentiation. Biol Reprod 59:476–482
21. Richards JS, Russell DL, Ochsner S, Hsieh M, Doyle KH, Falender AE, Lo YK, Sharma SC 2002 Novel signaling pathways that control ovarian follicular development, ovulation, and luteinization. Recent Prog Horm Res 57:195–220
22. Wayne CM, Fan HY, Cheng X, Richards JS 2007 FSH-induces multiple signaling cascades: evidence that activation of SRC, RAS and the EGF receptor are critical for granulosa cell differentiation. Mol Endocrinol 21:1940–1957
23. Arden KC 2007 FoxOs in tumor suppression and stem cell maintenance. Cell 128:235–237
24. Brunet A, Bonni A, Zigmond MJ, Lin MZ, Juo P, Hu LS, Anderson MJ, Arden KC, Blenis J, Greenberg ME 1999 Akt promotes cell survival by phosphorylating and inhibiting a Forkhead transcription factor. Cell 96:857–868
25. Rudd MD, Gonzalez-Robayna I, Hernandez-Gonzalez I, Weigel NL, Bingman III WE, Richards JS 2007 Constitutively active FOXO1a and a DNA-binding domain mutant exhibit distinct co-regulatory functions to enhance progesterone receptor A activity. J Mol Endocrinol 38:673–690
26. Li G, Robinson GW, Lesche R, Martinez-Diaz H, Jiang Z, Rozengurt N, Wagner KU, Wu DC, Lane TF, Liu X, Hennighausen L, Wu H 2002 Conditional loss of PTEN leads to precocious development and neoplasia in the mammary gland. Development 129:4159–4170
27. Froment P, Bontoux M, Pisselet C, Monget P, Dupont J 2005 PTEN expression in ovine granulosa cells increases during terminal follicular growth. FEBS Lett 579:2376–2382
28. Goto M, Iwase A, Ando H, Kurotsuchi S, Harata T, Kikkawa F 2007 PTEN and Akt expression during growth of human ovarian follicles. J Assist Reprod Genet 24:541–546
29. Kiyokawa H, Kineman RD, Manova-Todorova KO, Soares VC, Hoffman ES, Ono M, Khanam D, Hayday AC, Frohman LA, Koff A 1996 Enhanced growth of mice lacking the cyclin-dependent kinase inhibitor function of p27(Kip1). Cell 85:721–732
30. Robker RL, Richards JS 1998 Hormone-induced proliferation and differentiation of granulosa cells: a coordinated balance of the cell cycle regulators cyclin D2 and p27Kip1. Mol Endocrinol 12:924–940

31. Auer KL, Park JS, Seth P, Coffey RJ, Darlington G, Abo A, McMahon M, Depinho RA, Fisher PB, Dent P 1998 Prolonged activation of the mitogen-activated protein kinase pathway promotes DNA synthesis in primary hepatocytes from p21Cip-1/WAF1-null mice, but not in hepatocytes from p16INK4a-null mice. Biochem J 336:551–560

32. Reddy P, Shen L, Ren C, Boman K, Lundin E, Ottander U, Lindgren P, Liu YX, Sun QY, Liu K 2005 Activation of Akt (PKB) and suppression of FKHRL1 in mouse and rat oocytes by stem cell factor during follicular activation and development. Dev Biol 281:160–170

33. Carambula SF, Matikainen T, Lynch MP, Flavell RA, Goncalves PB, Tilly JL, Rueda BR 2002 Caspase-3 is a pivotal mediator of apoptosis during regression of the ovarian corpus luteum. Endocrinology 143:1495–1501

34. Carambula SF, Pru JK, Lynch MP, Matikainen T, Goncalves PB, Flavell RA, Tilly JL, Rueda BR 2003 Prostaglandin F2α- and FAS-activating antibody-induced regression of the corpus luteum involves caspase-8 and is defective in caspase-3 deficient mice. Reprod Biol Endocrinol 1:15

35. Fan H-Y, Shimada M, Liu Z, Cahill N, Noma N, Wu Y, Gossen J, Richards JS 2008 Selective expression of KrasG12D in granulosa cells of the mouse ovary causes defects in follicle development and ovulation. Development 135:2127–2137